THESIS

BUILDING

TECHNOLOGY

FIRE SAFETY AND SUPPRESSION IN MODERN RESIDENTIAL BUILDINGS |

Research on the Influence of the Building Skin on the Fire Behaviour in Well Insulated and Airtight Dwellings and Consequences for the Safety of the Occupant and Fire Service

This thesis is submitted in order to acquire the title MSc for the master track Building Technology, of the Department Architecture, Building and Planning at the Eindhoven University of Technology

THESIS

BUILDING

TECHNOLOGY

- Department Architecture, Building and Planning -

Building Technology

Student

V. van den Brink
078 3686

Supervisors

Prof. dr. ir. H.J.H. Brouwers (Chairman)
Ir. R.A.P. van Herpen FIFireE (Fellow TU/e)
Dr. ir. R. Weewer (Instituut Fysieke Veiligheid - Brandweeracademie)
Ir. A.C.J. de Korte (Supervisor TU/e)

Date: 21-04-2015

Preface

In the context of the study Building Technology, which is a part of the department Architecture, Building and Planning of the Eindhoven University of Technology, I conducted this research which focuses on the fire behaviour and the occurrence of pressure build-up in well insulated and airtight dwellings. This research is conducted in response to the problem statement which has been provided by Brandweer Nederland. During their daily activities the trend is observed that window panes withstand the fire longer before they lose its structural integrity. Because this has major implications for the fire scenario and safety of fire fighters during the suppressive phase, the question was initially aimed to provide an insight in the pane behaviour of modern dwellings.

In a recently conducted research of Ronald Huizinga, a thorough study to the performance of double and triple glazing on the fire behaviour was already carried out. In his thesis, the fall out period of double and triple glazing was identified. Another study presented on the National Congress Fire Safety Engineering in 2013 by Brecht Debrouwere, was a research to the fire behaviour in low energy houses. It was found that the fire behaviour in this kind of dwellings is more extreme compared to conventional dwellings. One interesting conclusion was that the inner pressure in low energy houses might reach values in the order of hundreds of Pascal. From the perspective of the fire service this would mean that the observed trend will not continue as this magnitude of pressure will have a certain effect on the structural integrity of window panes. The findings of these studies have in consultation with Brandweer Nederland led to the research question as formulated in chapter two.

The first part of this report is theoretical in nature. In this part the research methodology is pointed out and the basics of pressure during a fire will be pointed out. In the second part of the report, simulations will be carried out to identify the fire behaviour in well insulated and airtight dwellings and in the third part these results will be validated by conducting experiments and the results are described.

This study has been realized in cooperation with Stichting Fellowship FSE WO^2 and Brandweer Nederland. In addition, several people have contributed to this research. I would take this opportunity to thank the supervisors Prof. Brouwers, Ir. Van Herpen, Ir. De Korte and Dr. Weewer for their support during the graduation process.

Moreover I want to thank the Fire Department Twente, and in particular Folkert van der Ploeg for the pleasant cooperation, practical guidance and the possibilities that were offered to conduct the experiments on TroNed (Trainings- en Oefencentrum brandweer Oost-Nederland). This made it possible to investigate the pressure build-up during a fire in a well insulated dwelling on real scale, and was therefore essential for my research. The materials for the experiments are sponsored by Mr. Cleef of Rockwool. I want to thank for your contribution to this research. Additionally I would like to thank Sylvia Brandenburg, Martin Harbers and Ronald Huizinga of Nieman Raadgevende Ingenieurs for the support during the Voltra analysis as the preparation for the real scale fire experiments and their support with the blowerdoor test. Finally I want to thank Dr. Regterschot from the Eindhoven University of Eindhoven for the contribution to the research. His view and critical comments has led to an improvement of the quality in general and in particular the statistical part of the study.

Vincent van den Brink

Eindhoven, 21 April 2015

Table of contents

Summary viii

Terminology ix

Nomenclature xii

1. Introduction 1

2. Methodology 2

3. Theoretical background of pressure differences in dwellings 5

3.1 Cause of pressure differences 5

3.2 Modern dwellings 9

3.3 Closure 9

4. Computational approach 11

4.1 Input parameters 11

4.2 Results 14

4.3 Probabilistic scenario analysis 16

4.4 Connection with practical situations 19

4.5 Discussion 21

4.6 Conclusion 22

5. Experimental approach 25

5.1 Work plan 25

5.2 Method 27

5.3 Experimental results 30

5.4 Discussion 34

5.5 Conclusion 42

6. Discussion 45

7. Conclusion 47

8. Recommendations 49

References

Appendices

Appendix 1: Classification air tightness 56

Appendix 2: Input Ozone Chapter 4 “Computational Approach” 57

Appendix 3: Alternative approach iterative calculation process 62

Appendix 4: Uncertainties in simulations 64

Appendix 5: Parameter study – Results 66

Appendix 6: Results probabilistic scenario analysis 72

Appendix 7: Multiple linear regression model 74

Appendix 8: Calculation insulation covering for experimental enclosure 75

Appendix 9: Results blowerdoor test 77

Appendix 10: Simulation experimental scenarios 79

Appendix 11: Fuel calculation experiments 83

Appendix 12: Analysis moment of deflection of the temperature curves on the basis of the slope of the line 86

Appendix 13: Overview fitted simulation models 87

Appendix 14: Mass loss rate free burning rate 88

Appendix 15: Stepwise increase RHR in 20 s. 89

Appendix 16: Temperature behaviour scenario 3 and 4 91

Summary

During their daily activities the fire service observed that there is a trend that glass fallout occurs at a later stage of the fire. The extended period of time before the window pane fallout has major implications for the fire behaviour, and therefore also the strategy of the fire service. As a result, it is expected that the fire service will face more ventilated controlled fires in the near future, which result in a faster increase of the temperature, the production of more toxic gases whereby the survivability for the occupant decrease dramatically. The occurrence of a quick increase of the Rate of heat Release (RHR), backdraft, smoke gas explosion or a sudden window pane failure as a result of high pressures might result in more casualties among fire fighters. The Dutch building code will prescribe that in the year 2020 all buildings must be energy neutral. An insight in the consequences for the safety of the occupant and fire service is therefore essential.

In this research, a study to the influence of the building skin on the fire behaviour, and in particular the pressure increase during fire in well insulated and airtight dwellings, is carried out. This makes it possible to make statements about the safety of the occupant and the fire service during suppressive actions in modern dwellings.

The literature study identified that the pressure build-up mainly depends on thermal expansion. The thermal expansion is determined by six concrete variables which are the Rate of Heat Release (RHR), amount of infiltration ($q_{v;10}$ value), volume of the room, mechanical ventilation, type of enclosure and the R_c- value of the enclosure. The $q_{v;10}$ value, size of the compartment and the RHR have the largest influence on the pressure behaviour.

It appeared that on the basis of the simulation programme Ozone, it is difficult to give an insight in the fire and pressure behaviour of well insulated and airtight dwellings as a flow exponent of $n \neq 0.5$ cannot be applied. The magnitude of the air flow is calculated at a fixed pressure difference of 10 Pa and an oxygen dependent combustion model is lacking. With regard to the first two aspects an iterative calculation tool is developed to make a closer approach for the pressure behaviour. However, it appeared that this results in an underestimation of the pressure.

For the simulated scenario in an enclosure of 4.0 x 5.0 x 2.6 m (l x w x h), this results in a pressure peak of 64 Pa. As a result of the stochastic deviation of the variables and a lack of knowledge about practical situations, it can be expected that the pressure peak of 64 Pa will be exceeded. A multiple linear regression model is used to develop an equation to predict the pressure peak within a range of the variables of +/- 50% with regard to that scenario in practical situations.

The results of the conducted experiments show that that high pressures in the order of hundreds of Pa can occur during fires in passive dwellings. But also for well insulated dwellings significant higher pressures are observed. In the situation in which the amount of infiltration is doubled with regard to the maximum amount of infiltration according the passive house standard, still a pressure peak is 173 Pa observed.

Although in theory a ventilation controlled fire can be expected in modern dwellings, in practice the fire and pressure behaviour will be determined by coincidental factors like opened door and windows. Therefore, the fire service can expect a wide range of scenarios. The pressure peak will occur before arrival of the fire service at the fire scene and will therefore have no direct influence on the safety of the fire service.

The high pressures will have an influence on the safety of the occupant as the pressure peak will occur during the fire growth stage. This may prevent the occupant to escape the dwelling as it will be difficult or even impossible to open inward turning doors. In combination with the strong temperature increase this will lead to fatal circumstances within a minute.

Terminology

Adiabatic	A process is adiabatic when there is no heat exchange with the environment.
Backdraft	A phase transition whereby a sudden supply of oxygen into an enclosure with depleted oxygen supply leads to a rapidly and sudden combustion of the gaseous combustion products.
CFAST	A two zone mathematical model which evaluate the distribution of smoke, fire gases en temperatures throughout compartments of a building during fire.
Computational Fluid dynamics (CFD)	Advanced computer models in general which describes on the basis of a certain mesh (local) flows, velocity, temperatures and concentration of fluids and gases. Allows solving problems which cannot be solved analytically.
Deterministic model	Model which present its output as a single value. No variation limits are given, and so no uncertainty is taken into account.
Equivalent surface	One single opening which corresponds to the sum of all infiltration openings.
External validity	Relationship between the scientific model and real situations; To which extent predicts the research design real world conditions.
Fire Dynamics Simulator (FDS)	An open source Large Eddy Simulation CFD model, which numerically solves equations which describes low speed flows with the emphasis on heat and smoke transport during fires.
Fire Safety Engineering	A scientific and project specific approach to create a certain level of building safety based on the application of engineering principles.
Flashover	A rapid phase transition whereby the hot gases within the compartment set the entire compartment on fire in a short period of time by convection or radiation.
Fuel controlled fire	Fire scenario in which enough oxygen is present for combustion. The existence of the fire depends on the amount of fuel present in the fire room.
Internal validity	The extent to which the reasoning in the research is carried out correctly; Is measured what was intended to be measured.
Laboratory conditions	The extent to which the researcher can control the environmental factors of the experiment.
Local fire	Situation whereby the fire is limited to its initial object or surrounding objects; only a part of the compartment is burning.

Mass loss rate	The mass released per second from a material during fire.
Model	A combination of several hypotheses with regard to the distribution and consistency between the variables.
Neutral plane	Horizontal plane in the fire room with an equal pressure as the ambient pressure
One zone model	A zone model in which the assumption of a uniform temperature in the fire room is made.
Ozone	A two zone mathematical model which evaluate the temperature development in a single compartment during a fire.
Passive house	Building concept which emphasizes the use of little energy in order to relieve the environment with respect to the carbon dioxide release. This is achieved by applying small, properly orientated windows, high R_c-values and a high degree of air-tightness.
$q_{v;10}$	Volume of the air flow through the building envelope measured at a pressure difference of 10 Pa.; A term for the degree of air-tightness of a building.
Rate of Heat Release (RHR)	The heat released per second from a material during fire.
R_c***- value***	Thermal resistance of the building envelope; The resistance of a structure against heat transition.
Risk	The multiplication of the probability that an unwanted event occurs with the consequences.
Stoichiometry	A situation in which the molar ratio is such that there is enough oxygen for complete combustion.
Thermal thick	In a thermal thick structure, accumulation takes place when the temperature within the enclosure increases. When the temperature within the enclosure decreases, the heat will be dissipated.
Thermal thin	In a thermal thin structure no accumulation of the heat can take place. In case of an uninsulated thermal thin structure the heat will be dissipated to its environment.
Two zone model	A zone model in which during the simulation a hot upper layer under the ceiling with an uniform temperature and a lower layer in which no smoke is present with an uniform temperature are distinguished. The layers are separated from each other by a neutral plane.
Validation	Determining the correctness of the applied model and to which extent the made assumptions are correct.

Ventilation controlled fire	Situation in which there is not sufficient oxygen for complete combustion. The Rate of Heat Release is then controlled by the amount of oxygen available in the fire room.
Verification	Determining to which extent the result of the model is correct.

Nomenclature

Symbol	*Description*	*Unit*
A	Area	m^2
A_e	Equivalent surface	m^2
A_n	Equivalent surface upper opening	m^2
A_u	Equivalent surface lower opening	m^2
c	Partial air leakage coefficient	$dm^3/s.m^1.Pa^n$
c_v	Specific heat	J/kg.K
C	Total air leakage coefficient	$dm^3/s.\ Pa^n$
C_p	Wind pressure coefficient	[-]
g	Gravitational constant	m/s^2
h	Height	m
h_n	Height above the neutral plane	m
h_u	Height below the neutral plane	m
H_c	Heat of combustion	[-]
k	Extinction absorption coefficient	[-]
l	Length	m
m	Mass	kg/m^3
m”	Corrected free burning rate	kg/s
m∞”	Free burning rate	kg/s
n	Flow exponent	[-]
n_m	Number of moles	[-]
N	Ventilation rate	[-]
p_1	Fire activation probability	[-]
p_{fi}	Probability of the occurrence of fire	[-]
$p_{f;fi}$	Probability of failure	[-]
p_t	Failure probability	[-]
P	Pressure	Pa
P_w	Wind pressure	Pa
ΔP_n	Pressure difference in the dwelling	Pa
ΔP_u	Atmospheric pressure	Pa
q	Volume flow per unit area	$m^3/s.m^2$
$\dot{Q}$	Rate of Heat Release	kW
r	Air flow resistance	m^{-4}
r_e	Air flow resistance exhaust branch	m^{-4}
r_i	Air flow resistance inlet branch	m^{-4}
r_l	Air flow resistance leakages	m^{-4}
R	Gas constant	J/mole.K
t	Time	s
T	Temperature	K

Symbol	*Description*	*Unit*
T_e	Temperature of the outflowing gases	K
T_g	Temperature inside the dwelling	K
v	Air current speed	m/s
v_a	Air current speed into enclosure	m/s
v_g	Air current speed out enclosure	m/s
V	Compartment volume	m^3
w	Width	m
	Greek symbols	
ß	Regression coefficient	[-]
λ	Thermal conductivity	W/m.K
χ	Combustion efficiency	[-]
ε	Error term	[-]
μ	Contraction coefficient (Bernoulli coefficient)	[-]
ρ	Density	kg/m^3
ρ_a	Air density outside the dwelling	kg/m^3
ρ_g	Air density inside the dwelling	kg/m^3

1. Introduction

For new buildings the energy performance coefficient (EPC) is further reduced to 0.4 per 1 January 2015. It is assumed that this will have positive consequences for the environment, as the decrease of the EPC will lead to less energy use throughout the lifetime of a building. Some building concept are already developed which also meet the requirements for the year 2020 as new buildings will be energy neutral. The active and passive house principle are examples of these concepts. However, little is known about the effects of fire in these well insulated and airtight buildings with regard to the safety of the occupants and emergency services.

On annual basis, approximately 4100 fires occur in residential buildings [1]. Nevertheless, there are no known cases of fire in these active and passive houses. This does not prevent that the fire service will be confronted with fires in these types of dwellings in future. The window pane fall out is an important event in dwelling fires as it determines the fire development. It is suspected that with an increase of the thermal properties of the glass the mechanical strength of the glass also increases. This is supported by field observations of the fire service. As a result, ventilation controlled fires become are expected to become more common.

This has major implications for the strategy of the fire service. The sudden failure of glass or opening a door can lead to a backdraft within a few seconds, which is very dangerous for the fire fighters. Until now, it was assumed that the window pane fall out was a result of a temperature difference over the window pane. However, several recent studies, of which one of them was presented during the 6th National Congress Fire Safety Engineering, suggests that as a result of the new building strategies the pane behaviour might be affected by the pressure build-up generated by the fire. Knowledge about this process is therefore essential to ensure safety for the occupant and safety during suppressive actions of the fire service in modern dwellings. To this end, the following research question is formulated:

*"*To what extent has the building skin an influence on the fire and pressure behaviour in well insulated and airtight dwellings, and can statements be made about the safety of the occupant and the safety for the fire service during an intervention based on this behaviour?*"*

The goal of the study is to identify the expected fire scenario in well insulated and airtight dwellings and in particular, as a result of the fire scenario, the magnitude of the pressure increase during a fire. Therefore statements can be made about the safety of the occupant and fire service during the suppressive phase. This research will focus on modern dwellings in general in order to determine the range of the phenomenon. The passive house concept will be used as a guideline to make statements about well insulated and airtight dwellings. The requirements of passive houses are quantified and measured after the realization of the building and provides therefore a good starting point.

The scope of the research will be discussed in Chapter 2. In this chapter the research methodology is pointed out. Then, the basic physical aspects of air pressure during fire will be explained (Chapter 3). The relevant variables will be selected based on the conducted literature study. In the fourth chapter simulations will be carried out in order to define the fire scenario in a fictive dwelling with the use of the one zone model Ozone. To achieve this, a more realistic model for the airflow is developed. On the basis of this model a sensitivity analysis will be carried out and a degree of importance of the various parameters for the pressure build-up and a connection with practical situations will be obtained. These results will be validated by real scale experiments carried out at the Troned Safety Campus (Trainings- en Oefencentrum brandweer Oost-Nederland) in Enschede, and are described in the fifth chapter. Besides the validation of the simulated results, the aim of the experiments is to identify if the assumed high pressures also can be observed in practice. Finally, all results will be interpreted in the discussion and an overall conclusion will be drawn. Recommendations are made in Chapter 8.

2. Methodology

Problem field

As a result of political reasons and social trends about an increasing sustainable awareness, the energy consumption of buildings is severely reduced over the last two decades. As agreed in the Kyoto protocol in 1997 the energy consumption and the greenhouse gas emissions of the industrialized countries will be reduced. At national level, for the Dutch building industry this has lead to regulations in the building code. As a result of these regulations enshrined in the building code from 2012 and the goals of the government as described in *Koepelconvenant Energiebesparing Gebouwde Omgeving*, the energy demand of buildings will be only be the half in 2015 compared to buildings build in 2007 [2]. The goal for the year 2020 is that buildings are nearly energy neutral. There are already a few concepts to achieve this goal like passive and active building strategies. In these concepts, the goals regarding the energy aspect are achieved by applying sophisticated installations and more thermal insulation. A consequence of the last aspect is that buildings must be more airtight due to comfort, acoustics and health [3]. However, it can be expected that these changes in building envelopes affect the fire dynamics in buildings. Recent studies stated that a fire in a well insulated house will reach in three minutes fatal circumstances [4, 5, 6, 7, 8].

Beside this change, also other trends may contribute to changed fire dynamics. For example, different home geometries like open floor plans are more applied, new construction materials are used and new hollow construction elements are introduced. Another important factor that may affects the fire dynamics in dwellings is the interior. The use of more synthetic materials for the interior leads to an increase of the fire load in dwellings [5]. The result is a strong decrease in available egress time in case of fire. Was the time before a flashover occur a few decades ago 30 minutes, nowadays as a result of a modern interior, this time is expected to be only 5 minutes [5].

In the period from 2008 until 2011, in the Netherlands unfortunately 282 people lost their lives as a result of a fire. As many as 132 people lost their lives due to dwelling fires (suicide cases are excluded) [9]. With a share of 47%, dwelling fires are the main cause of casualties during fire. Although this number remains constant since the year 2009 up to 2012, it can be expected that in the future the amount of casualties will rise due to the changing fire dynamics in dwellings and aging of the population. The age group of 60+ is already the group with the most casualties as they need more time to leave the dwelling [9,10]. An insight in the fire behaviour in well insulated and airtight dwellings is therefore essential.

Until now, the Dutch fire service assumed that the increase of temperature will lead to a flashover. The steady temperature increase provides time for the occupant to leave the dwelling and it provides the fire fighters time to reach the fire scene. It is expected that during the temperature increase window panes fall out as a result of internal material stresses, particularly during the flashover when a rapid temperature rise occur. Glass breakage is an important event because it has a major influence on the fire dynamics. Before breaking, the pane acts as a barrier while it acts as a vent opening after the pane fall out. This allows the fire to grow but also to preventing to the hot smoke and gas to accumulate. A part of the heat is also removed. Therefore glass breakage is expected to be a critical stage in the fire development. However, observations of the fire service shows a trend that glass fall out occurs in a later stage of the fire. This research is a response to the field observations of the Dutch fire service and has led to the formulation of the research question.

Problem statement

The performance of the building skin is improved over the last years and will be further improved in the next few years. It is expected that this affects the fire behaviour and results in a ventilated controlled fire scenario whereby the temperatures in the building will increase rapidly and the pyrolyzing objects produce more toxic gases whereby the chance of surviving decrease dramatically,

especially in dwellings. The trend is also dangerous for the fire service. A sudden supply of oxygen to a ventilated controlled fire can result in a backdraft or smoke gas explosion and therefore cause casualties. Therefore, the improved performance of the building skin has major implications for the strategy of the fire service and it constitutes a risk for both the occupant and fire fighters. So knowledge about the fire dynamics and the different variables of glass breakage is important for strategic choices of the fire service and the safety of the occupant and fire service. Until now it was assumed that internal material stresses as a result of thermal differences within a window pane is the main cause for fall out. However, recent research shows that for well insulated dwellings the increasing inner pressure may become an important factor for determining the moment of window pane fall out. More knowledge about the fire and pressure behaviour in well insulated and airtight dwellings is therefore required.

Research objective

The objective of the research is to contribute to the safety of the dwelling occupant and the fire service during suppressive actions in case of fires in well insulated dwellings. The goal is to identify the influence of the building skin on the expected fire and pressure behaviour in well insulated and airtight dwellings by taking all possible fire scenarios into account. Recommendations for the strategy of fire suppression will be provided.

Theoretical model

The theoretical model (Figure 1) describes the different factors that are involved in order to be able to give an answer on the research question. Moreover, the model defines the scope of the research. The figure shows that the fire safety in dwellings depends on the fire scenario as each scenario has its own type of hazards. However, the fire scenario determines whether the window pane will withstand the fire. This is essential for the pressure build-up in the dwelling and determines the safety during the suppressive phase. However, the fire scenario, window pane behaviour and the pressure build-up are interrelated. This is visualised by the arrows.

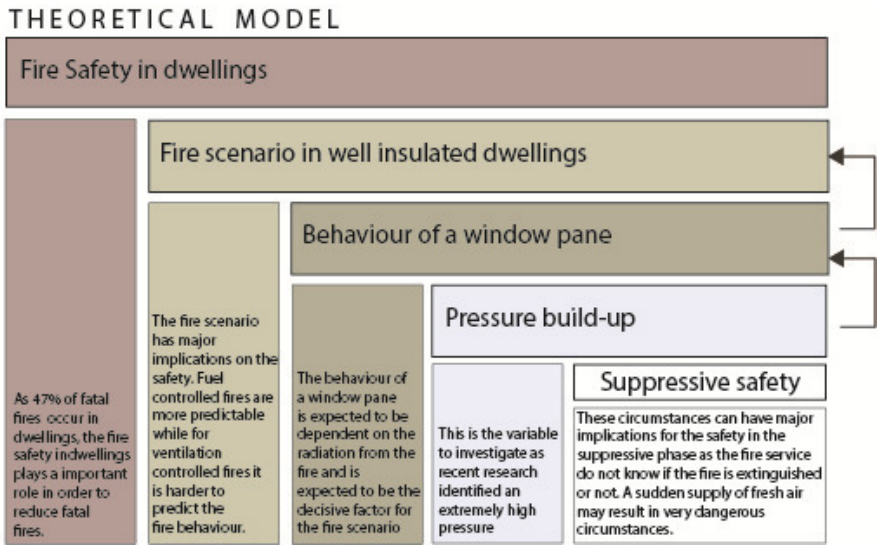

Figure 1 Theoretical model

Research model

The used research model in this study is shown below (Figure 2). In the upper part the research the research method is determined. As preparation for this research a literature study is carried out in a separate report in the field of the pane behaviour, fire dynamics and pressure behaviour.

During the experimental phase of the research, simulations in the field of the fire behaviour will be conducted. This data will be used to carry out a parameter study. In this way the sensitivity

and the standard deviation of the parameters can be determined. In order to validate the simulations real scale experiments will be carried out.

These results will then be analysed with regard to the influence of the pressure build-up on the safety of the occupant and the fire service. Then, it can be determined what the influence is on the safety, and statements about the reliability of the results can be made. This will result in a judgement about the fire dynamics in modern dwellings and a judgement about the influence of well insulated and airtight dwellings on the safety of the fire service and occupant.

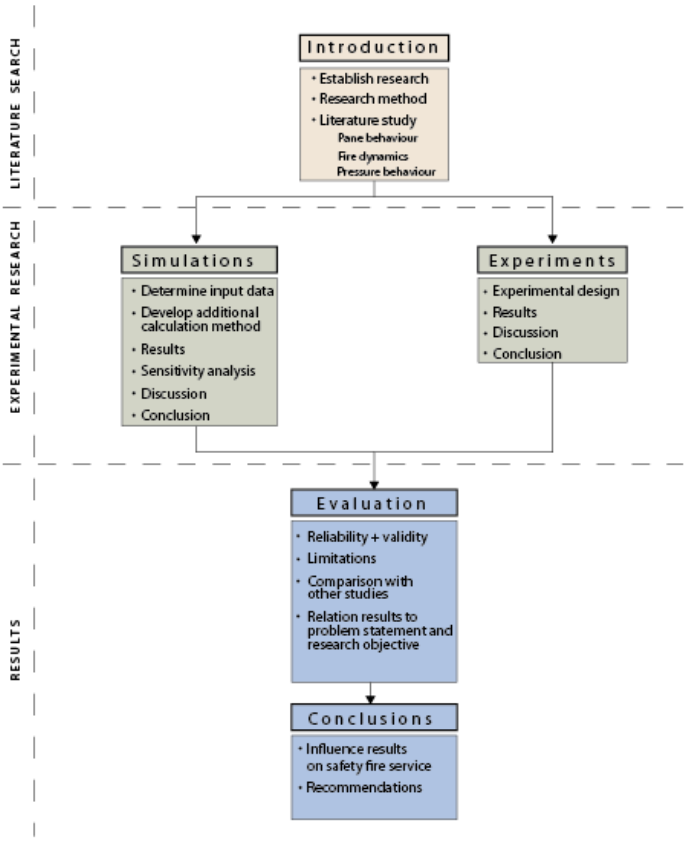

Figure 2 Research model

Research question

To what extent has the building skin an influence on the fire and pressure behaviour in well insulated and airtight dwellings, and can statements be made about the safety of the occupant and the safety for the fire service during an intervention based on this behaviour?

Sub questions

- What is the expected fire behaviour and quantity of the pressure build-up during a fire in well insulated and airtight dwellings?

- Which variables contribute mainly to the pressure build-up in well insulated and airtight dwellings during fire?

- To what extent has the pressure build-up an influence on the fire scenario?

- To what extent it is possible to simulate the fire and pressure behaviour in well insulated and airtight dwellings using the fire simulation model Ozone?

3. Theoretical background of pressure differences in dwellings

3.1 Cause of pressure differences in dwellings

The inner pressure in dwellings depends on different factors [11, 12]. A first distinction can be made by normal pressures, which are always present, and pressure that are generated in case of fire. In this paragraph, a brief overview of the pressure determining variables is given. In order to make estimations for the magnitude of the variable, equations are provided.

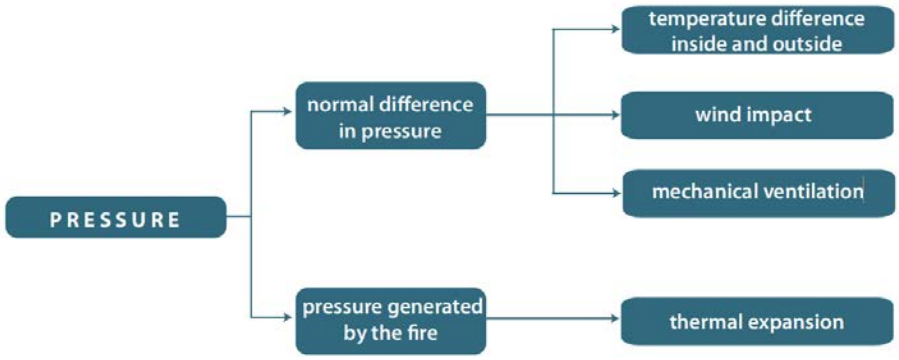

Figure 3 Aspects of the pressure in dwellings

Temperature difference inside and outside

In most cases the inner pressure inside a dwellings is higher compared to the environment. This difference is caused by the fact that in general the temperature in dwellings is higher than the surrounding. As the air heats up, it will expand which cause the pressure difference with respect to outside. As the pressure strives towards an equilibrium with its surrounding, the air will start to flow. The inflow will take place by the lower opening (Figure 4).

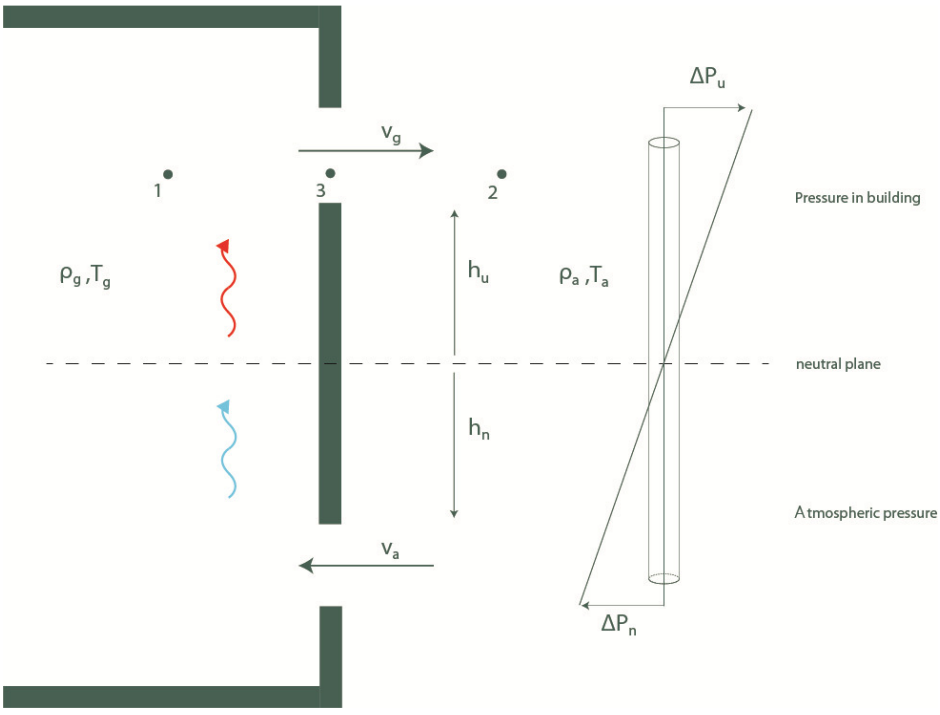

Figure 4 Pressure difference between inside and outside a building caused by temperature difference [12]

As hot air rises the air will flow out at higher openings. If the openings are large or if the pressure differences are small, the airflow can take place through one opening whereby the air intake takes place in the lower part of the opening and the air is flowing out at the upper part of the opening. When the inner pressure is higher or openings are smaller, the air will flow via the lower opening into the room and via the upper opening the air is flowing out of the room. The relation between pressure, flow and the velocity is described by the Bernoulli equation. A derivative of the Bernoulli equation can be used for the hydrostatic pressure between the upper and lower part:

Bernoulli's equation:

$$P_n + \rho_n g h_n + \frac{\rho_n v_n^2}{2} = \qquad P_u + \rho_u g h_u + \frac{\rho_u v_u^2}{2} \tag{1}$$

On the basis of this equation, the equations for the hydrostatic pressure difference between the points 1 and 2, and the hydrodynamic pressure difference between point 1 and point 3 and the velocity of the air flowing through the upper opening can be obtained [12].

Hydrostatic pressure between point 1 and 2:

$$\Delta P_u = h_u * g * (\rho_a - \rho_g) \tag{2}$$

Hydrodynamic pressure between point 1 and 3:

$$\Delta P_u = \frac{1}{2} P_g * v_g^2 \tag{3}$$

Air flow velocity through the upper opening:

$$v_g = \sqrt{\frac{2 h_u g (\rho_a - \rho_g)}{\rho_g}} \tag{4}$$

Similar, the equations for the lower opening can be obtained. When Equation (4) is equalised with the equation for the air velocity, the position of the neutral plane in relation with the surface of the openings can be determined with the equation below. This can be in terms of air density or temperature. Under normal circumstance it is assumed that the pressure difference over one, or a few storeys is that low that it can be neglected.

Position neutral plane:

$$\frac{h_n}{h_u} = \left(\frac{A_u}{A_n}\right)^2 * \frac{\rho_a}{\rho_g} \quad \text{or} \quad \frac{h_n}{h_u} = \left(\frac{A_u}{A_n}\right)^2 * \frac{T_a}{T_g} \tag{5}$$

Wind impact

The wind speed can have a significant influence on the on how gases flows within a building during a fire [11, 12]. In practice, it can be observed that no smoke and gases escape from the building at the façade were the wind is blowing on. An indication of the distribution of pressures around a dwelling is depicted in Figures 5 and 6.

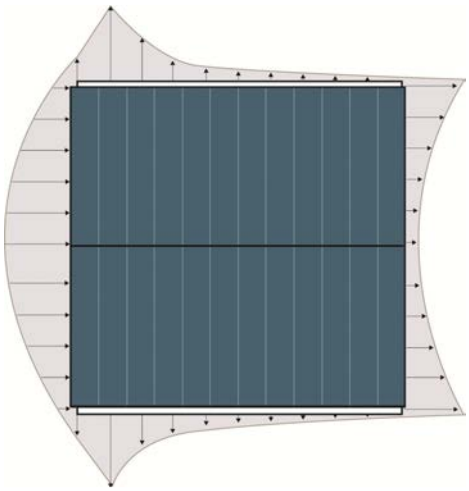

Figure 5 Top view distribution of pressure [12]

The magnitude of the pressure at the wind side can be approximated with Equation (6) [12]. For the magnitude of the negatives pressures at the leeward side, it can be generally stated that these are the half of the positive pressure.

$$P_w = C_P * 0.5 * \rho * v^2 \quad (6)$$

The distribution of the forces above the building depends on the shape of the roof [12] and is expressed in the factor C_p. The shape of the roof determines whether the pressure will be positive or negative. In Figure 6 the distribution of the forces with respect to the roof shape are depicted.

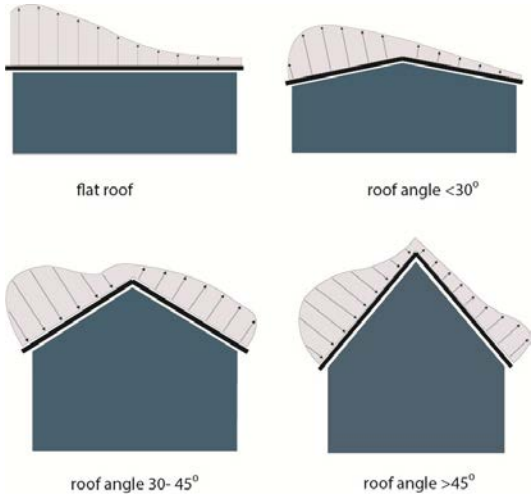

Figure 6 Distribution of pressure in relation to roof shape [12]

When a flat roof, or a roof with an angle of < 30^0 is applied, a negative pressures over the entire roof will occur. When the roof has an angle between 30^0 and 45^0 a positive pressure arise at the wind side and negative pressure arises at the leeward side. The same counts for roof angles larger than 45^0. In this case the pressures are larger compared to roofs with an angle between 30^0 and 45^0. Gable roofs are an exception. These roofs can be exposed to a negative pressure over the entire roof if the wind is blowing parallel to the ridge. The angle of the roof does not matter in this situation.

For the velocity of the wind, there is an important correlation with the surrounding. The surrounding buildings will affect the wind speed and causes turbulent flows. The surrounding built environment have a significant influence on the flows inside a dwelling.

Mechanical ventilation

Ventilation systems are based on pressure difference. This pressure is created by fans that push or suck the air trough the air ducts, this dependents on the system. For passive dwellings the ventilation consists of a forced supply and forced exhaust of air. In these situations there is no influence of the ventilation system on the inner pressure.

In case of a natural supply and a forced exhaust of air, the airflow on the basis of a pressure difference of 1 Pa. can be calculated according the equation below [13]:

$$q_v = C * (\Delta P)^n \quad (7)$$

Thermal expansion

Pressure as a result of thermal expansion is caused by the fact that air expands when it is heated up. The thermal pressure generated by the fire in a completely air tight enclosure can be calculated by Equation (8) [11]:

$$\frac{(P - P_a)}{P_a} = \frac{\dot{Q}}{V * \rho_a * c_v * T_a} \quad (8)$$

In a completely closed room the pressure will increase rapidly and will reach very high values. In practise, these high values will never be reached. In addition, in Equation (7) there is no relation with the availability of air for combustion inside the enclosure. In a completely closed room the available air for combustion will decrease rapidly what will cause extinction of the fire. For an approximation of the pressure during a fire in a building, Equation (9) [12] can be used. This equation takes also the leakage of the compartment into account.

$$\Delta P = \frac{(\dot{Q} / C_v * T_e * A_e)^2}{2\rho_a} \quad (9)$$

In this equation, the pressure is mainly influenced by $\dot{Q}$ (the RHR) and the size of the openings. The other variables depends on material characteristics and can be determined from tables. This equation also do not take the oxygen volume into account. In case of a constant fire, the pressure will drop linearly over time.

In a calculation the assumption of an ideal gas can made. Then it is assumed that the molecules take up no space and do not attract or repel each other, except in case of collisions of the molecules. An ideal gas is a good assumption for diluted gases [14]. For an ideal gas the following equation applies:

$$P = \frac{n_m * R * T}{V} \quad (10)$$

The density of air is defined as mass per volume:

$$\rho = m / V \quad (11)$$

Temperature differences in case of fire

When gases are heated up and gets an higher temperature, the density of the gases become lower than the surrounding air. As a result the gases will rise upwards. This is the principle of thermal buoyancy. The generated pressure difference can be approximated with [12]:

$$\Delta P = (\rho_a - \rho_g)\, g * h \quad (12)$$

Or in terms of temperature:

$$\Delta P = 353\left(\frac{1}{T_a} - \frac{1}{T_g}\right) g * h \quad (13)$$

In Equations (12) and (13) the variable *h* represents the height of the hot smoke layer. In an ideal situations there is a strict separation between the upper and lower layer. However, the practice will be more complicated as flows will arise due to oxygen supplies by leakage areas for example.

3.2 Modern dwellings

As mentioned in the literature study [15], little research is done with regard to the pressure build up during fire in well insulated and airtight dwellings. However, in the field of the nuclear industry extensive research is done to investigate the pressure increase in confined enclosures in case of fire [16, 17, 18, 19]. Although the research focus on a single aspect, the involved variables can be roughly divided into three groups of parameters [16]:

- RHR
- (Thermal) properties of the compartment
- Ventilation network and air flow resistance

To which extent modern dwellings and passive dwellings can be compared with the situations described in the literature study depends on the characteristics of the dwelling. For passive dwellings the characteristics are quantified during the design phase but are also measured before the completion of the dwelling, and can therefore provides valuable information about practical situations. The concept can therefore be the basis for the parameter study whereby statements about modern dwellings in general can be abstracted by changing the values of the parameters. The passive house concept defines the boundary conditions for the (thermal) properties of the compartment and can be defined as follows [20, 21]:

- The annual primary energy demand is not more than 120 kWh/m^2 per year
- The annual heating demand for space heating is not more than 15 kWh/m^{2}per year
- The maximum infiltration rate is n = 0.6 h^{-1}. This can be translated into a $q_{v;10}$ value of 0.15 dm^3/s.m^2 (Appendix 1)
- The frequency of overheating (inner temperature of > 25 ^{0}C) is at most 10%

The boundary conditions for an ‘average’ dwelling are expected to lie between the passive dwellings and the minimum prescribed amount of insulation in the building code and will have a significant impact on the fire behaviour.

The passive house concept provides a guideline for this research as it will always meet the requirements of the third category and make therefore possible to make statements, in contradiction to modern buildings. For that reason, the passive house concept will be used as a starting point to make statements about the fire safety of modern dwellings. In order to make statements about well insulated and airtight dwellings, a risk based approach will be used in Chapter 4 “Computational approach”.

3.3 Closure

In a dwelling, there are always pressure differences as a result of the temperature difference between inside and outside the dwelling, wind impact and the mechanical ventilation. Although they may have an influence on the pressure build-up during fire, they are hard to simulate and are characterized by large deviations. However, it is expected that they will be subordinate to pressure differences which are generated by thermal expansion in case of fire. To that end, these factors are excluded and the research will focus only on the pressure differences generated by the fire. The provided equations in this chapter can be used as a guideline for the magnitude, and so the influence of these factors.

4. Computational approach

In this chapter a computational approach of the problem is made. The goal is to identify and visualize the fire scenario which can be expected during a fire in a well insulated and airtight dwelling, in order to predict the pressure difference within the enclosure. Although the focus is on the passive house standard, also less good insulated dwellings will be examined as it gives an indication of the pressure build-up in more common dwellings. The standards of the passive house concept provides quantified characteristics and are therefore a good starting point for the research. In this chapter, Ozone will be used to provide the simulations. In the first paragraph the input parameters, values and assumptions will be accounted and in the second paragraph the fire scenario will be determined. In the third paragraph the uncertainty will be considered and finally, a sensitivity analysis over the identified parameters from the literature study will be carried out and a connection with practical situations is made.

4.1 Input Parameters

Compartment

For the fire room an enclosure with the internal dimensions of 4.0 x 5.0 x 2.6 meter (w x l x h) is maintained. This enclosure is not representing a specific function and the size is chosen arbitrary. But the dimensions are chosen such that the enclosure could represent a bedroom or kitchen, the rooms in a dwelling wherein a fire mostly occurs [9]. In the model, the situation is assumed to be adiabatic in order to exclude the influence of the enclosure. The influence of the enclosure will be investigated in a later stage, in the sensitiveness analysis. The entire Ozone input and made assumptions can be found in Appendix 2.

Air-tightness of the compartment

Ozone assumes that the input geometry is completely air-tight. Therefore the infiltration must be defined by hand and must be entered as a constant opening in de Ozone model. Conform the passive house standard, the maximum amount of infiltration is 0.15 $dm^3/s.m^2$, at ΔP = 10 Pa. So the maximum infiltration in the fire room of 20 m^2 at a pressure difference of 10 Pa. must be 3.0 dm^3/s. However, the amount of infiltration of the passive standard applies only to the facades. As the fire room is a part of a larger dwelling, the inner walls will have a lower air tightness as the outer walls as they do not have to meet the requirements for the amount of infiltration.

However, this amount of infiltration can never be higher than the maximum infiltration on the basis of the $q_{v;10}$ value of the remaining area of the floor plan of the dwelling of 100 m^2 (Figure 7). It is determined that the maximum infiltration of the $q_{v;10}$ value of the remaining area of the floor plan is normative. With regard to the infiltration for the inner walls a value of
80 x 0.15 $dm^3/s.m^2$ = 12 dm^3/s will be maintained. The total infiltration of 15 dm^3/s must be entered in Ozone as an equivalent opening. This opening must be applied over the entire height of the compartment in order to affect the fire behaviour within the enclosure as little as possible.

Figure 7 Fire area in relation to total area of the dwelling of 100m^2

The equivalent opening in Ozone, due to air-infiltration, can be calculated according to Equation (14), with a pressure difference of 10 Pa:

$$A_{e;10} = \frac{q_{v;10}}{0.833 * \sqrt{10}} \quad (14)$$

However, when the pressure difference is significantly higher it make sense that a higher inner pressure leads to a larger air flow through the slit whereby these deviations become too large to ignore. Therefore, for this specific situation a correction must be applied. Equations (15) and (16) [22] are the basic equations needed for the correction:

$$A_{e;p} = \frac{C * \sqrt{\rho}}{1000 * 2^n} \quad (15)$$

$$q_{v;p} = \sum C * (\Delta p)^n \quad (16)$$

The amount of infiltration is a building characteristic, which can be translated into a equivalent surface of the slit. In the model, the size of the slit must be based on the maximum pressure difference. As the pressure peak is not known in advance, an iterative calculation must be carried out to adapt the slit on the maximum pressure difference. As openings can only be inserted in Ozone as time dependent or temperature dependent, an alternative method must be created to adjust the slit on the occurring inner pressure. This iterative calculation process is depicted in Figure 8.

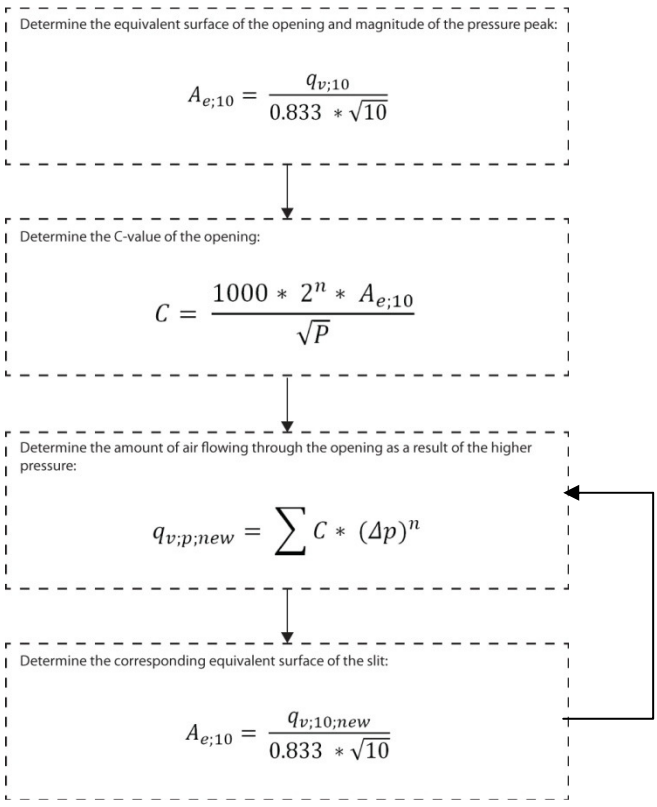

Figure 8 Iterative calculation process for adapting the equivalent surface of the slit on higher pressure differences as input for Ozone

In the first step the amount of infiltration is translated into an equivalent surface for Ozone. With Equation (15) the C- value of this slit is determined. Then the magnitude of the airflow a result of the

higher pressure can be calculated with Equation (16). In the last step, this airflow must be translated back into an equivalent surface of the slit which can be entered in Ozone.

By calculating the equivalent surface for a number of pressure intervals, the slit can be adjusted on the outcome of the pressure peak of Ozone.

With regard to determining the C- value a remark must be placed. When the size of the equivalent opening is changed, this value will also change. In order to simplify the approximation, the amount of variables is limited to one. Therefore, the C- value is considered to be constant. In order to overcome this shortcoming and the shortcoming of the flow exponent n ≠ 0.5, also other simulation software like CONTAM is considered. However, there is no simulation software currently available which contains the possibility to apply a RHR curve as temperature input and an air infiltration model as well.

The calculation is adapting the equivalent surface of the slit on the pressure peak. The moment before and after the pressure peak occurs, the slit will therefore be too large in relation to the occurring pressure which results in an underestimation of the pressure curve in the Ozone model. The expected curve is indicated with the dashed line in Figure 9.

The magnitude of the pressure peak will depend on the pressure behaviour before the moment the pressure peak occurs. As a result, it can be expected that the magnitude of the pressure peak of is therefore also underestimated. Therefore, the peak pressure for the dashed line will be higher in practice.

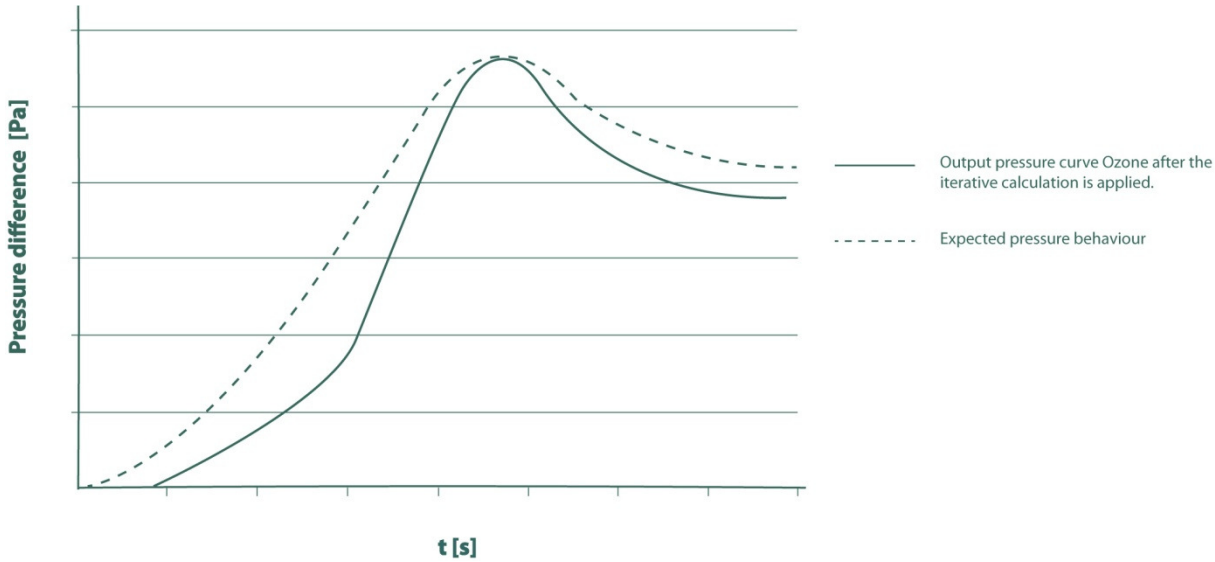

Figure 9 Model uncertainty: Effect of iterative calculation of the pressure behaviour

Also a variant for the iterative calculation process, whereby the size of the slit is linearly increased, is studied and described in Appendix 3.

Rate of Heat Release

The standard NEN-EN 1991-1-2/NB "*Loads on structures exposed to fire"* provides the required fire density. For the fire curves in dwellings a reference fire density of 250 kW/m^2, a variable fire load of 780 MJ/m^2 and a fire growth rate t_c = 300 curve is prescribed. However, research indicated that due to a changing fire load the fast growth curve (t_c = 150 curve) might fit the real situation better [23]. Therefore, for this study the t_c = 150 curve is maintained.

The combustion model of Ozone is turned off. Therefore, Ozone keeps the calculation running, even when the fire in practice will already be smothered. The moment that the fire extinguishes must be determined manually. Figure 10 gives an indication of the moment when the fire smothers or

extinguishes. This model is based on the current temperature and the oxygen volume in the fire room. If the oxygen volume is below a percentage at a given temperature it can be assumed the fire is out. The oxygen volume fraction can be determined with the oxygen mass volume given in the output of Ozone.

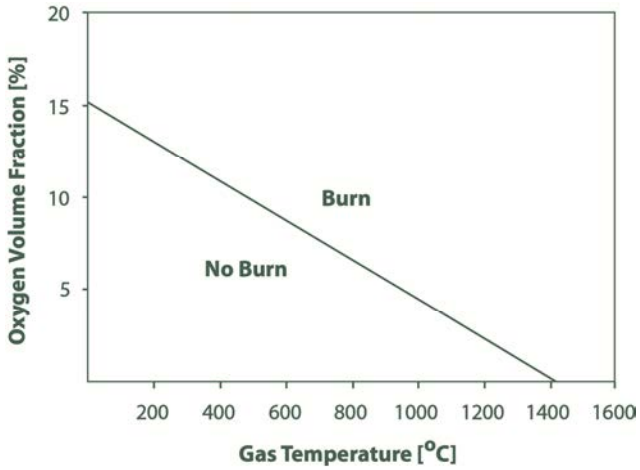

Figure 10 Model for determining moment that the fire will go out as a lack of oxygen or remain smouldering [24]

One zone model

Although a two zone model is specifically used for localized fires in a pre flashover, an one zone model is used for the simulations. This model is chosen because the fire is expected to be strongly ventilation controlled and produce therefore large amounts of unburned combustion products. In that case the height of the upper layer will increase rapidly whereby the lower layer will be very weak. Therefore an one zone model will approach the practical situation better.

4.2 Results

In this paragraph, the results of the simulation are presented. A brief description of the RHR, temperature, oxygen and pressure difference for this scenario is given. The simulated fire behaviour is the result of the input values as described in the previous paragraph.

Rate of Heat Release

The graph of the rate of heat release shows a quadratic curve. The maximum RHR of 0.644 MW is reached after 110 seconds. On the basis of the oxygen mass it can be determined that the fire has gone out or remain smouldering after that moment as a result of a shortage of oxygen.

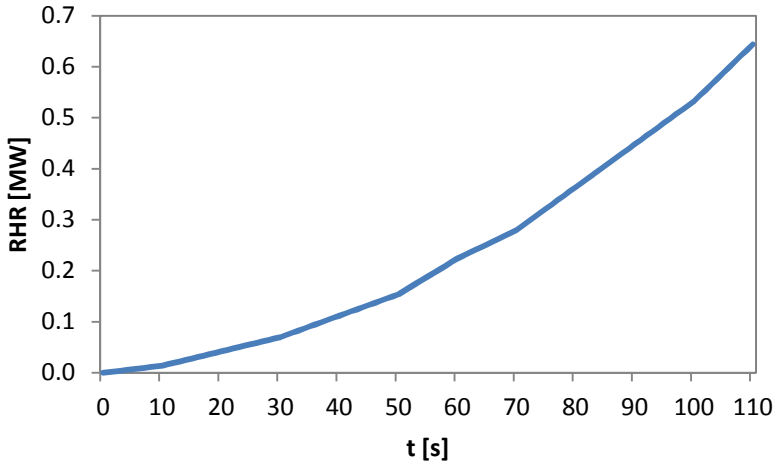

Figure 11 Rate of Heat Release curve

Temperature

During the burning period there is a temperature increase of 165 ^{0}C. In this period the temperature increases from 20 ^{0}C up 185 ^{0}C. It can be observed that a quadratic curve arise whereby the slope of the line declines but the line will be not become linear. On the basis of this graph it can be expected that the strongest pressure increase occurs between 20 s. and 80 s. as the pressure is caused by the expansion of air as a result of the heat.

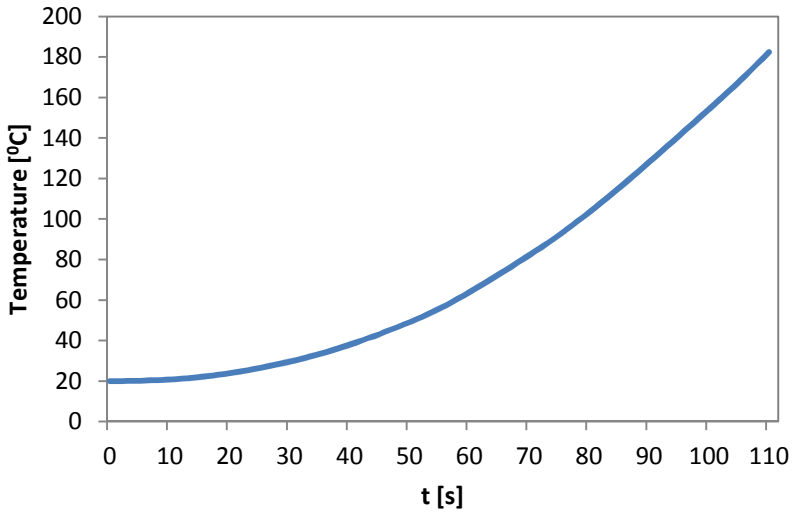

Figure 12 Temperature curve

Oxygen

The oxygen mass decrease from 14.221 kg to 8.998 kg after 110 s. of burning. As discussed in the last paragraph, the oxygen volume fraction can be determined since it is known that air contains 21% oxygen. Therefore it is easy to determine that after 110 s. the oxygen volume fraction is 13.27% at 185 ^{0}C. On the basis of Figure 10 it can then be assumed that the fire goes out as a result of a lack of oxygen or remain smouldering. On the basis of this calculation the simulation is stopped.

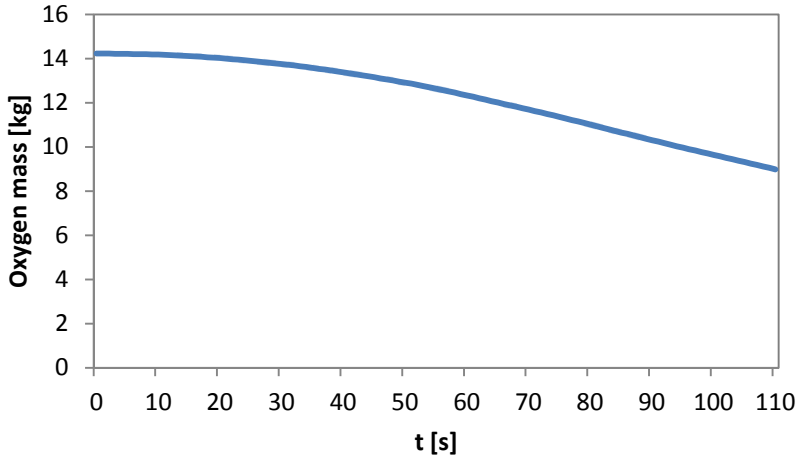

Figure 13 Oxygen mass

Pressure difference

It can be observed that the curve for the pressure difference (with respect to the normal atmospheric pressure of 101300 Pa) is characterised by a stepwise increase. During the first 14 s. after ignition the pressure difference is slightly negative with a minimum of -0.157 Pa. The strongest increase of the pressure can be found between 60 s. and 70 s. In this short period of time the

pressure increases with 20.6 Pa from 24.9 Pa up to 45.5 Pa. The absolute pressure peak can be found at 98 s. after ignition and has a value of 64 Pa.

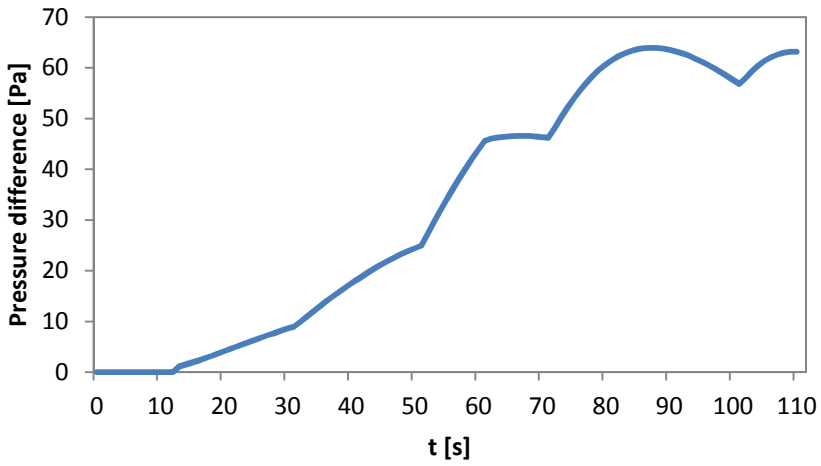

Figure 14 Pressure difference

4.3 Probabilistic scenario analysis

Ozone can be classified as a deterministic model [25]. The model is shown schematically in Figure 15. As a result, no uncertainties are taken into account. However, these uncertainties may have a significant influence on the results. The levels at which uncertainties are introduced is pointed out in Appendix 4.

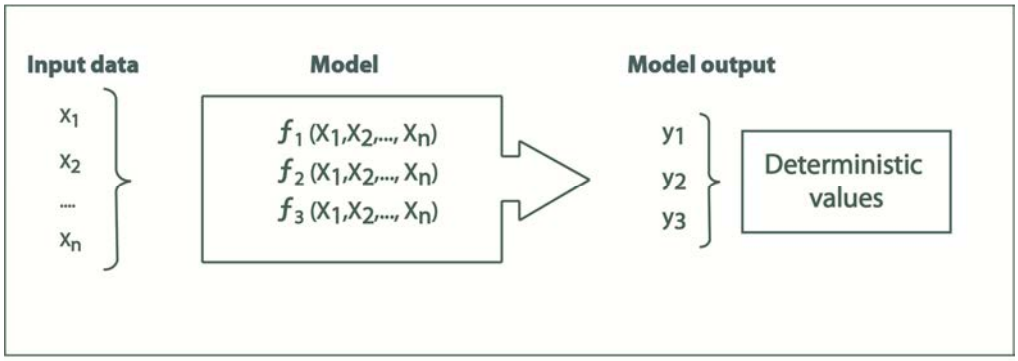

Figure 15 Schematic overview Ozone as time-dependent deterministic model [25]

To give an insight in the effects of the uncertainty on the pressure build-up and the dynamics of the parameters, first the influence of the separate variables on the magnitude of the pressure peak is analyzed. This is done by varying the size of the parameters RHR, $q_{v;10}$, volume of the room, mechanical ventilation, enclosure type, and the R_c- value of the enclosure in steps of 10% with a fixed value. For identifying the dynamics, the range of -50% up to 50% is taken into account. The input values and the resulting pressure curve for each variable can be found in Appendix 5.

In Figure 16 the sensitivity of the variables according to the pressure difference is summarized. With respect to the basic calculation, the RHR shows a difference of 13.6 Pa when the RHR is decreased with 50% . A decrease of the $q_{v;10}$ value results almost in a doubling of the pressure. When the $q_{v;10}$ value is halved, the pressure difference according the basic situation is 56.2 Pa. Increasing the volume of the room results in a pressure increase of 17.1 Pa. The influence of the variables mechanical ventilation and the enclosure type is much smaller. A decrease of the amount of ventilation results in a maximum pressure decrease of merely 2.2 Pa and the application of a timber frame construction results in a pressure increase of 4.0 Pa.

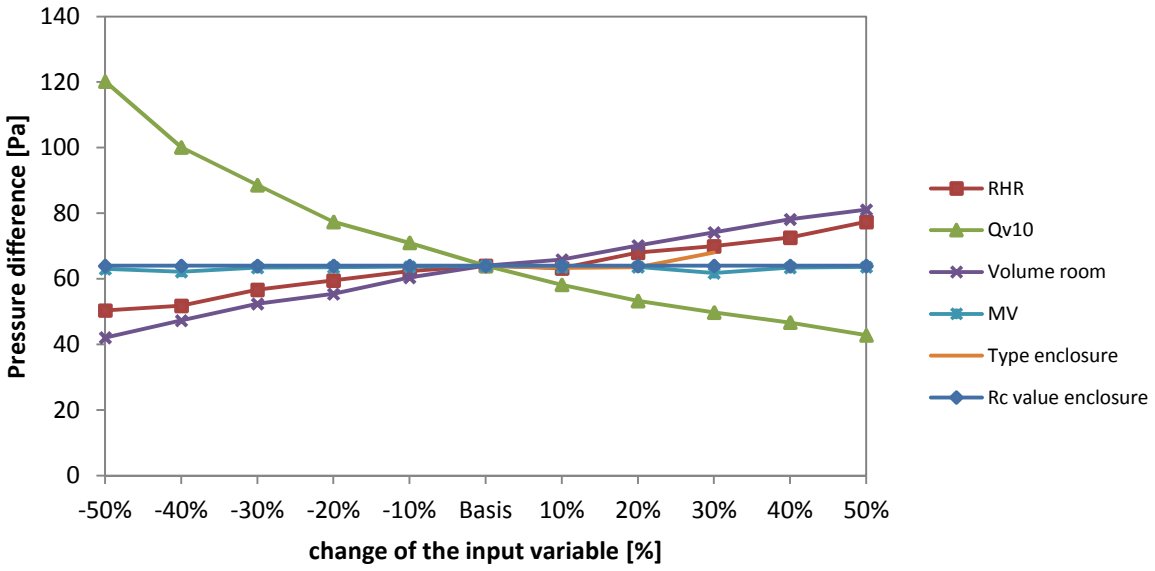

Figure 16 Sensitivity of pressure difference given the variation of the 6 different boundary conditions

Probabilistic scenario analysis

As a result of a natural variation of the stochastic variables (RHR, time constant, $q_{v;10}$ value, mechanical ventilation), the pressure peak of the scenario described in paragraph 4.2 will contain a certain deviation. As only a higher pressure peak, with respect to the defined pressure peak of 64 Pa., will influence the defined fire scenario, statements will be made about the exceedance probability. A probabilistic scenario analysis on the basis of the natural variation of the variables will be carried out. For the underlying theory of this approach is referred to [26] and [27].

Estimation of standard deviations

For the simulation in paragraph 3.2 the fast growth curve (t_c = 150) is applied. The adjacent growth curves that can be applied are t_c = 75 and t_c = 300. If the time constant will be faster than 112.5 s., the t_c = 75 curve will be applied. 112.5 Seconds is therefore the upper limit. In like manner the lower limit can be determined and is 225 s. Therefore, in practice the possible range for the time constant will be from 112.5 s. up to 225 s. The average is expected to be 150 s.

With regard to the mechanical ventilation the lower limit is defined at 80% (0.0144 m^3/s) of the average capacity of 0.018 dm^3/s, and the upper limit is defined at 150% (0.027 m^3/s) of the average as a lower capacity is be seen as a larger shortcoming compared to a higher ventilation rate.

With regard to the infiltration rate, it is assumed that a $q_{v;10}$ value of 0.15 is the average. The maximum infiltration rate is (0.16 $dm^3/s.m^2$) and the minimum infiltration rate is defined at the half of this standard (0.075 $dm^3/s.m^2$).

With regard to the RHR, the fast growth curve is expected to be the upper limit, and the lower limit is defined by halving this RHR.

Empirical data for these variables is lacking. Although the classifications above are rough estimations, it will give an indication about the magnitude of the pressure peak in practice and the influence of each variable on this scenario.

The results show that the possibility that the pressure peak of 64 Pa for that particular scenario as a result of the uncertainty will be exceeded is large. This probability is depicted in Figure 17. In Table 1 the results for the sensitivity analysis can be seen. For a complete overview of the results is referred to Appendix 6. Due to the rough estimation of the boundary limits for each variable, a standard deviation of 31 Pa. in relation to a pressure peak of 64 Pa is present. This implies that more knowledge about practical situations is required to make reliable estimations for that particular scenario.

Table 1 Overview sensitivity analysis

	variant study / boundary conditions		deterministic		sensitivity analysis				probability distribution		
			avarage x	pressure peak Pa	variation V	st. deviation s	variant x + dx	pressure peak Pa	dt/dx	s·dt/dx	(s·dt/dx)²
RHR	rate of heat release	MW	0.64	64	0.5	0.32	0.96	90	81.25	26	676
t_c	time constant	s	150	64	0.4	60	210	48	-0.2666667	-16	256
mv	mechanical ventilation	dm^3/s	18	64	0.38	6.84	24.84	65	0.1461988	1	1
$q_{v;10}$	infiltration	dm^3/s	15	64	0.45	6.75	21.75	59	-0.7407407	-5	25
										variance (P)=	958
										s (P)=	30.951575

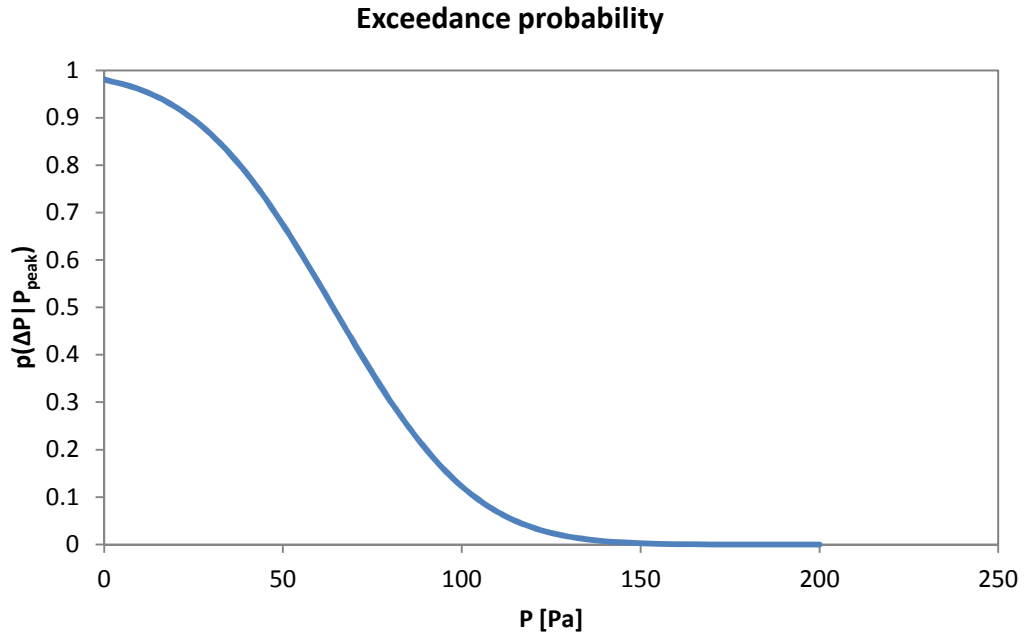

Figure 17 Exceedance probability

To make statements whether the exceedance probability for ΔP_{max} is acceptable or too large, a value must be determined for the maximum accepted exceedance. This can be defined according Equation (17) [27]. For the underlying theory is referred to 'Normalisatie fysisch brandmodel; Statistische en probabilistische aspecten' [27], Paragraph 3.1.

$$P_{f;fi} \leq \frac{P_t}{P_{fi}} \tag{17}$$

The calculation value for the occurrence of fire (P_{fi}) can be defined with Equation (18). For this scenario, the calculation value for the occurrence of fire is only determined by the activation probability of the fire and the area of the compartment. The normative event is expected to be a local fire. Therefore, no reduction factors for fire safety measures will be applied. According the literature, a standard fire activation probability (P_1) of $4E^{-7}$ per m^2 can be maintained [27]. To consider a worst case scenario, a very high fire activation probability is assumed and so an activation probability of $4E^{-5}$ per m^2 is applied.

$$P_{fi} = p_1 * \prod_i (P_i) * A_{fi} * n \tag{18}$$

The probability for the occurrence of a fire will therefore be $P_{f\,i} = 4E^{-5} * \frac{100}{25} = 1.6E^{-4}$.

As for this purpose no maximum values for the accepted probability of failure (P_t) are mentioned in the Dutch building regulations, a connection is made with the safety requirements for building structures, which are defined in the Dutch building code. As a risk based approach is not common in the Dutch building regulations, this is the only possible reference with regard to failure probabilities and so the minimum required safety level. The Eurocode EN 1990, annex B [27] describes that for a residential building (Construction Class 2) the acceptable probability of failure (P_t) for the building structure is $7{,}23E^{-5}$. This corresponds to a fixed reliability index of ß ≥ 3.8. As the reliability index for this scenario will also depend on the risk of fire, the reliability index can be defined as follows [27]:

$$ß_{fi;t} = Ø^{-1}\left(\frac{P_t}{P_{fi}}\right) \quad (19)$$

As can be found in appendix 6, the limit value for a dwelling in the CC2 class, with a probability of the occurrence of fire of $4E^{-5}$, is 0.12. This line is drawn in Figure 18. As can be seen in Figure 18, the intersection between the lines is at 70 Pa, which according to Figure 17 corresponds to an exceedance probability of 0.45. Therefore the exceedance probability is higher than the accepted failure probability according the safety level of the Dutch building regulations. Therefore, it can be concluded that the failure probability for this scenario, or in this case the uncertainty for the pressure peak for this scenario, is too large with regard to the desired certainty in the Dutch building regulations.

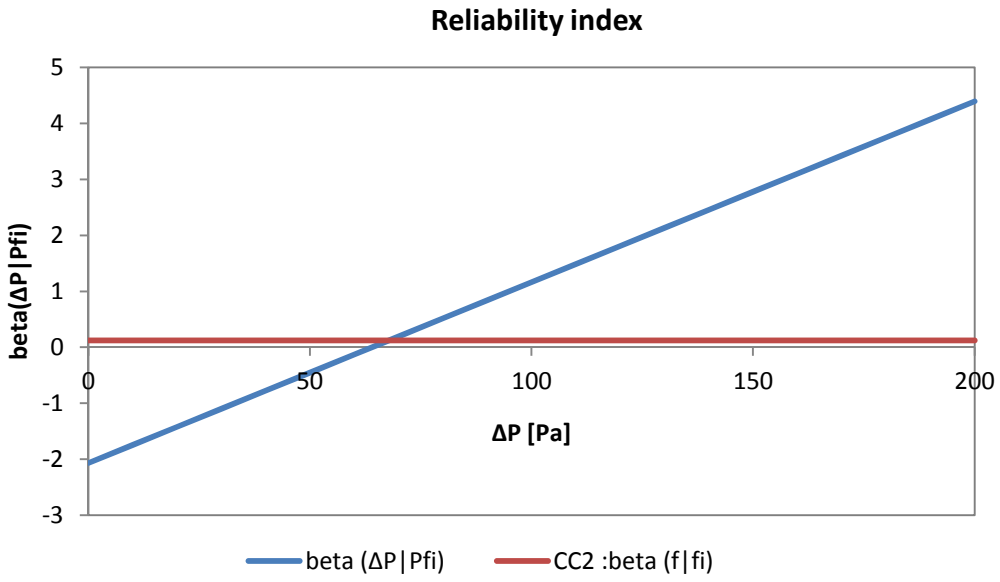

Figure 18 Reliability index

4.4 Connection with practical situations

To give an indication of the pressure peak in a simple manner for practical situations, a linear regression model is developed on the basis of Figure 16. To make the equation applicable for practical situations, the amount of involved variables must be reduced. This reduction in variables is achieved by assuming that 80% of the problems is caused by 20% of the most important causes, and is called a Pareto analysis.

The Pareto analysis can be worked out on the basis of the data which is generated for the pressure dynamics from Figure 16 and Table 5.1 in Appendix 5. The change of the parameters can also be defined as a percentage with respect to the basic situation (Table 5.2 in Appendix 5). On the basis of

these percentages, the cumulative proportion of each variable can be determined. Figure 19 shows the proportion of the variables which are classified ascending by size.

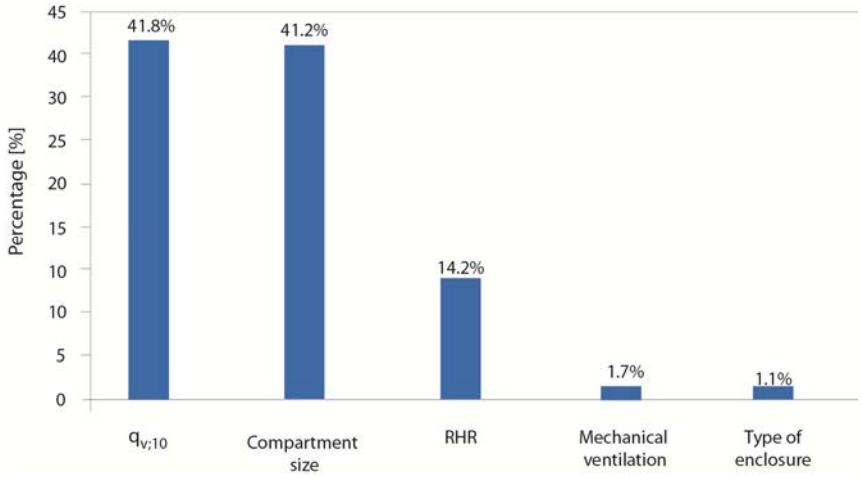

Figure 19 sensitivity of the variables as percentage

When both the $q_{v;10}$ value and the RHR are taken into account, the pressure difference can be explained for 56%. However, the $q_{v;10}$ value and the size of the room explain 83% of the pressure difference. When all three variables are taken into account 97.2% of the pressure difference can be explained. As the Pareto analysis assume that 20% of the causes explain 80% of the results, it is sufficient to focus on the $q_{v;10}$ value and the size of the room.

Because there are two variables (X_1 and X_2) which have a certain influence on another variable (Y), the manner of influence of X_1 and X_2 on Y can be described by multiple linear regression. Multiple linear regression is based on Equation (20) and will provide a linear curve which fits the data for the $q_{v;10}$ value and the compartment size as best as possible.

$$Y = \beta_0 + \beta_1 x_1 + \beta_2 x_2 + \varepsilon \tag{20}$$

Whereby $ß_0$ and $ß_i$ can be determined by :

$$\beta_i = \frac{n \sum X_i Y_i - \sum X_i \sum Y_i}{n \sum X_i^2 - (\sum X_i)^2} \quad (\text{with } n = 1; 2) \tag{21}$$

and

$$\beta_0 = \bar{Y} - b\,\bar{X} \tag{22}$$

The regression analysis identified that the influence of the $q_{v;10}$ value and the size of the compartment in relation to the occurring pressure peak can be described by Equation (23), whereby the $q_{v;10}$ value must be entered as the infiltration of the dwelling per m^2. The size of the fire room is entered in m^2 as in the building sector a compartment height of 2.6 m. is standard for newly build houses.

$$\Delta P_{max} = 102.83 + 1.737 * A_{fire\ room} - 471.52 * q_{v;10} \tag{23}$$

In this equation the floor area of the fire room must be entered in m^2, and the $q_{v;10}$ value in $dm^3/s.m^2$. Hereby it is assumed that the total floor area of the dwelling is 100 m^2.

To which extent this curve fits to the data from Table 2 is indicated by the adjusted least square coefficient (R^2_{adj}), this value is 0.887 and can be calculated on the basis of Equation (24). As this value is high, it means that the developed equation fits the data from Figure 16 very well. The fact that the R^2 - value and the R^2_{adj} in Appendix 7 are close to each other is caused by the small sample size. As the F- value of the results is 1.14E-09, statements can be made based on a 98% confidence level with regard to the data of Figure 16. An overview of the results can be found in Appendix 7.

$$R^2_{adj} = \frac{SS_{error}/(n-p)}{SS_{tot}/(n-1)} \quad (24)$$

In Figure 20 the iso pressure curves on the basis of Equation (23) depicted. In this figure the size of the fire room is plotted against the $q_{v;10}$ value and provides with regard to equation (23) a graphical insight in the peak pressures in relation to the combination of the two variables. The line shows which combinations lead to a certain pressure peak.

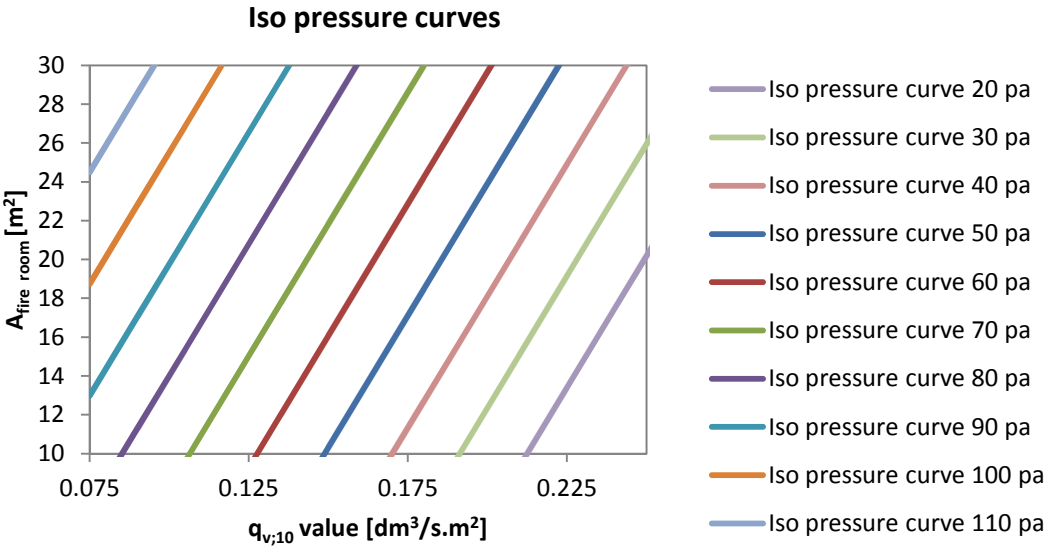

Figure 20 Iso map pressure curves

4.5 Discussion

For a room with the dimensions of 4.0 x 5.0 x 2.6 the results shows that the fire is expected to remain small with a RHR of only 0.644 MW and a peak temperature of 182 ^{0}C. A pressure peak of 64 Pa is simulated. This pressure peak is low compared to the results from other research. Although only a single scenario is simulated, it implies that large pressures differences in the order of hundreds of Pascal will not occur during dwelling fires. This seems to be caused by the approach of the higher infiltration rate for the inner walls, which is expected to be a more realistic approach for dwellings.

However, the lack of the possibility to apply a flow exponent of n ≠ 0.5, and the standard pressure difference of 10 Pa at which the outgoing airflow is calculated seems to be the most important obstruction for determining the pressure behaviour as the slit is characterized by a flow exponent of 0.625 and higher pressure are expected to occur.

The iterative calculation approach seems to give more realistic approach but has some shortcomings. The size of the slit is adjusted to the maximum occurring pressure. This means that the pressure curve in the moments before the peak occurs, is underestimated as the slit is adjusted to a higher pressure. As the pressure peak is correlated to the pressure behaviour before the moment the peak pressure occur, the simulated peak pressure is expected to be underestimated.

Moreover, it is possible that the calculated C- value, which is determined for the iterative calculation process, is not accurate enough as the C- value of the opening varies during the fire.

The results for this particular scenario cannot exclude that high pressures might occur as some input values can be considered as a result of a lack of knowledge about practical situations.

The used $q_{v;10}$ value, for example, is the minimum level for a passive dwellings. An enclosure which is 50% more airtight will lead to a pressure peak of 120 Pa, which is an increase of 87.8%. Moreover, the volume of the enclosure may vary in practice and it expected to lead to a higher pressure peak. With the common open floor plans for dwellings it can be expected that the chosen geometry is a best case scenario as a larger floor plan leads to higher pressure peaks.

On the other hand, the enclosure in the simulations is assumed to be adiabatic and the simulation is based on the fast growth curve instead of the according the standard NEN-EN 1991-1-2/NB prescribed medium growth curve. Moreover, no coincidental factors as opened doors and windows are incorporated.

The probabilistic scenario analysis is used to overcome these uncertainties. As the building code is characterized by prescriptive rules instead of a probabilistic approach, no minimum level of certainty is defined. To that end, as indication for the minimum required level of safety the failure probability for building structures is maintained. This probabilistic approach makes it only possible to make statements about the described scenario.

To give an indication of the magnitude of the pressure peak at a higher level, the multiple linear regression model is developed. This equation is only applicable for practical situations within the range of -50% up to +50% with respect to the variables of the above described enclosure. Caution is required when results are extrapolated as this might results in larger deviations.

4.6 Conclusion

As a result of the incorporated fixed flow exponent n = 0.5 and a pressure difference of 10 Pa. whereby the magnitude of the airflow is calculated in Ozone, the pressure behaviour in passive dwellings cannot be simulated accurately. To that end, the size of the slit which represents the infiltration of a passive dwellings in the model is adapted on the calculation method of Ozone.

An enclosure which meets the requirements of a passive house with the dimensions of 4.0 x 5.0 x 2.6 m (l x w x h) is modelled. These dimensions are arbitrary but are chosen such that it could represent a small living room or a large bedroom, the rooms in which a fire mostly occur. In the model it is assumed that the enclosure is adiabatic. The enclosure is expected to be a part of a dwelling of 100 m^2 which results in a higher amount of infiltration for the inner walls.

The results for this scenario indicates that the fire remains small with a RHR of 0.644 MW. The fire is expected to spontaneously go out as a result of a lack of oxygen after 120 s. During these two minutes the temperature increases to 182 ^{0}C and a pressure peak of 64 Pa is reached after 98 s. Although it can be assumed that this pressure is underestimated as a result of the size of the slit, it can be concluded that a pressure increase in the order of hundreds of Pascal is not obvious for this scenario. Nevertheless, it can be stated that the occurring pressure is higher compared to fires in conventional dwellings. Coincidental factors like opened doors and windows are not included in the simulation. Therefore, a wide range of scenarios is possible.

As a result of natural variation for the input parameters (RHR, time constant, $q_{v;10}$ value and the mechanical ventilation) the standard deviation for the pressure peak is 31 Pa. Taking into account the maximum failure probability for building structures from the building code, it must be concluded that the exceedance probability for the pressure peak is too large. This is caused by a lack of knowledge about the values of the parameters in practical situations.

The $q_{v;10}$ value and the compartment size affects the magnitude of the pressure peak at most. To that end, these to variables are used for a multiple linear regression model to predict the magnitude of the pressure peak. Within a range of +/- 50% with respect to the initial values for the $q_{v;10}$ value and the compartment size the magnitude of the pressure peak can be estimated with the following equation:

$$\Delta P_{max} = 102.83 + 1.737 * A_{fire\ room} - 471.52 * q_{v;10}$$

In this equation the floor area of the fire room must be entered in m^2, and the $q_{v;10}$ value in $dm^3/s.m^2$. Hereby it is assumed that the total floor area of the dwelling is 100 m^2.

5. Experimental approach

Purpose of the experiments is on the one hand identifying if high pressures can occur during fire in well insulated and airtight dwellings and on the other hand generating data in order to validate the simulations as conducted in Chapter 4 'Computational approach'. To this end, real scale fire experiments are conducted at the Troned (Trainings- en Oefencentrum brandweer Oost-Nederland) on the Twente Safety Campus in Enschede. The Safety campus provides the ability to generate data by conducting fire tests under realistic conditions. In this chapter, the experimental design will be described and the results of the experiments will be described and analyzed. In the discussion the experimental results will be interpreted and then compared to the preliminary calculations. Then differences between the calculations and experimental results will be explained and the simulation models from the preliminary calculations will be fitted subsequently on the experimental results

5.1 Work plan

Description of test facility

The experiments will be carried out in a test set-up of 20.7 m^3 which is depicted below (Figures 21 and 22). The fire room comprises a space with the dimensions 3.6 x 2.4 x 2.4 m (length x width x height). The front façade of the object consists of a steel frame whereby the walls on the inside are covered with a Fermacell gypsum fibre board and on the outside a cement fibre board. Between the framework 120 mm mineral wool is present. An air cavity of 20 mm is present between the rockwool and the outer fibreboard. In this front façade two window openings are present which are closed with plywood before the start of the experiments. The dimensions are approximately 500 mm by 800 mm. The other walls consist of a steel frame covered with a gypsum fibre board. In the end wall a door is present. The floor and ceiling are also build-up from a steel frame and are not insulated.

Figure 21 Test setup

Figure 22 Test setup

Test setup

Because in this stage of the research, it is assumed that the window pane fall out occurs in a later stage of the fire, the fire in the experiments will only consuming oxygen which is already available in the fire room. Therefore, the present window openings in the enclosure are not applicable and will be closed with plywood.

In the parameter study as described in paragraph 4.3, the influence of six variables on the pressure build-up in dwelling fires has been identified. It has been found that the level of air-tightness of the enclosure is one of the main factors which determine the magnitude of the pressure build-up. To this end, the enclosure will be upgraded to the passive level in terms of air-tightness.

This will be done by applying a vapour-resistant and airtight foil at the inner side of the wall structure (Rockwool PE). To keep the heat within the room, the walls are covered with rockwool (Figures 23 and 24).

Figure 23 Applying vapour resistant and airtight foil

Figure 24 Foil is protected by rockwool

On the basis of some simple calculations the required thickness of the rockwool can be determined for a steady state situation. Based on the calculation in Appendix 8 it can be concluded that as a result of the 80 mm Rockwool, the temperature at the location of the foil will not exceed 155 ^{0}C. As in the other three walls no insulation is present, the surface temperature at the location of the foil will even be lower. Therefore it will be sufficient to apply 80 mm Rockwool to protect the foil.

The insulation will be attached with long screws with a metal rosette. Despite the fact that the screws will pierce the foil, it is expected that this will not affect the air-tightness such that it will lead to an exceedance of the maximum $q_{v;10}$ value of 0.15 dm^3/s.m^2. With the use of the programme Voltra a more detailed calculation for the heat transport through the rosettes and screws is made in order to determine to which extent the heat is conducted to the foil (Appendix 8). Based on the output it can be concluded that the small temperature increase as a result of the thermal conductivity through the screws will not lead to a degradation of the air tightness of the foil.

Experimental scenarios

In order to identify the fire behaviour in well insulated and airtight dwellings, four different scenarios are constructed.

Scenario 1

In scenario 1 the enclosure will meet the requirements of a passive dwelling and have the aim to identify if high pressures can occur in practice in modern dwellings. With regard to the air tightness, all four walls will meet the requirements according the passive house standard. So the maximum infiltration of air should be 0.15 dm^3/s.m^2. As the ground surface of the enclosure is 8.64 m^2, the maximum infiltration for the test facility amounts 1.296 dm^3/s. By applying this standard it can be obtained whether it is possible that a significant pressure rise can occur during fire. The amount of infiltration will be measured before the start of the experiment by conducting a blowerdoor test.

Scenario 2

In scenario 2 a more realistic approach with regard to practical situations is chosen. The approach will be equal to the parameter study described in chapter 3. For scenario 2 it is assumed that the enclosure is a part of a dwelling of 100 m^2 (Figure 25). This has consequences for the air-tightness of

the compartment whereby a higher amount of infiltration is caused by the inner walls. Conform the passive standards, only the outer wall must meet the standards of 0.15 $dm^3/s.m^2$. Therefore, in practice it can be expected that the inner walls have a higher degree of infiltration. However, the infiltration of the inner walls is restricted by the $q_{v;10}$ of the remaining area of the floor plan, so the total infiltration of a dwelling of 100 m^2 can never be higher than 15 dm^3/s, conform the passive standard. The maximum infiltration for scenario 2 is determined as follows:

Table 2 Infiltration approach scenario 2

$q_{v;10}$ outer wall	: 0.15 x 8.64 = 1.296 dm^3/s
$q_{v;10}$ inner wall, based on the remaining area of the floor plan	: 0.15 x (100-8.64) = 13.704 dm^3/s
Total infiltration	15 dm^3/s

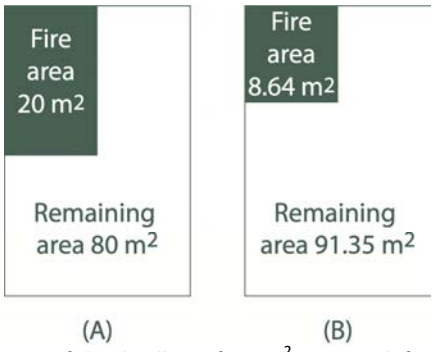

Figure 25 Fire area in relation to total area of the dwelling of $100m^2$. Approach from Chapter 4 (a) and for scenario 2 (b)

Scenario 3 and 4

For scenario 3 and 4 the influence of varying the parameters on the pressure build-up compared to scenario 2 will be examined. In scenario 3 the influence of the RHR on the pressure curve will be examined. To that end, the RHR will be halved by declining the burning area of the pan fire. The amount of infiltration will be the equal to scenario 2.

For scenario 4 the influence of a higher amount of infiltration on the pressure build-up will be examined. To that end the $q_{v;10}$ value will be doubled. This results in a doubling of the equivalent size of the slit. The size of the pan fire will be equal to scenario 2.

5.2 Method

Before the experiments are conducted the amount of infiltration of the enclosure will be defined. Therefore a quantitative and qualitative evaluation of the air-tightness of the enclosure will be carried out. The quantitative approach (Figure 26) will be made by conducting a blowerdoor test conform the standard NEN 2686 *Air permeability of Buildings – Measurement methods* (Appendix 9). It appeared that the enclosure of scenario 1 is characterized by a $q_{v;10}$ value of 0.173 $dm^3/s.m^2$ and a flow exponent of 0.8.

In addition, the location and influence of the air leakages can be analyzed qualitatively. With the use of a smoke tube, the location of the leakages can be identified (Figure 27). If the smoke is blown away measures can be taking in order to reduce the infiltration at this point.

Figure 26 Blowerdoor test

Figure 27 Smoke tube

During the experiments, the pressure differences within the enclosure will be measured as well as the temperature. Thermocouples will be placed into the enclosure, but also the temperature on the foil will be measured. On the basis of the measurements of these thermocouples it will be concluded if the air-tightness of the enclosure may be affected.

The place of the pressure gauges should be chosen such that these are affected as less as possible by disruptive air currents. To this end, the sensors will be mounted on the wall on the opposite of the door. A pressure gauge will also be placed on the longest side of the enclosure. The pressure gauges will be placed at a height of 1.60 m. This is based on the fact that the height between the floor and the bottom of the window in dwellings is often 900 mm and the height of the window is 1500 mm. Therefore, 1.60 m. is in the middle of the window pane whereby an average for the vertical pressure profile for the window pane is measured. In order to define the temperature profile within the enclosure, the thermocouples will be placed on 0.3 m., 1.20 m. and 2.10 m height. The illustration below provides an overview of the location of the sensors and the number of the thermocouples. In order to affect the air flows and so the pressure measurements as little as possible, the fire will be ignited using a long stick through a hole (Figure 29) with a limited size. This makes it possible to seal the opening quickly and easily from the outside.

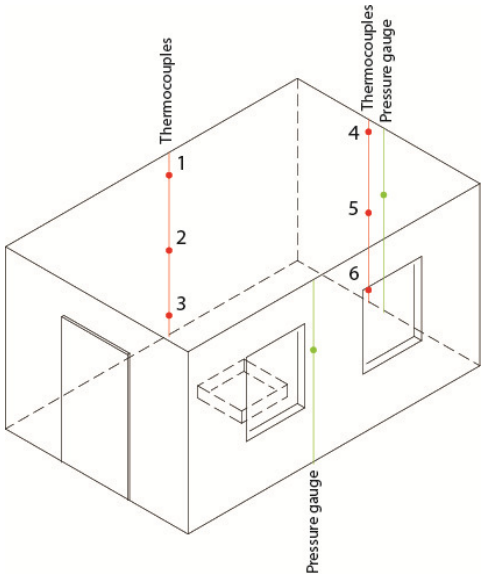

Figure 28 Overview location of the sensors

With regard to the different scenarios, the opening which can be seen in Figure 29 will be used to create the correct equivalent surface of the opening. For scenario 1 the opening will be closed and sealed after the pan fire is ignited. For scenario 2 the created additional opening can be obtained with Equation (14) and will be 0.04 x 0.15 m. For scenario 3 the size of the opening will equal to scenario 2 and for scenario 4 the opening will be 0.08 x 0.15 m.

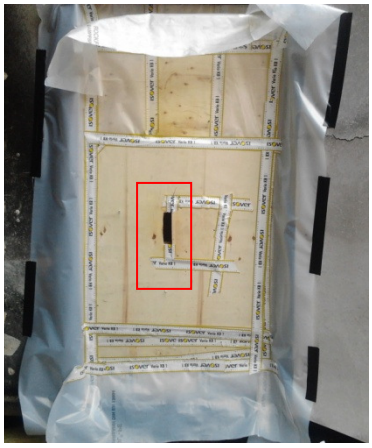

Figure 29 Sealed door with gap

Because bio ethanol has a fairly clean burning, a purity of nearly 100% and evaporates not quickly, this fuel will be used for the experiments. The pan will be levelled horizontal to ensure the burning area will not decline during the experiment and therefore affect the RHR. An excess of fuel will be placed into the pan. The calculations for the pan size and the minimum required amount of fuel depends on the conducted simulations for the four scenarios. These simulations can be found in Appendix 10. The fuel calculations can be found in Appendix 11. Table 3 gives a summary of the experimental scenarios.

To obtain a higher reliability is to define a basic situation before the start of the experiments. In this way, the same starting temperature will be used. This starting temperature depends on the temperature during the test day. After each experiment the enclosure will be cooled to the starting temperature with a fan. For the test run a fuel pan of 0.221 m^2 is used. This resulted in such high pressures that this pan is used instead of a pan with a surface of 0.335 m^2.

Table 3 Overview of the scenarios

Scenario	Description	$q_{v;10}$ *[dm^3/ $s.m^2$]*	Equivalent surface opening created in door *[m]*	Flow exponent *[-]*
1.	$q_{v;10}$ based on the blowerdoor test Pan surface of 0.221 m^2	0.17	-	n = 0.8
2.	Assumption is made that the enclosure is 100% airtight, fire room is part of a dwelling of 100 m^2. Equivalent size of the added opening is based on a dwelling of 100 m^2. Pan surface is 0.221 m^2.	0.15	0.04 x 0.15 m	n = 0.5
3.	Assumption is made that the enclosure is 100% airtight, fire room is part of a dwelling of 100 m^2. Equivalent size of the added opening is based on a dwelling of 100 m^2. Pan surface is 0.117 m^2	0.15	0.04 x 0.15 m	n = 0.5
4.	Assumption is made that the enclosure is 100% airtight, fire room is part of a dwelling of 100 m^2. Equivalent size of the added opening is based on a dwelling of 100 m^2. $q_{v;10}$ value is doubled.	0.3	0.08 x 0.15 m	n = 0.5

5.3 Experimental results

Scenario 1

For the first experiment the level of air tightness is defined by the blowerdoor test. The results indicated that the air tightness of the enclosure was at least 0.17 $dm^3/s.m^2$. An overview of the results and explanation of this blowerdoor test can be found in Appendix 9.

The fire is ignited at t = 0. The temperature curve of thermocouple 1 is linear for the first 45 s. This is determined by identifying the slope (Appendix 12). The peak temperature of 420 ^0C is reached at t = 294 s.

Due to the occurring temperatures one pressure gauge melted which may affected the measurements. Therefore no pressure behaviour is registered with a time logger. The highest observed value by personal observation was 1165 Pa., but higher values may occurred.

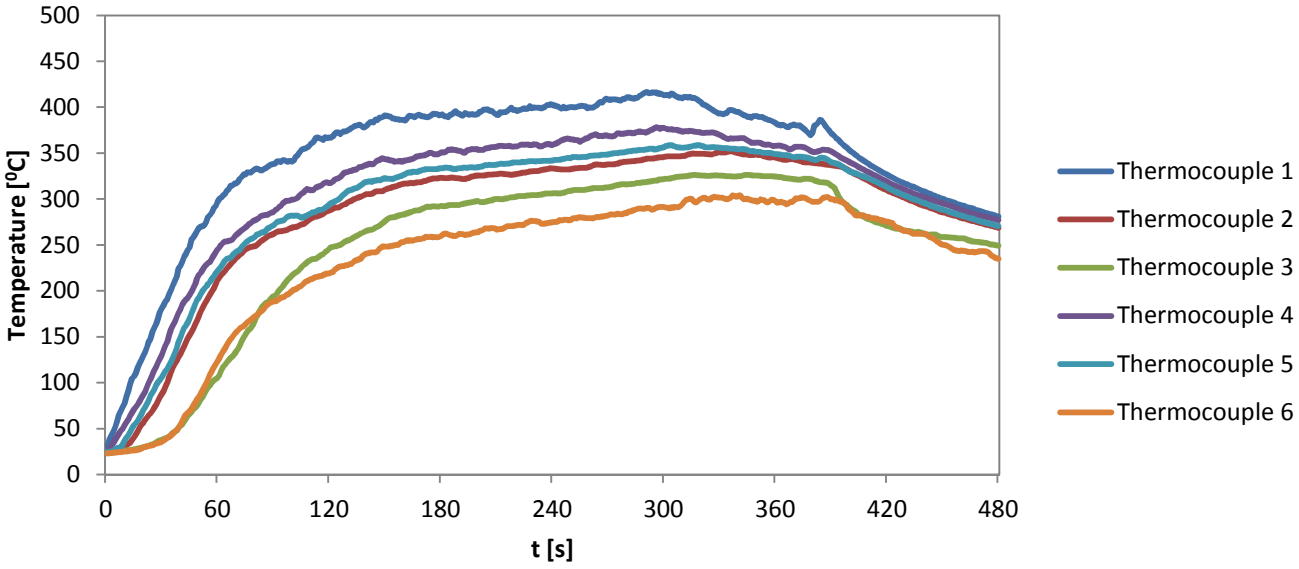

Figure 30 Measured temperatures scenario 1

Scenario 2

The graphs for the pressure difference and the temperature within the enclosure are depicted in Figure 31 and 32 respectively. For the pressure difference within the enclosure, a strong increase can be noticed shortly after the fire is ignited. The pressure peak is reached after 16 s. and has a magnitude of 530 Pa, which corresponds with 53 kg/m^2 on the walls. After this peak is reached, the pressure decreases exponentially. After 35 s. a strong decrease in pressure is noticed. In only one second the pressure decreases in two steps from a positive pressure of 292 Pa to +9 Pa and then to a negative pressure of -243 Pa. At 36 s. the pressure increases with 518 Pa so there is a positive pressure of 275 Pa. On the basis of the audio file this remarkable behaviour can be explained by the fact that someone stepped on the tube of the pressure gauge. A sudden pressure increase can also be noticed at 143 s. after ignition, but the effect is less strong. In one second the pressure increases from 4.5 Pa up to 89.6 Pa. Although no explanation for this event can be given, it may also be caused by the fact that someone stepped on the pressure gauge tube.

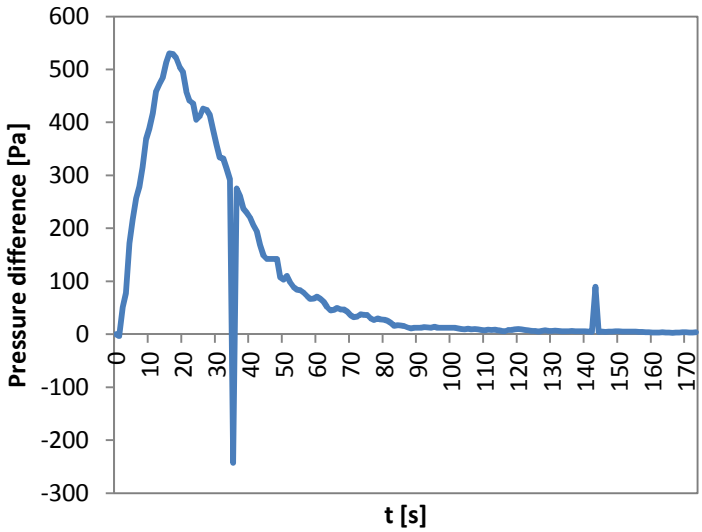

Figure 31 Measured pressure difference scenario 2

With regard to the temperature measured by thermocouple 1, the first 38 s. after ignition the temperature curve shows linear behaviour. The upper thermocouple measured a value of 100 ^{0}C after 17 s., which is almost equal to the moment the pressure peak is observed. At t = 217 s. A sudden increase in temperature can be noticed where after the peak temperature of 354 ^{0}C was reached at t = 227 s.

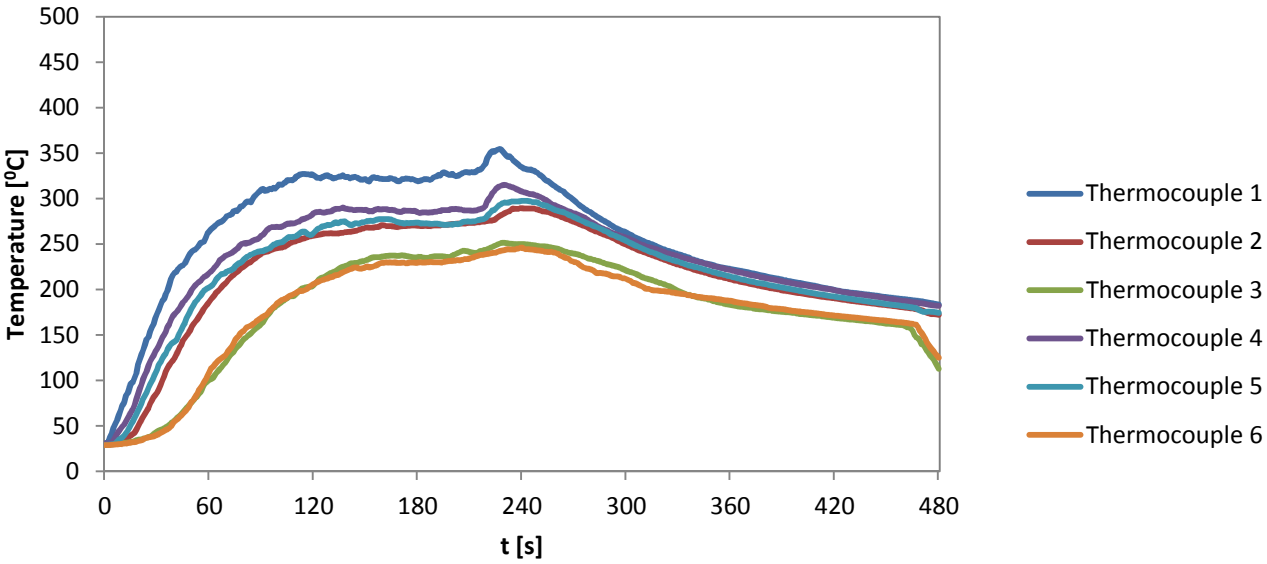

Figure 32 Measured temperatures scenario 2

Scenario 3

The graphs with the pressure results and the temperature within the enclosure are depicted in Figures 33 and 34 respectively. For the pressure, a strong increase can be noticed after the fire is ignited. Within the first 5 s. the pressure increase is 104 Pa., after which the pressure is increasing up to 163 after 20 seconds. After that moment the pressure still increase, but less strong compared to the first 20 s. The absolute pressure peak is reached after 39 s. and has a magnitude of 172 Pa.

The starting temperature of 41.6 ^{0}C is higher compared to the first two scenarios. The temperature increase is approximately constant for the first 78 s. After 20 s. the temperature of 100 ^{0}C is reached and is approximately equal to scenario 1 and 2. The peak temperature of 355 ^{0}C is reached at t = 208 s.

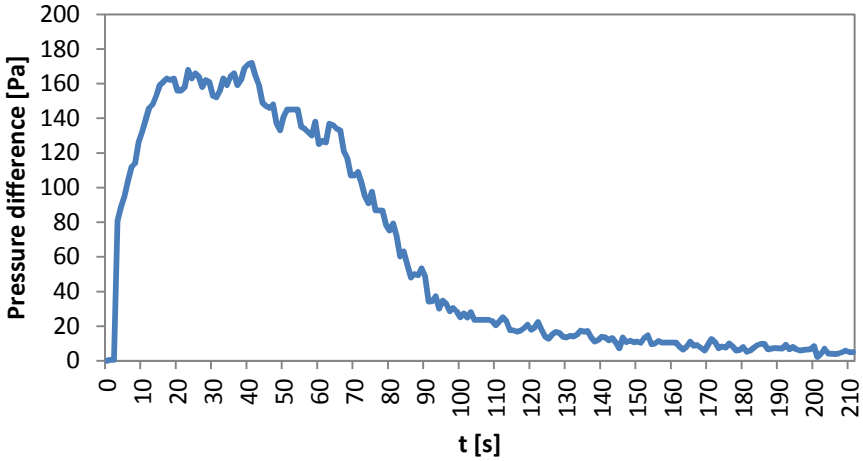

Figure 33 Measured pressure differences scenario 3

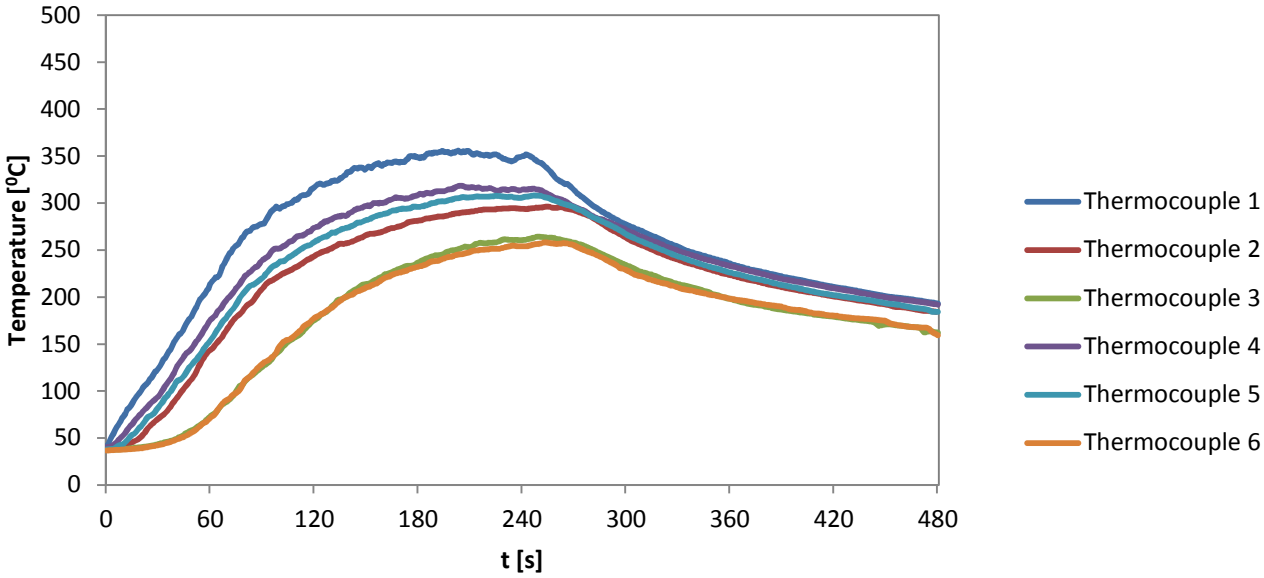

Figure 34 Measured temperatures scenario 3

Scenario 4

The graphs with the results for the pressure difference and the temperature within the enclosure are depicted in Figures 35 and 36 respectively. At t = 11 s. the maximum pressure difference of 172 Pa is reached. After this moment the pressure decreases approximately linearly.

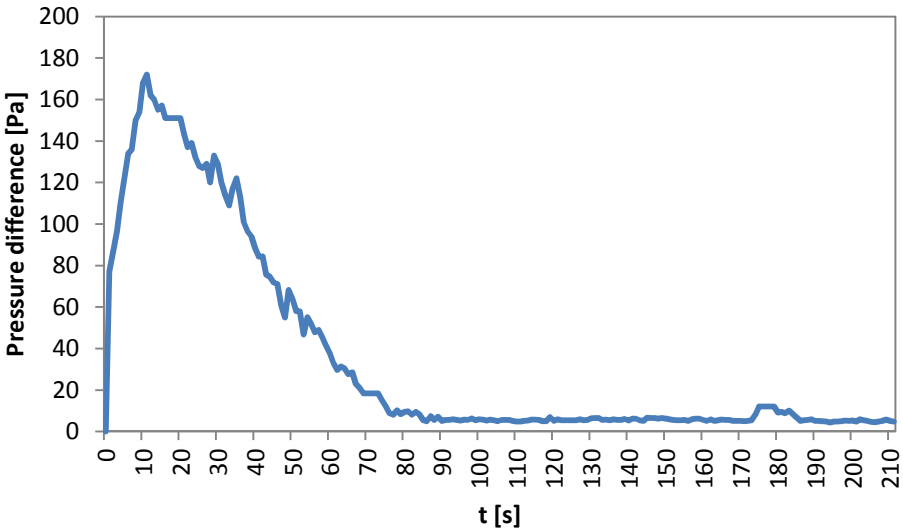

Figure 35 Measured pressure differences scenario 4

The starting temperature at the start of this experiment is 40 ^{0}C, which is higher compared to the first two scenarios. After ignition the temperature increase of thermocouple 1 has a linear progress. The time period after ignition in which the temperature increase is linear cannot be determined exact from Figure 36. Also with the approach whereby the slope of the line is determined, it is difficult to identify if the line deflects after 43 s. or after 70 s. But the temperature increase is significantly lower after 70 s. The temperature reach a peak value of 476 ^{0}C after 263 s. At t = 309 s. a strong temperature increase is measured by the lower two thermocouples (thermocouple 2 and 3) on the long side of the enclosure. This was caused by a wooden plate in the door which caught fire.

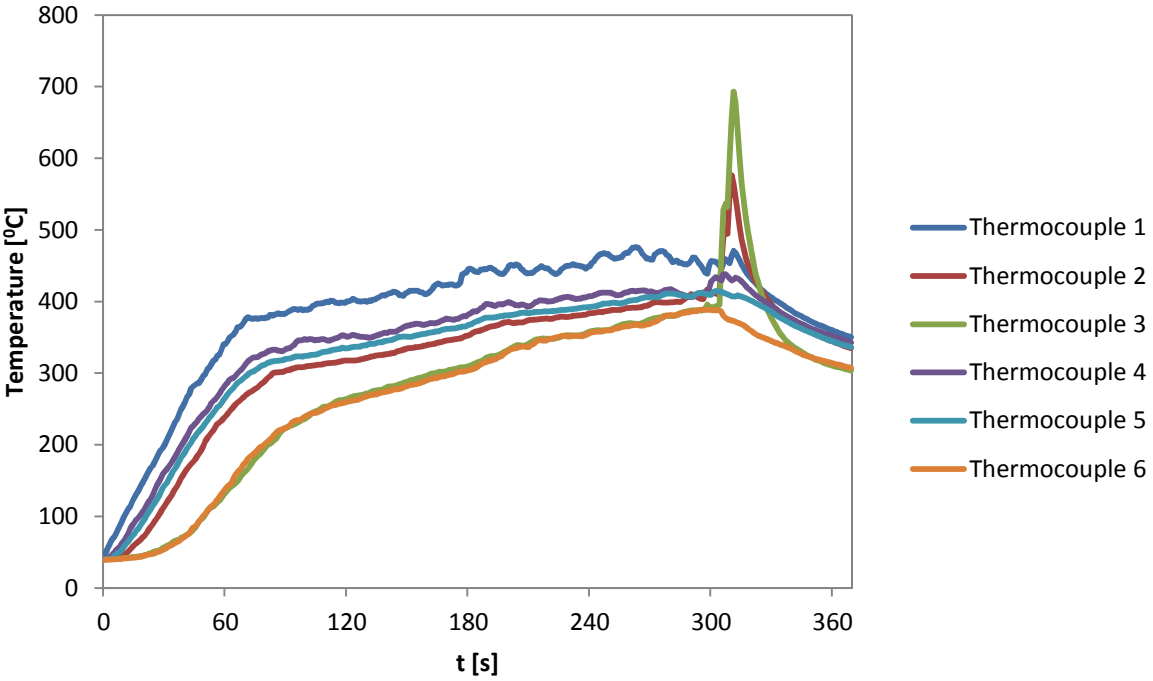

Figure 36 Measured temperatures scenario 4

5.4 Discussion

It was not possible to carry out the blowerdoor test conform the standard NEN2686. This was caused by the fact that the small floor area resulted in such a small air flow that the equipment was not able to measure the magnitude of the flow. The equipment could not found a balance between the incoming and out coming air flow. Thereto, four pressure differences at which the flow is measured are determined manually. Conform the standard NEN 2686, this had to be at least six points. By using points with higher pressure differences the air flow increased so the equipment was able to measure these flows. All measurement points are within the error range of 5% of the regression line so the measurement of the infiltration is valid, despite it is not carried out conform the NEN 2686. Therefore the results of the blowerdoor test can be used for further calculations.

However, the measured values of n_{50} = 1.0 and a $q_{v;10}$ value of 0.17 $dm^3/s.m^2$ should be considered as a conservative performance of the enclosure. Due to the small floor surface, the influence of the installed test door may be too large. In theory, all the infiltration could take place by the connection of the fan with the test door. So, in an extreme situation the enclosure could be completely airtight. The qualitative analysis with the smoke tube showed that merely no infiltration take place through the screws which penetrates the foil. This supports the assumption that the enclosure has a higher air-tightness than is measured with the blowerdoor test.

This assumption may explain the occurring extreme pressures during the experiment of scenario 1 as it is not obvious that high pressures in completely sealed enclosures occur. On the other hand, after ignition of the fuel in the first scenario, the door was sealed by a wooden plate with two screws at the bottom. As a result of the occurring pressure the wooden plate bowed outward and a significant slit arose. According Equation (16), the equivalent surface of the opening for a passive dwellings to represent the infiltration according the passive standard is only 4.92E-4 m^2 (= 4.92 cm^2). As the width of the wooden plate was 150 mm, a slit of 3 mm is enough to represent the equivalent surface of a slit in a passive dwelling, which was present as a result of the air which was pushed out the enclosure.

As a result of the high pressures during the test run for scenario 1 with a fuel pan of 0.221 m^2, there is chosen to conduct the experiments for scenario 1,2 and 4 with this pan size. The calculated pan size according the simulations will have lead to even higher pressures. For comparison, for scenario 1,2 and 4 the RHR in the conducted experiment is only 0.1 MW which can be compared with the RHR from ten burning trashcans.

The shape of the temperature curves are remarkable as the temperature remains constant after a period. At this moment, flames where still visible while it could be expected that the fire is strong ventilation controlled. This indicates there is a balance between the produced and heat extraction which cannot be explained.

Comparison pressure build-up between the scenarios

Scenario 3 and 4 provides information about the pressure behaviour. With regard to scenario 2 the RHR is halved and the $q_{v;10}$ value is doubled for scenario 3 and 4 respectively. In Figure 37, the pressure curves are depicted in one graph. It can be observed that, compared to scenario 2, halving the fire surface in scenario 3 has the same effect on the magnitude of the pressure as doubling the equivalent surface of the opening in scenario 4. This ratio corresponds to the sensitivity analysis in Chapter 4 (Appendix 5).

However, the period that the pressure persists varies significant between scenario 3 and 4. When the opening is made larger the pressure peak is reached in the first moments after ignition whereupon the pressure drops. A smaller RHR leads to a longer duration of the high pressure which is remarkable and against the expectations. A larger sample size will be necessary to exclude deviations. On the basis of this data it is suggested that the RHR has an influence on the magnitude, duration and the moment of the pressure peak. Compared to scenario 2 the magnitude of the

pressure peak in scenario 3 and 4 is significant lower. Halving the RHR or doubling the size of the opening leads to a pressure decrease of 67.5%.

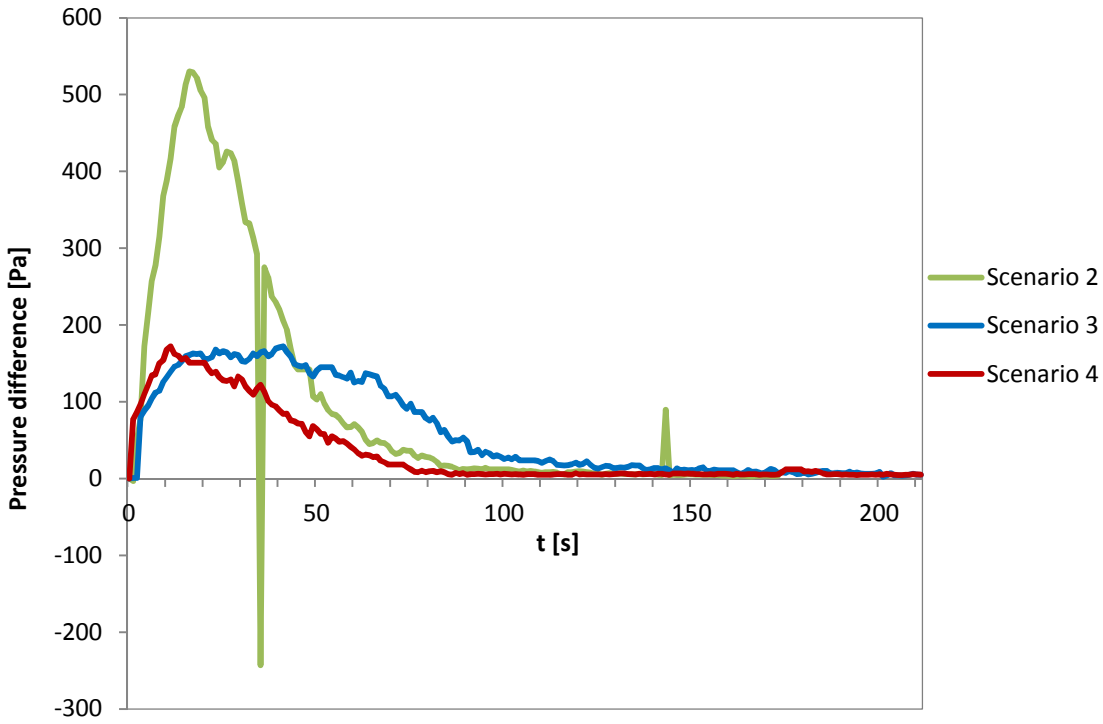

Figure 37 Overview pressure curves

It can be observed that the maximum pressures are reached approximately at the same time. In Figures 38 up to 40 it can also be noticed that all pressure peaks occur around the temperature of 100 ^{0}C, measured by upper thermocouple in the fire room (thermocouple 1). In Table 4 the magnitude, moment and temperature at which the pressure peak occurs are listed. Although for scenario 3 the absolute pressure peak of 172 Pa occurs at 39 s., a pressure of 163 Pa is observed after already after 23 s. After that moment the pressure fluctuates, but the pressure curve remains more or less horizontal. These results suggest there is a certain correlation between the temperature and the occurring pressure peak.

Table 4 Overview peak values

Scenario	**Pressure peak** *[Pa]*	**Time** *[s]*	**Temperature** *[^{0}C]*
2	530	16	98.1
3	172	39	93.0
4	172	11	105.8

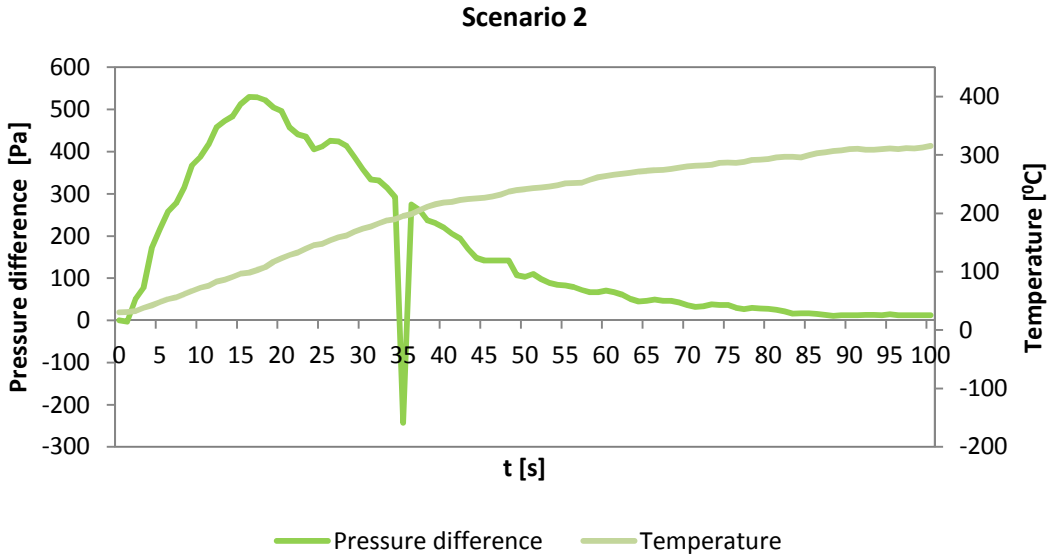

Figure 38 Measured pressure difference and temperature scenario 2

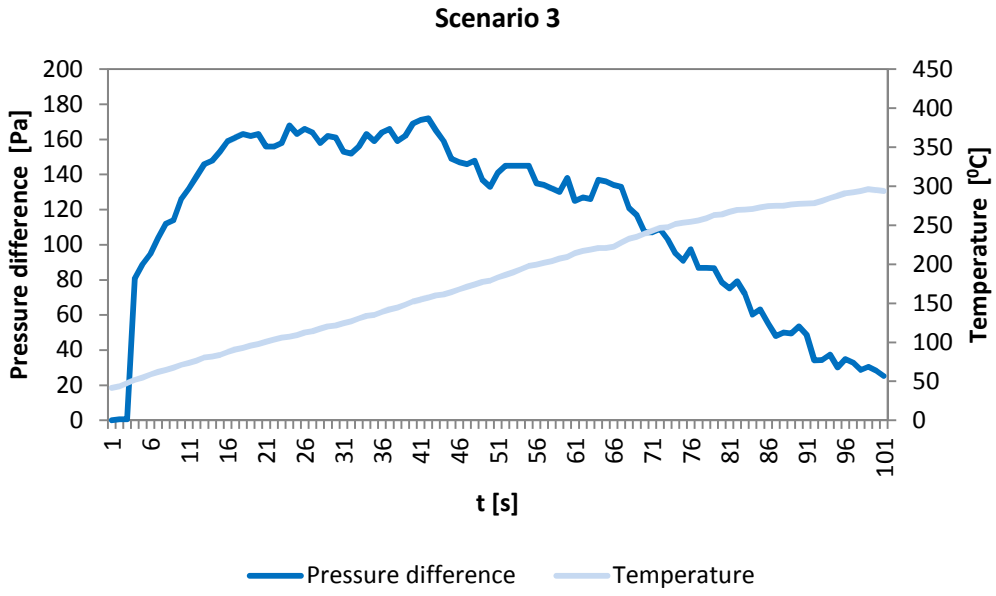

Figure 39 Measured pressure difference and temperature scenario 3

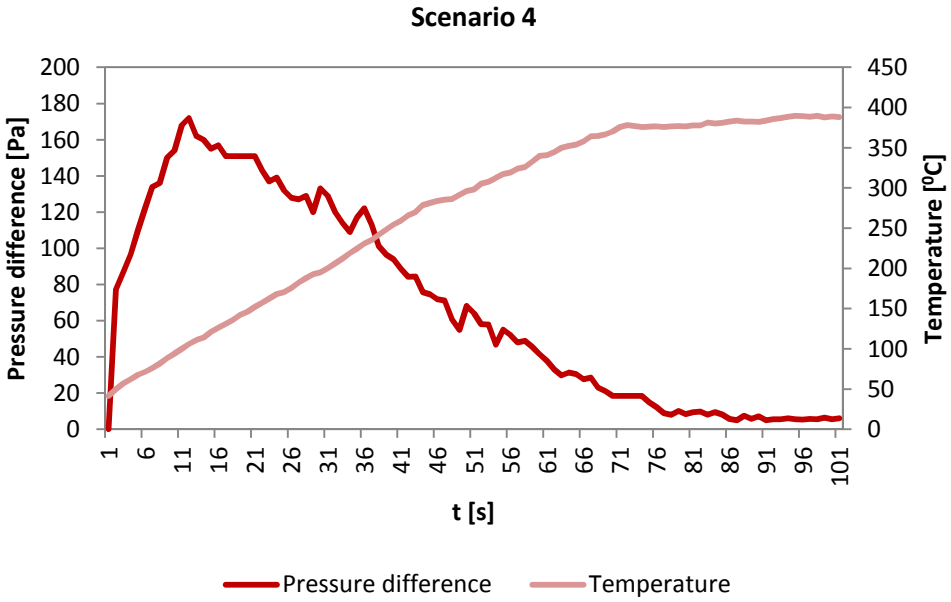

Figure 40 Measured pressure difference and temperature scenario 4

To verify this correlation, the proportional pressure build-up is plotted against the temperature up to the moment the pressure peak occur. In Figure 41 it can be observed that in the period from 50 s. up to 100 s. there seems to be a relation between the temperatures and the proportional pressure. However, the pressure measurements are not carried out with a time logger. As a result, and the fact that the sample size is limited, no statements can be made about the fact that all pressure peaks occur around 100 ^{0}C.

The fact that the lines are corresponding with each other may be explained by the law of Regnault. This law describes the behaviour of an ideal gas at a constant volume:

$$\frac{p}{T} = constant \qquad (25)$$

This equation states that in case of a constant volume of the gas the pressure is directly proportional with the absolute temperature. To apply this equation, two assumptions must be made. The first one is the presence of an ideal gas. The second assumption is that there is a constant volume, so a confined enclosure. With respect to the experimental enclosure this is not the case due to the presence of the gap. But the ratio of this gap with respect to the total enclosure is small. This may explain the suggestion of the correlation between the temperature and the occurring pressure. This is supported by the fact that the curve of scenario 4, which has the largest gap, is the most non-linear curve as it does not meet the requirements to apply the law of Regnault.

The irregular shape of the curves up to 50 ^{0}C might be explained by the number of measurement point or the fact that a constant RHR is assumed while in practice the RHR must be build up in the first moments after ignition.

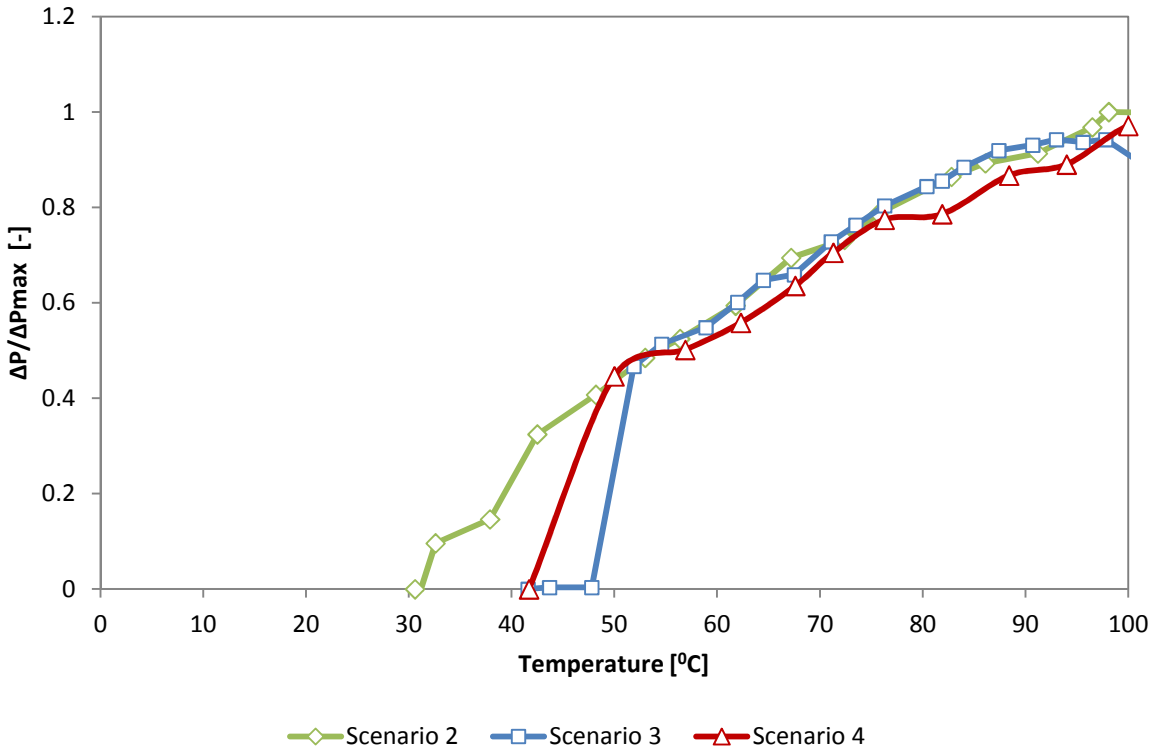

Figure 41 Proportional pressure plotted against the temperature

Comparison and fitting experimental and simulated results

When the experimental results are compared with the preliminary calculations for the experimental scenarios (Appendix 10), it can be observed that these are not in line with each other. To identify the cause of the difference, the possible variations for the Ozone models are identified. As the experimental enclosure is assumed to be adiabatic, these models can be defined by combine all possibilities of the following variables: shape of the equivalent surface, combustion model and the in Paragraph 4.1 developed iterative calculation model. This result in 6 relevant models. These models with corresponding results for the peak pressures of scenario 2 are summarized in Appendix 13.

From the results of Appendix 13 it can be observed that the application of the equivalent surface as a gap instead of the simulated slit from the preliminary calculations gives the closest approach for the experimental results. Nevertheless, with respect to the experimental pressure peak of scenario 2, this model has still a deviation of 228 Pa.

A possible explanation for the difference between model 4.1 in Appendix 13 and the experimental results of scenario 2 may be the fact that the RHR during the initial phase of the simulation is overestimated. In the simulation model, the full RHR is directly present at t = 0 s. A stepwise increase of the RHR will fit the practical situation better.

Before the experiments in the enclosure are conducted, the free burning rate of the fuel is determined (Appendix 14). The measured RHR is depicted in Figure 42. It appeared that the full rate of heat release is present after approximately 20 seconds. The weight of the fuel is read every 10 seconds which explains the irregular deviation of the points. Moreover, as the weight of the fuel is read for every 10 seconds, the moment when the full rate of heat release is present must be seen as a rough estimation.

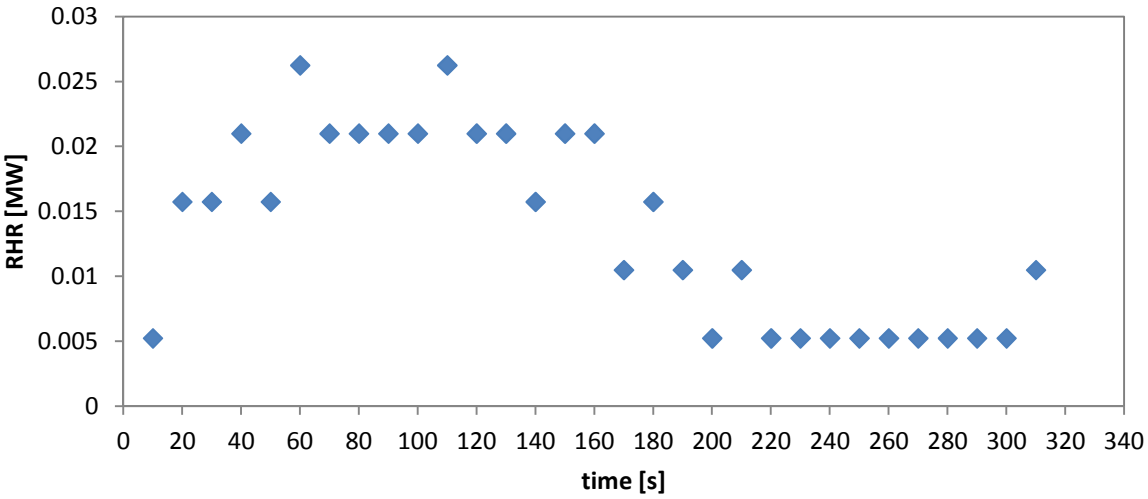

Figure 42 heat release rate of the free burning experiment

When the RHR for the simulations is build up in 20 seconds, the pressure peaks are 474 Pa, 114 Pa. and 118 Pa for scenario 2, 3 and 4 respectively (Appendix 15). The peak pressures are underestimated with 56 Pa. for scenario 2, 58 Pa. for scenario 3 and 54 Pa. for scenario 4.

As a result of the 10 seconds interval for reading the weight of the fuel during the free burning rate, the full RHR might be present earlier. To that end, the RHR is build up in 10 seconds. The resulting pressure curve for scenario 2 is depicted in Figure 43. It can be observed that the simulated pressure peak is 577 Pa. This is an overestimation of the experimental pressure peak with 47 Pa.

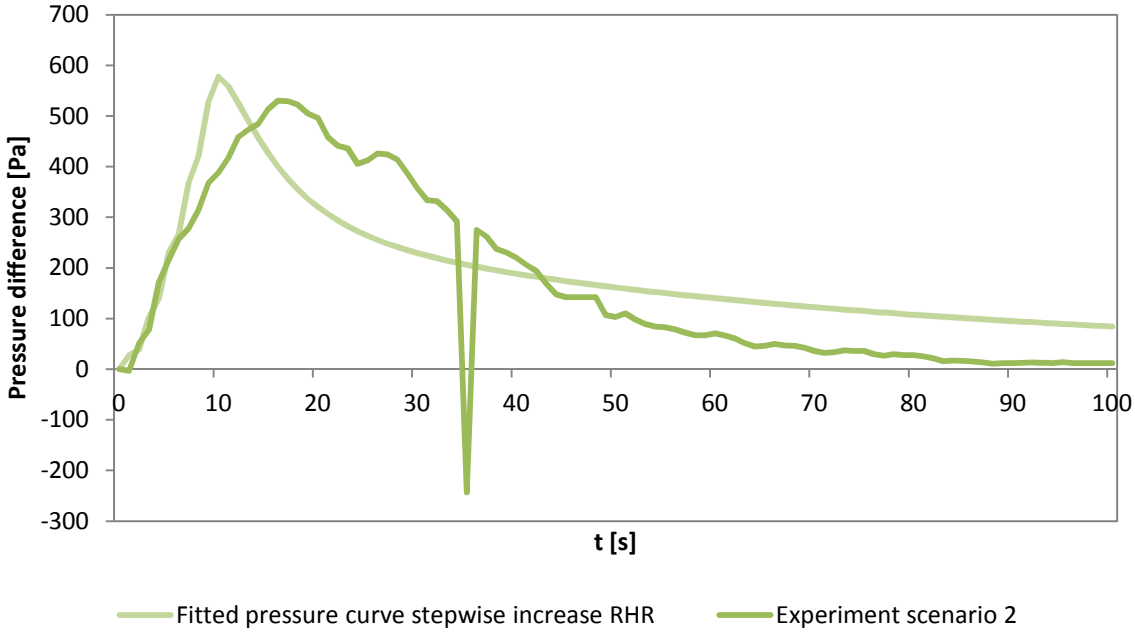

Figure 43 Fitted pressure curve scenario 2 with a stepwise increase of the RHR in 10 seconds

When the RHR for the simulation of scenario 3 is also build up in 10 seconds, the simulated pressure peak is 134 Pa. and so the pressure peak is underestimated with 38 Pa with regard to the experimental pressure peak for scenario 3. This can be seen in Figure 44.

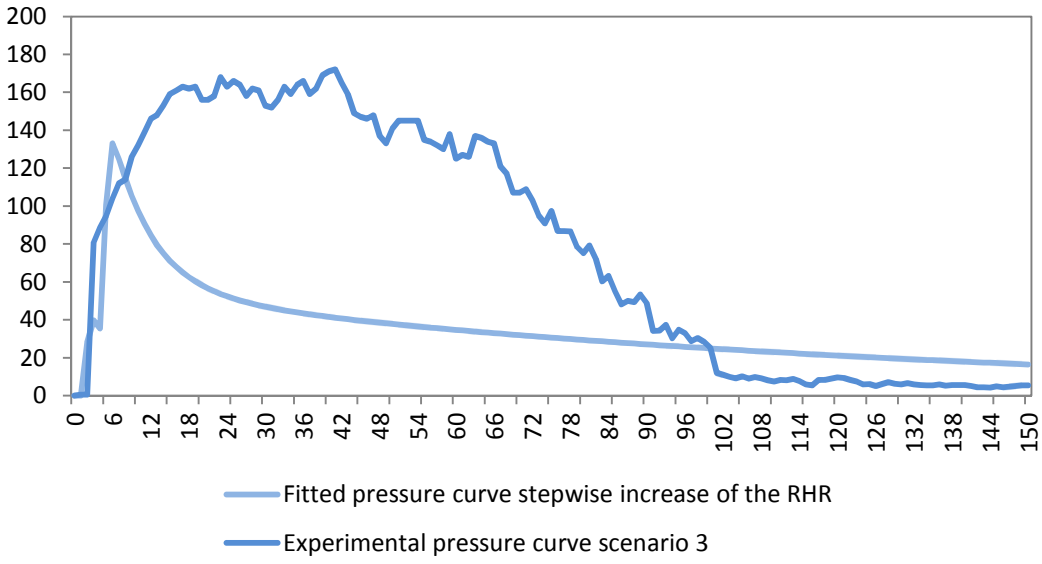

Figure 44 Fitted pressure curve scenario 3 with only a stepwise increase of the RHR in 10 seconds

The same approach is also applied for the simulation of scenario 4. When for the fourth scenario the RHR is increased stepwise in the first 10 seconds, it can be observed in Figure 45 that it will lead to a underestimation of the pressure peak with 20 Pa.

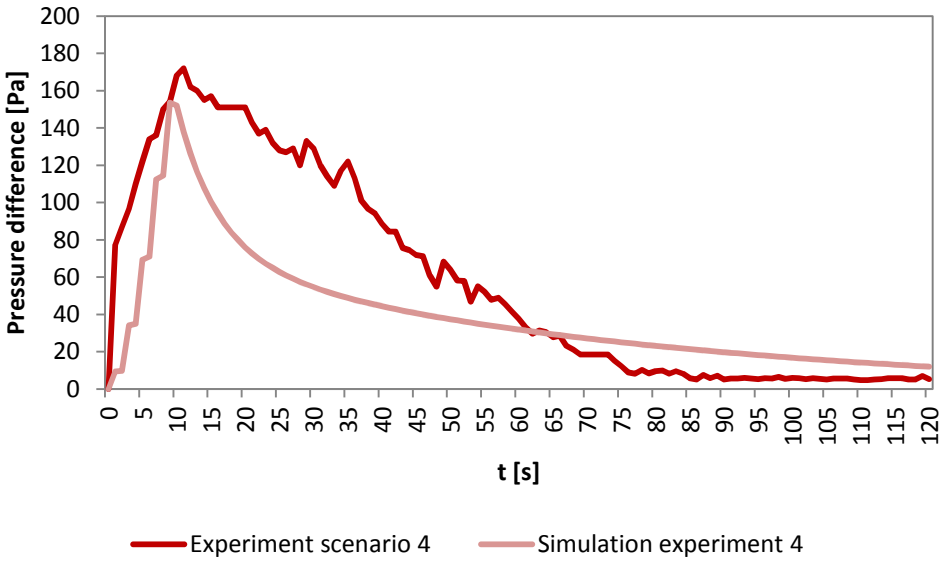

Figure 45 Fitted pressure curve scenario 4 with only a stepwise increase of the RHR in 10 seconds

Considering the results for the stepwise increase of the RHR in 10 and 20 seconds, it can be stated that simulation model 4.1 fits the experimental results fits quite well regarding the pressure peaks, provided that the RHR is increased stepwise in 10 up to 20 seconds.

Temperature curve

As both the experimental and the simulated enclosure are adiabatic, the temperature can only be influenced by changing the RHR and varying the size of the openings. As these two variables are measured and aligned with the experimental setup, there are actually no remaining tools for a better approach of the experimental temperature results. The experimental and simulated temperature curves for scenario 2 are depicted below.

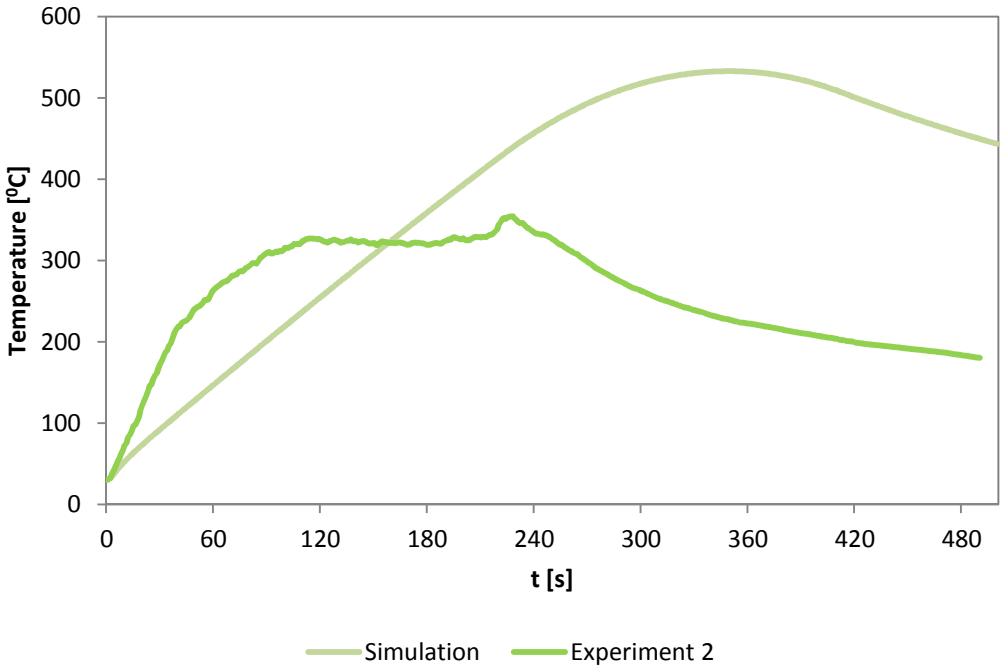

Figure 46 Simulated and measured temperature curve scenario 2

In Figure 46 it can be observed that there is a large deviation between the temperature curve of the experiment and the simulation. Moreover, the shape of the simulated temperature curve is remarkable. In contrast to a linear curve, a square root curve which deflects after a period as a result of a lack of oxygen for the combustion should be expected. The fact that the temperature lines from the simulations and experimental results are not in line with each other, might be explained by the fact that the thermocouples were not covered. Therefore the radiation heat is also measured and results therefore in higher temperatures.

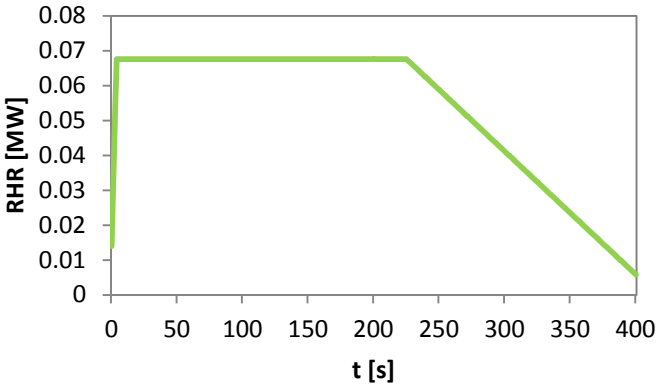

Figure 47 Stepwise increase of the RHR for the first 10 s. after ignition

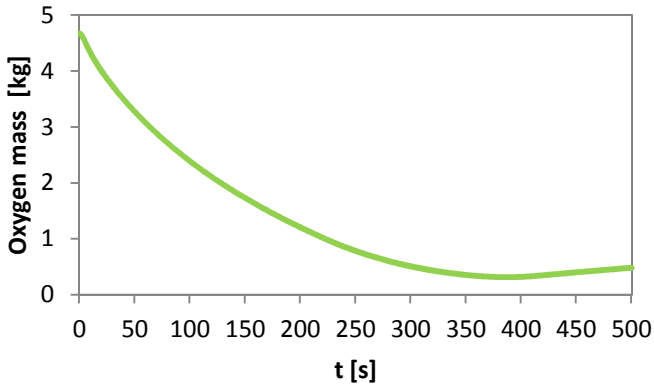

Figure 48 Oxygen mass simulation scenario 2

On the basis of output for the oxygen mass (Figure 48), it can be calculated by hand that the fire is smothering or extinguishes after already approximately 60 s. due to a lack of oxygen. The combustion model does not take this aspect into account (Figure 47). Although the moment at which the cooling down phase starts is different, the cooling down phase of the experiments and the simulation show similar behaviour.

With regard to the temperature behaviour, the same applies for scenario 3 and 4. These graphs can be found in Appendix 16. In both scenarios the temperature curve of the experiments is underestimated and have a remarkable shape. When the temperature curves of scenario 2 and 4 are compared, it can be observed that the shape of the simulated temperature curve of scenario 2 is

exact the same, but the 10 ^{0}C lower. This is caused by the fact that the starting temperature in scenario 2 in 10 ^{0}C lower. This implies that the size of the opening has no influence on the temperature curve. However, for the conducted experiment a temperature difference of approximately 17 % is measured between the curves of experiment 2 and 4. So in practice the size of the opening does play a role in the temperature behaviour.

Differences with real world situations

For the conducted experiments, the distribution of the created infiltration openings differs from practical situations. In the experiments 2, 3 and 4 only one opening represents the amount of infiltration, instead of a distribution of smaller openings at different locations at the enclosure as is usual in practice. Therefore the results may be overestimated as smaller openings may result in a more laminar air flow through these openings, and an opening with a laminar airflow has a higher capacity compared to openings of the same size with a more turbulent flow. Moreover, the mechanical ventilation, and so the supply of air, or the removal of air and heat is not taken into account.

Another aspect that differs from practical situations is that the heat generated by the fire cannot accumulate in the enclosure, as the insulation is applied at the inner side of the wall. This results in higher temperatures and so in a larger expansion of the air. However, it can be considered what the influence of the enclosure will be as the pressure peaks occur within the first 17 s. after ignition. In this period of time the heat extracted from the fire room by the enclosure will be limited due to the thermal inertia of the wall and will not have a large influence.

Last difference compared to practical situations is the fire source. In these experiments a pan fire is used. A result of the application of a pan fire is that the full RHR is more or less directly present. It should be mentioned that the area of the used pans in scenario 1, 2 and 4 (0.221 m^2) is significant smaller than the calculated size conform the fuel calculations (0.35 m^2). Using pans with a surface of 0.35 m^2 would resulted in a higher RHR, and so higher pressures.

5.5 Conclusion

According to the air-tightness of the test setup it can be concluded that the influence of the test door is too large to carry out a measurement of the air-tightness conform the standard NEN2686. Due to the small floor area, the air flow through the enclosure is too small to measure it conform the standards. Nevertheless, by using higher pressure differences for the blowerdoor test it was possible to define a n_{50} value of 1.0 h^{-1} and a $q_{v;10}$ value is 0.17 dm^3/s.m^2. Thus it can be concluded that the experimental enclosure approaches the requirements of the passive house concept. As the measured points are within a range of 5% of the regression line, the measurement is valid. However, these values must be interpreted as the minimum performance in terms of the air-tightness of the enclosure. As the influence of the test door on the small enclosure is large, in theory all infiltration can takes place at the connection of the fan with the test door whereby the enclosure itself will have a higher amount of air-tightness.

For scenario 1, in which all walls meet the requirements for the air tightness of 0.17 dm^3/s.m^2, the highest observed pressure by personal observation was 1165 Pa. But as a result of the melted pressure gauge a complete measurement for the pressure behaviour is not recorded. The pressure difference of 1165 Pa is measured by personal observation on a second pressure gauge.

A description of the other scenarios with corresponding results can be found in Table 5. On the basis of these scenarios it can be stated that higher pressures during a fire a passive dwelling can occur. But also in well insulated and airtight dwellings the pressure differences can be significant higher compared to conventional dwelling fires.

A distinction in the pressure behaviour can be made. According to the experimental results, it can be stated that increasing the degree of air-tightness leads to higher pressure peaks whereupon the pressure drops immediately. Remarkably, lowering the RHR leads to a lower pressure peak, but

also a longer duration of high pressures. But a larger sample size is required to make more reliable statements.

Table 5 Overview peak pressures of the experiments

Scenario	Description	$q_{v;10}$ *[$dm^3/s.m^2$]*	Equivalent surface opening created in door *[m]*	ΔP_{max} *[Pa]*
1.	n_{50} = 1.0, $q_{v;10}$ < 0.17 $dm^3/m^2.s$ Pan surface of 0.221 m^2	< 0.17	-	- (1165 Pa)
2.	Assumption is made that the enclosure is 100% airtight, fire room is part of a dwelling of 100 m^2. Equivalent size of the added opening is based on a dwelling of 100 m^2. Pan surface is 0.221 m^2.	0.15	0.04 x 0.15 m	530 Pa
3.	Assumption is made that the enclosure is 100% airtight, fire room is part of a dwelling of 100 m^2. Equivalent size of the added opening is based on a dwelling of 100 m^2. Pan surface is 0.117 m^2	0.15	0.04 x 0.15 m	172 Pa
4.	Assumption is made that the enclosure is 100% airtight, fire room is part of a dwelling of 100 m^2. Equivalent size of the added opening is based on a dwelling of 100 m^2. $q_{v;10}$ value is doubled.	0.3	0.08 x 0.15 m	172 Pa

For the survivability of the occupant the temperature at the lower part of the enclosure is of interest (Figure 49). There is no clear limit value for the temperature which results in fatal conditions. Whether a fire is lethal depends on many factors like the amount of heat radiation from the fire, received radiation doses, burned area of the skin, age, etc. [28]. The literature reveals that an exposure to a temperature of 53 ^{0}C during 100 s. results in 2nd degree burns. However, an exposure to a temperature of 65 ^{0}C will results in 2nd degree burns within only 3 s. [28].

But also the oxygen mass fraction must be taken into account. Therefore, for these experiments it is assumed that for all scenarios fatal conditions are reached within the first two minutes.

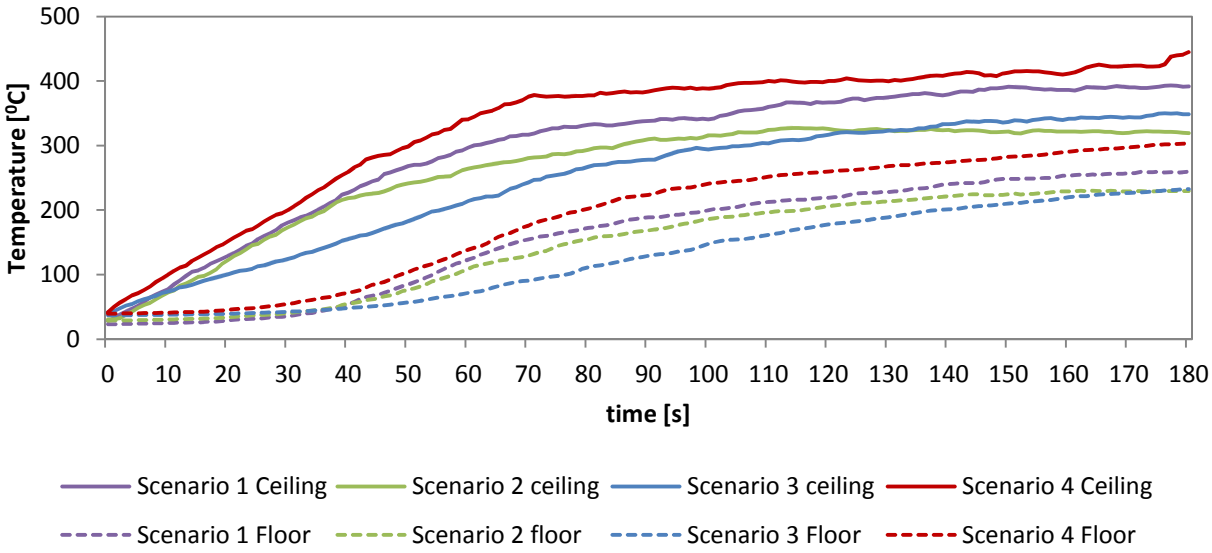

Figure 49 Temperature at ceiling height and floor height for all scenarios

The simulated pressure behaviour of each scenario differs significant from the experimental results. To that end, six simulation models are constructed for scenario 2 with three involved variables (shape of the opening, combustion mode and the application of the developed air model) in order to fit the peak pressures. It appeared that the simulation in where the shape of the opening is a gap and the combustion model is on, gives the best approach. However, there is still an overestimation of the peak pressure of 228 Pa.

The presence of the full RHR at t = 0 seems the cause of the overestimation of the pressure peak. From the experimental free burning rate it is calculated that the full RHR is present within 20 seconds. As the interval for reading the mass is 10 seconds, this must be seen as a rough estimation. Subsequently, when for the simulations the RHR is build up in 20 seconds, this results in an underestimation of the pressure peak. When the RHR is build up in 10 seconds, the simulations predicts the magnitude of the pressure peak quite well. The shapes of the pressure curves are not in line with the experimental results.

None of the predicted temperature curves satisfies the experimental results. The linear shape of the predicted curves differs greatly from the experimental results. This might be caused by the fact that the thermocouples where not covered during the experiments. Therefore, also the radiation heat is measured. On the other hand, the changed size of the gap in scenario 4 has no influence whatsoever on the simulated temperature curve of the, while in practice a temperature difference between the scenarios of 17% is measured between scenario 2 and 4. The absence of an oxygen dependent combustion model in Ozone results in inadequate predictions for the temperature.

6. Discussion

This research is focussed on the influence of the building skin on the fire behaviour in well insulated and airtight dwellings, and in particular the pressure behaviour with regard to the safety of the occupant and fire service. Until now it was assumed that window pane breakage as a result of internal material stresses was normative for the safety.

In order to give an answer, the relevant variables are selected by a literature study. The simulation programme Ozone is used to give an insight in the fire and pressure behaviour. In order to create a robust answer a probabilistic scenario analysis is carried out, and at a higher level, a regression analysis over the two most important variables is conducted. The results are validated by conducting real scale fire experiments.

With regard to the internal validation, it is sought to base the input parameters on standards and prescriptive rules like the Dutch building code, NEN2687, NEN-EN 1991-1-2/NB and the Eurocode EN 1990, annex B. With regard to the internal validation it is chosen to use the passive building concept as a starting point, as the characteristics are quantified.

In practice, the results will be strongly influenced by random factors. One can think of windows that are opened, window pane breakage and the initial fire object.

With regard to the simulations and the sensitiveness analysis it must be mentioned that these results only applies for dwellings of 100 m^2. A different dwelling size may lead to different results. To find a solution for the shortcoming of Ozone to apply a flow exponent ≠ 0.5, other programmes like CONTAM are considered. However, in these programmes it is not possible to apply a RHR curve. Finally, this research focuses at the fire behaviour at room level. Although there is looked at the influence of the remaining area of the dwelling on the fire room, a closer look at this interaction may result in different outcomes.

For each scenario only one experiment is conducted. As fire source a pan fire is used. As a result, the full RHR is directly present. Although the pan size is adjusted on the simulated pressure peak as a result of the curve from the EN 1991-1-2, and is even reduced on the basis of the pressure results after the test run for scenario 1, this may affect the pressure behaviour. Due to the clean combustion of the fuel, no smoke is produced. Moreover, the enclosure is expected to be adiabatic and the infiltration is translated into an equivalent opening. Due to the small floor area only a maximum value for the infiltration could be measured with the blowerdoor test.

The research objectives have been achieved in that an insight is given in the fire and pressure behaviour in well insulated and airtight and passive dwellings. Although there are some limitations, statements can be made. The fire behaviour and in particular the pressure behaviour has been observed in practice at full scale and recommendations for suppressive actions and safety for the occupant can be made.

The results of this research show that more knowledge is required about current practical situations and the ability to simulate fires in passive dwellings must be increased. The simplifications in the experimental rig resulted in a reduction of time and money. Now it has been shown that high pressures can occur, more extensive experiments can be conducted to overcome the limitations of this research.

7. Conclusion

Ability to simulate the fire and pressure behaviour

The simulation of the pressure behaviour in well insulated and airtight dwellings in Ozone is inadequate as a result of a fixed value of n = 0.5 for the flow exponent and the calculation for the magnitude of the air flow at a fixed pressure difference of 10 Pa. To determine the air flow as a result of the infiltration, which is translated into a slit over the entire height of the compartment, an additional iterative calculation tool is developed. This iterative calculation tool adapts the size of the slit on the occurring higher pressures. However, this results in an underestimation of the pressure peaks.

The simulation of the temperature behaviour in Ozone is inadequate as a result of the absence of an oxygen dependent combustion model.

Fire and pressure behaviour in well insulated and airtight dwellings

The pressure increase in dwelling fires is determined by 6 variables, which are the Rate of Heat Release, amount of infiltration ($q_{v;10}$ value), volume of the room, mechanical ventilation, type of enclosure and the R_c- value of the enclosure. The $q_{v;10}$ value, the size of the compartment and the RHR have descending the largest influence on the pressure build-up during fire.

For the simulated enclosure with the arbitrary dimensions of 4.0 x 5.0 x 2.6 m. (w x l x h), which can represent a small living room or large bedroom, a strong ventilation controlled fire with a RHR of 0.65 MW and a pressure peak of 64 Pa can be expected. As a result of the stochastic deviation of the variables and a lack of knowledge about practical situations it can be concluded that, with the required degree of certainty according the building code, the pressure peak of 64 Pa will be exceeded.

From the experiments it appeared that high pressures in the order of hundreds of Pa can occur during fires in both well insulated and passive dwellings. However, the extent to which these pressures really occur and so determines the fire scenario will depend on the building characteristics, heat release rate and coincidental factors. During the experiments, the temperature within the compartment increases rapidly. Within 75 seconds the temperature at floor level exceeds 100 ^{0}C for all conducted scenarios.

Safety for the occupant and fire service

The pressure increase will play a role in the safety of the occupant as the pressure peaks occurred within the first 23 seconds after ignition. It may prevent the occupant to escape the dwelling as it will be difficult or even impossible to open inward turning doors. In combination with the strong temperature increase this will lead to fatal circumstances within a minute.

Given the expected fire behaviour in well insulated and airtight dwellings, the fire service will not be able to carry out an offensive insight attack in order to rescue the occupant. If openings are created below the neutral plane the RHR will increase rapidly or a smoke gas explosion could take place. If openings are created above the neutral plane a backdraft could take place.

In theory, the fire service can expect a strong ventilation controlled fire which may have already been gone out as a result of a lack of oxygen. This results in a potential dangerous situation as it cannot be excluded that the fire is still smothering. In that case a sudden supply of oxygen can lead to a very rapid increase of the RHR, backdraft or smoke gas explosion.

In practice the fire and pressure behaviour will be determined by coincidental factors like opened door and windows. Another possibility is that the pressure increase may lead to the occurrence of unplanned ventilation openings as a pressure increase of several hundreds of Pa in combination with the occurring temperatures may have an influence on the structural integrity of

window panes. Therefore, the fire service can expect a wide range of scenarios. As the pressure peaks occurred at the first moments after ignition during the fire growth stage, it will have no direct influence on the safety of the fire service.

8. Recommendations

As a result of the findings in this research the following recommendations can be made:

- It is expected that the application of a flow exponent of $n \neq 0.5$ and oxygen dependent combustion model in Ozone will improve the ability to predict the fire and pressure behaviour in passive dwellings. This is supported by the fact that Ozone gives somewhat reasonable results for the peak pressures in the simulations of the conducted experiments when a gap is modelled and the RHR is increased stepwise. It can be recommended to integrate these possibilities in Ozone.

- No general recommendations for the strategy of the fire service in well insulated and airtight dwellings can be given, as the fire service can face a wide range of scenarios as a result of coincidental factors. However, a distinction in possible scenarios can be made. On the basis of the individual scenarios and the quadrant model [30] it is possible to make recommendations for the strategy of the fire service. The following scenarios are distinguished:

    - Local smouldering fire
    - Local flaming fire
    - Compartment on fire with external flames

  In case of a local smouldering fire without casualties it can be recommended to do nothing and wait until the fire spontaneously go out as a result of a lack of oxygen. In case of casualties, no inside attack can be carried out as the scenario is expected to be strong ventilation controlled and the fire source cannot be localized. Therefore it will be too dangerous to carry out an offensive inside attack.

  In case of a local flaming fire without casualties, an attack from the inside is not possible as additional openings may lead to a backdraft, smoke gas explosion or a very quick increase of the RHR. A defensive strategy from the outside can be applied. An offensive attack from the outside is possible to reduce damage. But any additional oxygen supply will result in greater damage and expose the fire fighters to danger.

  In case of casualties, in theory the offensive outside attack might be followed by an offensive inside attack, provided that it is certain that there are no heat sources anymore and the hot gases are cooled. However, given the time that has been elapsed since the ignition of the fire, it is expected that the survivability for the occupant is nil.

  In case of a compartment fire with external flaming, an offensive attack from the outside can be applied. A careful consideration must made to apply an attack from the inside as the fire can still be ventilation controlled, even when window panes are fallen out. An additional oxygen supply can therefore result in a quick increase of the RHR.

- For well insulated and airtight dwellings it can be recommended to apply a CO or smoke detection system in every room to establish detection in a very early state of the fire. However, with the moment of the pressure increase and the rapid temperature increase, this may not be sufficient to escape the dwelling on time in many situations. A rapid intervention to eliminate the cause of the hazards is required. This can be done by applying dwelling sprinklers.

- Dwellings should be designed such that at least for one escape route doors are turning open into the flee direction. Then it will be possible for the occupant to open doors. Therefore it can be recommended to flee through the back door since back doors always open to the outside. In absence of a back door it can be recommended to apply a pressure relaxation device in the façade which opens at a pressure increase of 50 Pa. This can be compared with a positive pressure system in stairwells.

- For further research, it can be recommended to conduct more experiments on a larger scale with multiple rooms in order to obtain a higher reliability for the blowerdoor test, and to give an insight in the interaction between the fire room and remaining area of the dwelling. This provides also an insight in the survivability in adjacent rooms and so the necessity for an offensive attack from the inside in case of a local flaming fire.

  For a better approximation of practical situations, a more accurate distribution of infiltration openings instead of an equivalent surface is recommended. Moreover, the application of solid fuels will result in a fire curve which fits practical situations better. This provides also the possibility to take the smoke layer height into account with regard to the safety of the occupant, and gives an insight in the ability of the occurrence of a smoke gas explosion.

- The sensitivity study identified that more practical data must be generated about the values for the amount of infiltration ($q_{v;10}$) and Rate of Heat Release in practical situations. This makes it possible to make more robust statements about the pressure behaviour in practical situations.

References

[1] Centraal Bureau voor de Statistiek, 2014. *Brandweerstatistiek 2013*. Available at:
< http://www.cbs.nl/nl-NL/menu/themas/veiligheidrecht/publicaties/publicaties/archief/2014/2014-brandweerstatistiek-2013-pub.htm>
[Accessed at 23 September 2014]

[2] Ministerie van Binnenlandse Zaken en koninkrijksrelaties, 2012. *Koepelconvenant Energiebesparing Gebouwde Omgeving.* Available at:
<http://www.rijksoverheid.nl/documenten-en-publicaties/convenanten/2012/06/28/koepelconvenant-energiebesparing-gebouwde-omgeving.html>
[Accessed 18 March 2014].

[3] Nieman, H., 2012. *Luchtdicht bouwen; De theorie en het waarom.* Available at:
<http://www.nieman.nl/wp-content/uploads/2012/05/Luchtdicht-bouwen-Harry-Nieman.pdf>
[Accessed at 14 August 2014].

[4] FOD Binnenlandse Zaken, 2010. *Brand in een passiefhuis = inferno?; Brandveiligheid in passiefhuizen*. Available at:
<http://besafe.ibz.be/publications/passief-huis.pdf>
[Accessed at 8 November 2013].

[5] Underwriters Laboratories, 2012. *Analysis of Changing Residential Fire Dynamics and its Implications on Firefighter Operational Timeframes.* Available at:
http://www.ul.com/global/documents/newscience/whitepapers/firesafety/FS_Analysis%20of%20Changing%20Residential%20Fire%20Dynamics%20and%20Its%20Implications_10-12.pdf
[Accessed at 18 November 2013].

[6] Underwriters Laboratories, 2010. *Analysis of One and Two-Story Single Family Home Fire Dynamics and the Impact of Firefighter Horizontal Ventilation.* Available at:
<http://www.ul.com/global/documents/newscience/whitepapers/firesafety/FS_Analysis%20of%20One%20and%20Two-Story%20Single%20Family%20Home%20Fire%20Dynamics_10-12.pdf. >
[Accessed at 18 November 2013].

[7] Herpen, Van R.A.P., 2011. *Passiefhuisconcept: brandveilig?* Adviesbureau Nieman. Available at:
<http://www.infopuntveiligheid.nl/Infopuntdocumenten/3.%20Ruud%20van%20Herpen.pdf.>
[Accessed at 23 November 2013].

[8] Debrouwere, B., 2012. *A study on initial fire behaviour in low-energy houses.* Gent University, Department of Flow, Heat and Combustion (Floheacom). Available at:
<http://www.vvba.nl/downloads/nominaties/A%20study%20on%20initial%20fire%20behaviour%20in%20low%20energy%20houses.pdf>
[Accessed at 23 November 2013].

[9] Instituut Fysieke Veiligheid, 2013. *Fatale woningbranden 2008 t/m 2012: een vergelijking.* Available at:
http://www.nifv.nl/web/show/file/id=253360/filename=Vergelijking_fatale_woningbranden_2008-2012.pdf/page=189250.
[Accessed at 20 November 2013].

[10] Hasofer, A.M., Thomas, I., 2006. *Analysis of fatalities and injuries in building fire statistics*. Fire Safety Journal; 41, 2-14.
[Accessed at 15 November 2013].

[11] Bengtsson, L.G., 2001. *Enclosure fires*. s.l.: Swedish Rescue Services Agency.

[12] Svensson, S., 2005. *Fire Ventilation*. s.l.: Swedish Rescue Services Agency.

[13] Herpen, R.A.P., 2013. Meerzone luchtstroommodellen. Available at:
< http://www.nvbv.org/index.php?option=com_edocman&view=document&id=312&Itemid=271 >
[Accessed at 2 May 2014]

[14] Mierlo, van R. and Tromp, A., 2013. *Fire Safety Engineering- handboek voor de bouw*. Delft: Eburon.

[15] Brink, Van den V., 2015. *Fire Safety and Suppression in Modern Residential Buildings*. An experimental research to the Influence of the Building Skin on the Fire Behaviour in Well Insulated Dwellings and its Consequences for the Safety of the Occupant and Strategy of the Fire Service – Literature study.

[16] Prétrel, H., Saux, Le W., Audouin, L., 2012. Pressure variations induced by a pool fire in a well-confined and force-ventilated compartment. *Fire Safety Journal*; 52, 11-24.

[17] Bonte, F., Noterman, N., Merci, B., 2013. Computer simulations to study interaction between burning rates and pressure variations in confined enclosure fires. *Fire Safety Journal;* 62,125-143.

[18] Suard, S., Hostikka, S., Baccou, J., 2013. Sensitivity analysis of fire models using a fractional factorial design. *Fire Safety Journal*; 62, 115-124.

[19] Chow, W.K., Zou, G.W., 2009. Numerical simulation of pressure changes in closed chamber fires. *Building and Environment;* 44, 1261-1275.

[20] PassivHaus Institut, 2013. Zertifiziertes Passivhaus; Zertifizierungskriterien für Passivhäuser mit Wohnnutzung. Available at:
< http://www.passiv.de/downloads/03_zertifizierungskriterien_wohngebaeude_de.pdf>
[Accessed at 2 September 2014]

[21] SBRCURnet, 2012. Passiefhuisconcept voor woningbouw. SBR. Available at:
< http://www.sbrcurnet.nl/producten/infobladen/passiefhuisconcept-voor-woningbouw>
[Accessed at 9 August 2014].

[22] SBRCURnet, 2013. *Luchtdicht bouwen; Theorie-ontwerp-praktijk.* SBR. Available at:
< http://www.sbrcurnet.nl/producten/kennisarchief/luchtdicht-bouwen/bijlage-1-voorbeeldberekeningen >
[Accessed at 24 April 2014]

[23] Linssen, J.P.A., 2011. *Brand in huis; Overleven of overlijden.* Available at:
http://www.infopuntveiligheid.nl/Infopuntdocumenten/20111001%20Linssen%20FSE%20Brand%20in%20huis_overleven%20of%20overlijden.pdf
[Accessed at 21 November 2013]

[24] Baum, R., Floyd, J., Hostikka, S., McGrattan, K., Rehm, R., 2007. *Fire Dynamics Simulator (Version 5) Technical Reference Guide*. NIST Special Publication 1018-5.

[25] Lundin, J., 1999. *Model Uncertainty in Fire Safety Engineering.* Department of Fire Safety Engineering, Lund University. Report 1020. Available at:
< https://lup.lub.lu.se/luur/download?func=downloadFile&recordOId=525794&fileOId=642195>
[Accessed at 22 November 2013]

[26] Herpen, R.A.P., 2014. *Fysisch brandmodel*; Afstemming risiconiveau aan publiekrechtelijke regelgeving constructieve veiligheid. Available at:
<http://www.nieman.nl/wp-content/uploads/2012/01/Fysisch-brandmodel-Afstemming-risiconiveau-aan-publiekrechtelijke-regelgeving-constructieve-veiligheid_Ruud-van-Herpen_2009.pdf>
[Accessed at 23 December 2014]

[27] Herpen, Van R.A.P.,2007. *Fysisch brandmodel.* Achtergronden; Normalisatie *fysisch brandmodel* - Statistische en probabilistische aspecten. Available at:
< http://nieman.nl/2007/06/fysisch-brandmodel/ >
[Accessed at 23 December 2014]

[28] Ministerie van Binnenlandse Zaken en Koninkrijksrelaties, 2003. *Publicatiereeks Gevaarlijke Stoffen 1*. Deel 1A: Effecten van brand op personen. Available at:
< http://content.publicatiereeksgevaarlijkestoffen.nl/documents/PGS1/PGS1-2005-v0.1-deel-1a.pdf>
[Accessed at 21 March 2015]

[29] Hagen, R., 2014. *Brandpreventie voor repressief leidinggevenden.* Available at:
< http://www.ifv.nl/kennisplein/Paginas/Lectoraat-Brandweerkunde.aspx#tab2 >
[Accessed at 11 February 2015]

In Appendix 11 :

[30] Karlsson, B., Quintiere, J.G., 2000. *Enclosure Fire Dynamics*. CRC Press LLC, Florida. Available at:
< http://unina.stidue.net/Politecnico%20di%20Milano/Ingegneria%20Strutturale/Corsi/Felicetti%20-%20Fire%20resistance%20of%20materials%20and%20structures/Books/Enclosure%20fire%20dynamics/Contents.pdf>
[Accessed at 23 March 2014]

Appendices

Appendix 1: Classification air tightness

Appendix 2: Input Ozone Chapter 4 “Computational approach”.

Appendix 3: Alternative approach iterative calculation process

Appendix 4: Uncertainties in simulations

Appendix 5: Parameter study – Results

Appendix 6: Results probabilistic scenario analysis

Appendix 7: Multiple linear regression model

Appendix 8: Calculation insulation covering for experimental enclosure

Appendix 9: Results blowerdoor test

Appendix 10: Simulation experimental scenarios

Appendix 11: Fuel calculation experiments

Appendix 12: Analysis moment of deflection of the temperature curves on the basis of the slope of the line

Appendix 13: Overview fitted simulation models

Appendix 14: Mass loss rate free burning experiment

Appendix 15: Stepwise increase RHR in 20 s.

Appendix 16: Temperature behaviour scenario 3 and 4

Appendix 1 – Classification air tightness

The air tightness of the façade is a primary factor to meet the requirements of the building concept and must therefore be quantified. Based on the standard NEN 2687, three categories of air-tightness can be defined [3] and are presented in Table 1.1. It can be observed that a separate air tightness category is used to meet the requirements of the passive house building concept.

The passive house concept provides a guideline for this research as it will always meet the requirements of the third category and make therefore possible to make statements, in contradiction to well insulated modern buildings. For that reason, the passive house concept will be used as a starting point to make statements about the fire safety of well insulated dwellings.

Table 1.1 Overview of the air-tightness categories based on the standard NEN 2687 [3]

Category	**Dwelling volume** *[m^3]*	**Maximum $q_{v;10}$** *[dm^3/s]*	**$q_{v;10}$/ m^2** *[$dm^3/s.m^2$]*
1. Basis	0-250	100	1,0
	250-500	150	1,0
	> 500	200	1,0
2. Good	≤ 250	50	0,6
	> 250	80	0,4
3. Excellent	≤ 250	15	0,15
	> 250	30	0,15

Appendix 2 – Input Ozone Chapter 4 "Computational approach"

The ventilation rate of the room is calculated on the basis of the Dutch building code. The building code prescribes a minimal ventilation capacity of 0.9 dm^3/s per m^2 floor space with a minimum of 7 dm^3/s. As the floor space is 20 m^2, the required amount of ventilation is 18 dm^3/s (= 0.018 m^3/s). With an air speed of approximately 3 m/s, the diameter of the ventilation duct can be determined according equation (2.1) which results in a diameter of the duct of 80 mm with a volume of 0.018 m^3/s.

$$V = \frac{Q_{vent}}{A_{duct}} \qquad (2.1)$$

$$3.0\ m/s = \frac{0.018}{A_{duct}}$$

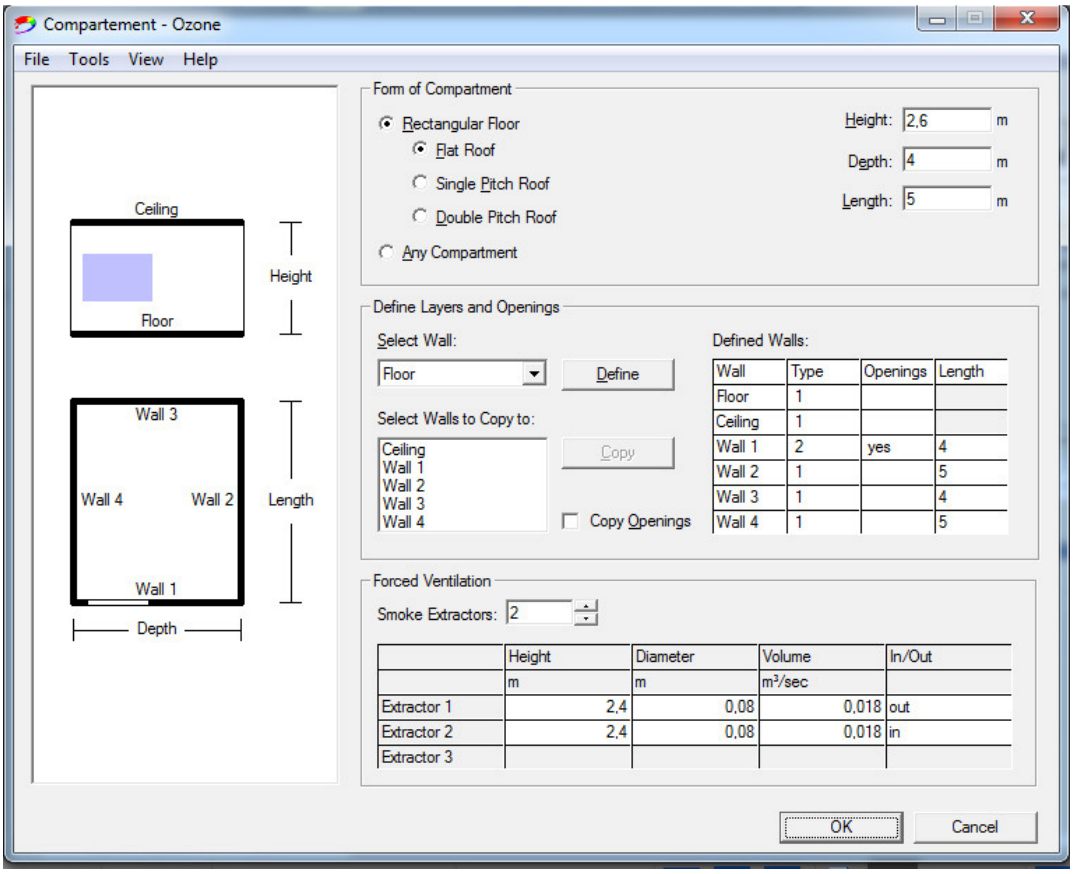

Figure 2.1 Characteristics of the enclosure

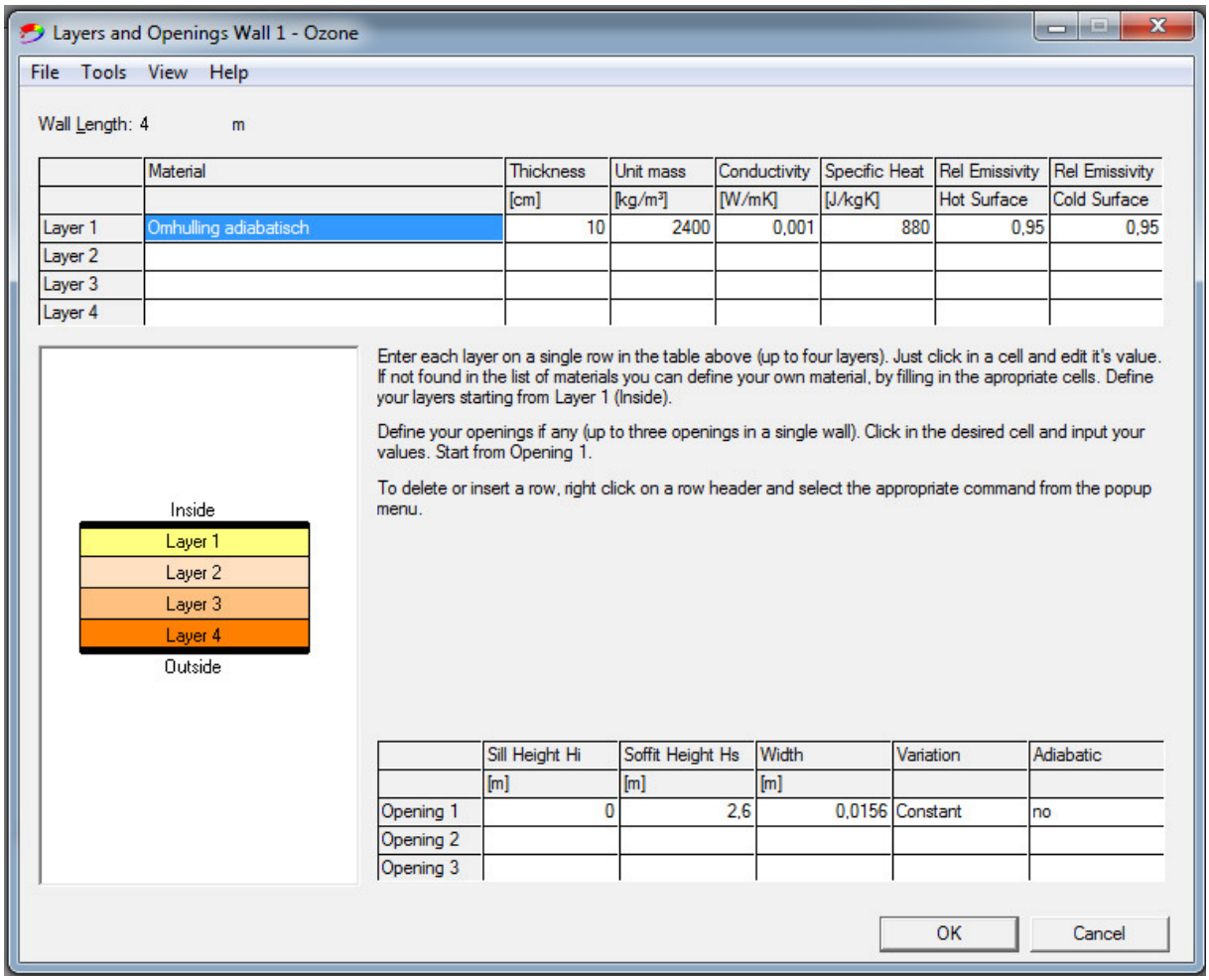

Figure 2.2 Adiabatic enclosure and infiltration translated into a slit over the entire height of the compartment

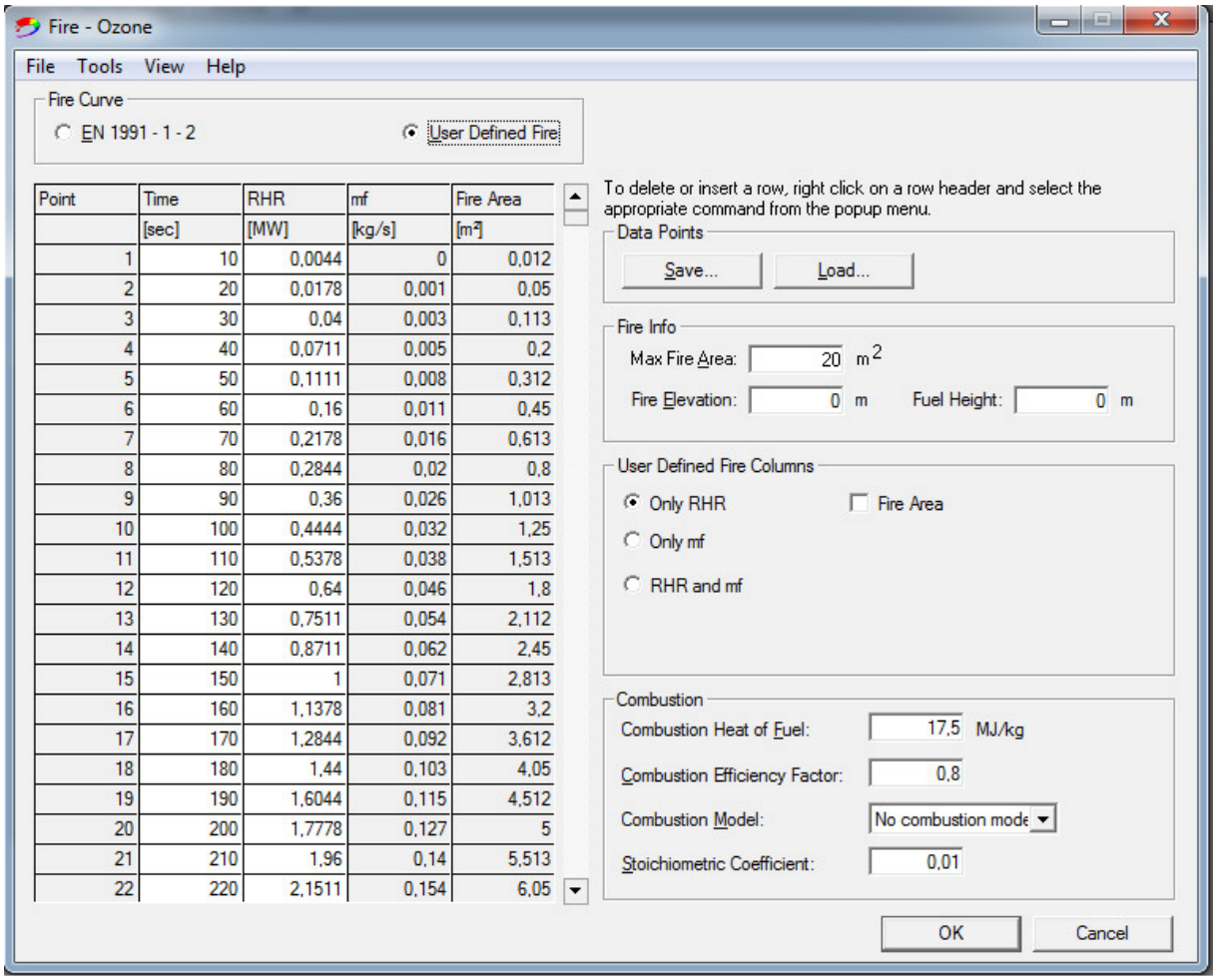

Point	Time [sec]	RHR [MW]	mf [kg/s]	Fire Area [m²]
1	10	0,0044	0	0,012
2	20	0,0178	0,001	0,05
3	30	0,04	0,003	0,113
4	40	0,0711	0,005	0,2
5	50	0,1111	0,008	0,312
6	60	0,16	0,011	0,45
7	70	0,2178	0,016	0,613
8	80	0,2844	0,02	0,8
9	90	0,36	0,026	1,013
10	100	0,4444	0,032	1,25
11	110	0,5378	0,038	1,513
12	120	0,64	0,046	1,8
13	130	0,7511	0,054	2,112
14	140	0,8711	0,062	2,45
15	150	1	0,071	2,813
16	160	1,1378	0,081	3,2
17	170	1,2844	0,092	3,612
18	180	1,44	0,103	4,05
19	190	1,6044	0,115	4,512
20	200	1,7778	0,127	5
21	210	1,96	0,14	5,513
22	220	2,1511	0,154	6,05

Figure 2.3 Applied t_c = 150 curve

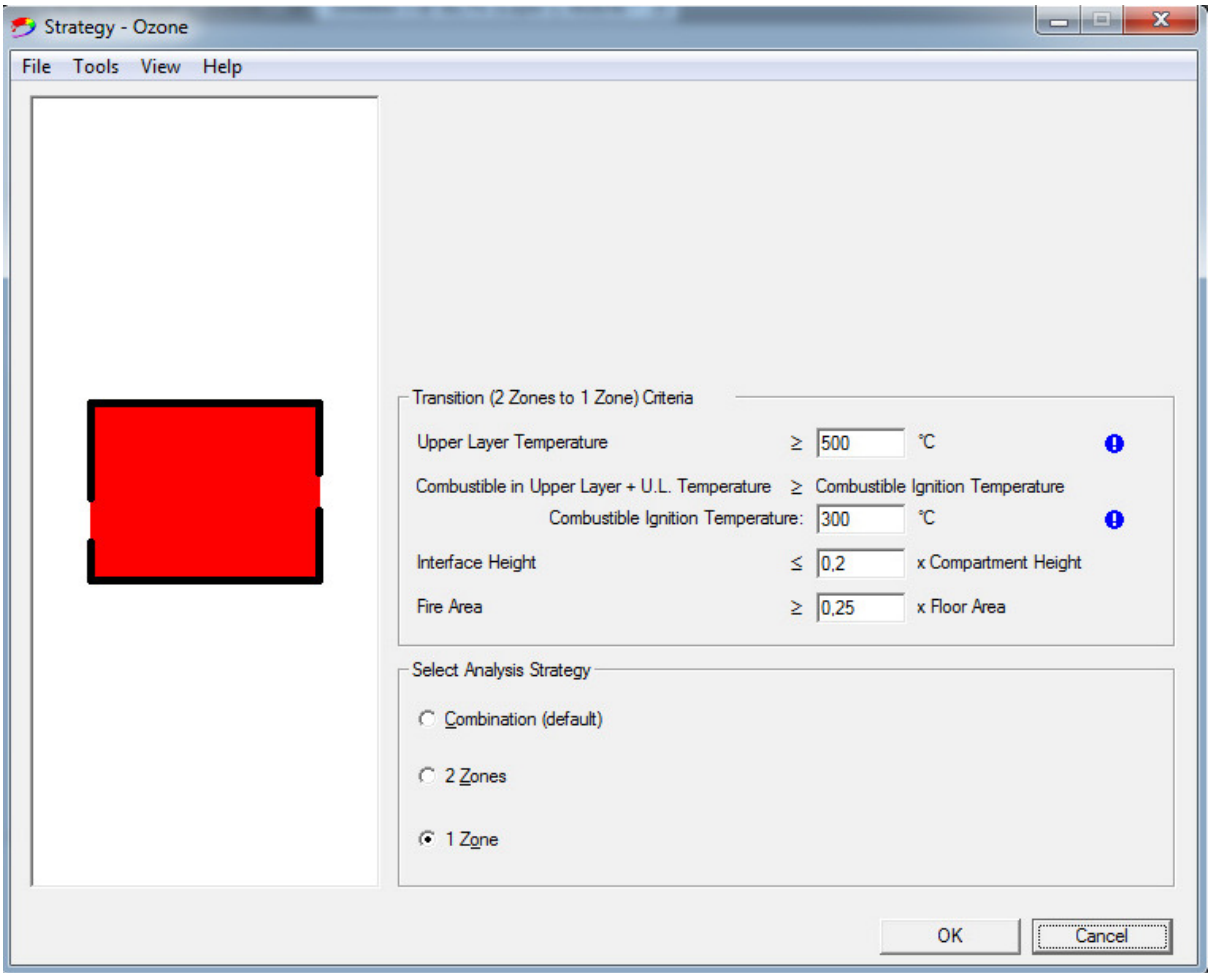

Figure 2.4 Strategy

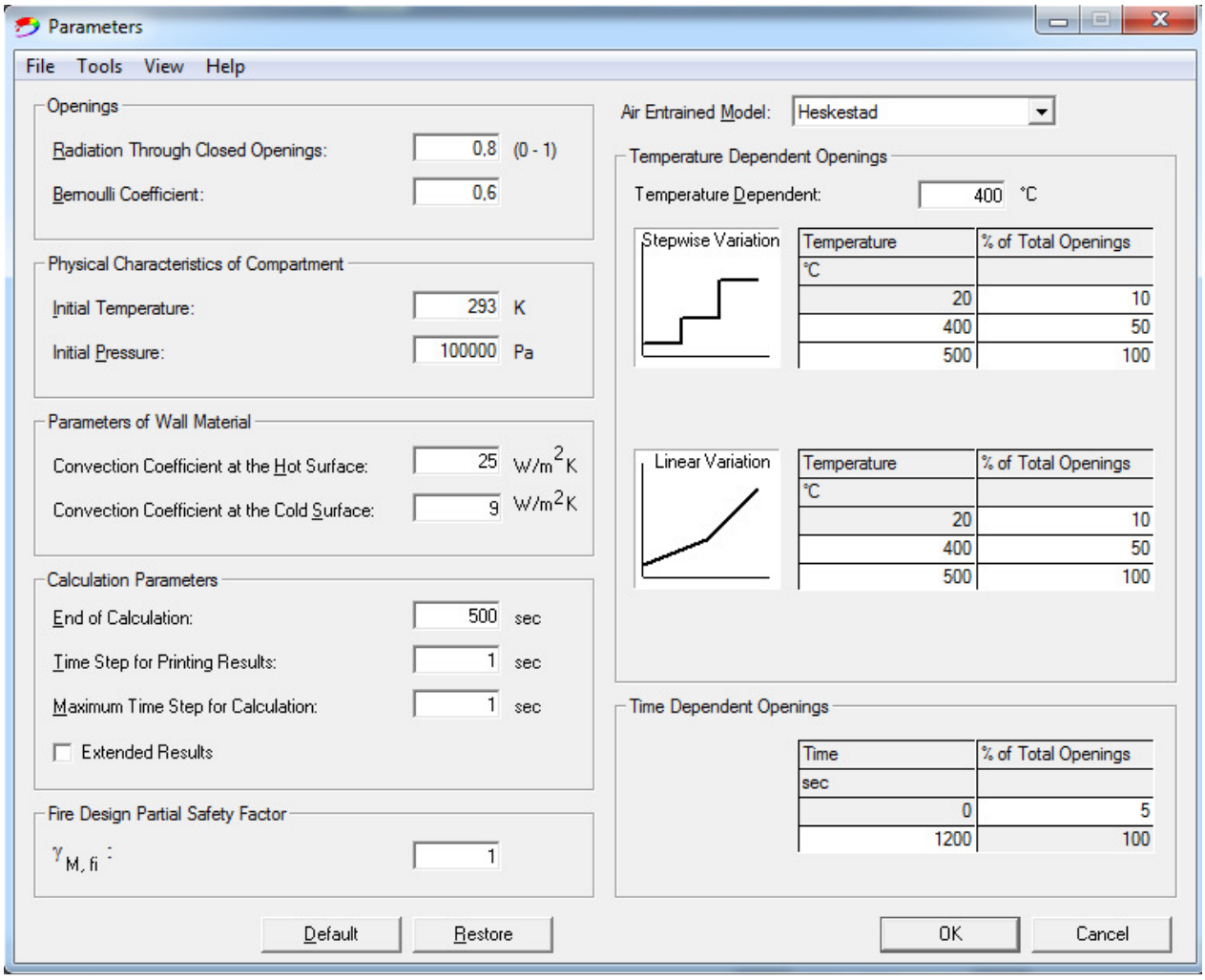

Figure 2.5 Parameters

Appendix 3 – Alternative approach iterative calculation process

Alternative approach

As the pressure depends on the magnitude of the pressure at the last time step, another approach is used to create a closer approach for the pressure curve. As openings in Ozone can also be inserted as temperature or time dependent, the effect of a temperature dependent variation for the size of the slit is observed. However, only one intermediate point between the moment of ignition and the pressure peak can be added in the programme. Therefore, a linear variation is chosen. Table 3.1 shows the input that is required for this approach.

Table 3.1 temperature dependent linear variation of the size of the slit

Temperature [^{0}C]	% of total opening
20	To determine percentage
T_1	To determine percentage
T_2	100%

As can be observed in Table 3.1, in Ozone only two temperatures can be used to create an adjusted slit. As the absolute pressure peak must be approximated T_2 must be used for the pressure peak. T_1 can be used for an intermediate point.

The best position of the intermediate point is expected to be the point in the middle between the moment of ignition and the moment of the pressure peak. Therefore, the position for the intermediate point will be at T_1 = 50 s. The best approximation for the size of the slit is equal to the method as applied in Figure 8, and is the iterative calculation process. It appeared that the influence of the size of the slit on the temperature curve is negligible. So for Table 3.1, both T_1 and T_2 can be filled in (40 ^{0}C for the T_1, and 250 ^{0}C for T_2). However, as a result of the Ozone interface, the size of the slit of the intermediate point at T_1 must be expressed as a percentage of the size of the slit of the maximum pressure. So now must be dealt with two variables; one for the percentage of the slit at T_1 = 50 s. with respect to the size of the slit at T_2 = 93 s., which is also unknown. However, as a result of this approach, the size of the slit must follow from the size of the slit at T_1.

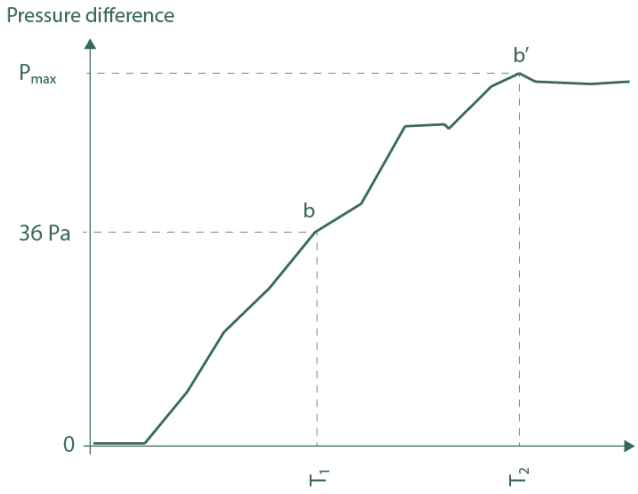

Figure 3.1 Principle adjusted pressure curve based on temperature dependent linear variation of the size of the slit

With respect to the size of the slit for T_1, it can be determined with respect to the moment of ignition that the equivalent surface is 0.2808 m^2. The equation for determining the percentage with respect to the equivalent surface can be defined as:

$$Percentage\ of\ opening\ at\ 50\ s. = \frac{0.02808\ m^2}{A_e\ corresponding\ to\ P_{max}} * 100\% \qquad (3.1)$$

On the basis of point b, as depicted in Figure 3.1, the magnitude of the pressure peak b' can be determined. This number must be determined by trial and error in the same way as the iterative calculation process. The required percentage for point b can then be determined. If the estimated pressure and so the percentage is correct, the line will intersect the 36 Pa at T_1. The result can be seen in Figure 3.3.

It can be observed that with this approach the pressure peak will be 84 Pa, which is 33% higher compared to the results from Figure 14. This shows that there is indeed an underestimation of the pressure peak as a result of the used approach. Between t = 0 s. up to t = 40 s. and t = 60 s. up to t = 70 s. the pressure curve shows the linear expected behaviour. Between t = 40 s. up to t = 60 s. and t = 70 s. up to t = 90 s. the line shows behaviour which cannot be explained.

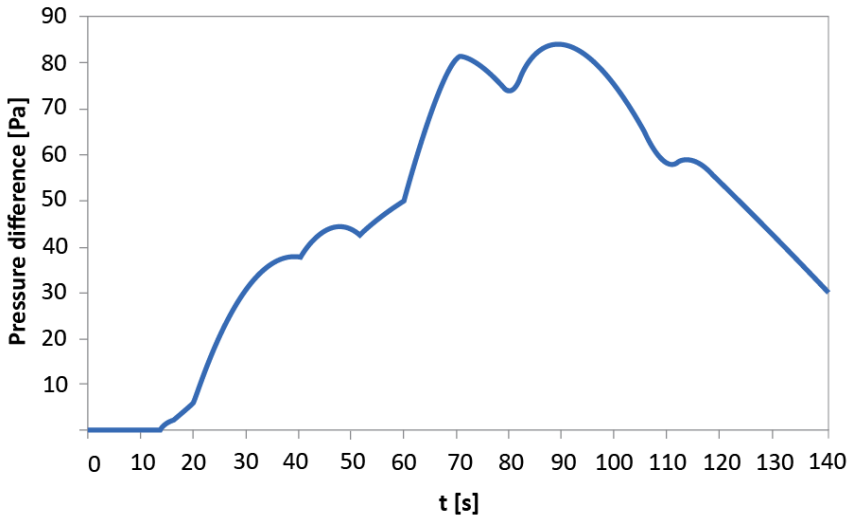

Figure 3.2 adjusted pressure curve based on temperature dependent linear variation of the size of the slit

In the same manner, more fitted openings can be added as time dependent for a closer approach of the equivalent size of the slit. However, this will result in 4 unknown variables. This will exceed a practical limit as in this situation it is hard to define the correct percentages as the line must intersect two and three points respectively, and must be determined by trial and error.

In addition to a stepwise increase of the opening, the effects of a linear increase of the opening is examined. It appeared that a linear increase of the opening result in higher pressure differences, and therefore a better approach for determining the size of the slit. However, when the size of the opening is compared to the occurring pressure difference at point b, it appeared that the equivalent opening is very small with regard to the occurring pressure. Therefore, a linear increase of the opening seems not be a valid approach.

Appendix 4 – Uncertainties in simulations

Uncertainties in calculations

In engineering, different classes of uncertainty can be distinguished [25]. In order to make statements about the uncertainty of the results and how the uncertainty affects the results, it is important to have an understanding at which levels uncertainties are introduced and with which magnitude in order to control the uncertainties. In Figure 4.1 [25], the different levels at which uncertainties are introduced are depicted. The factors 'resources' and 'assumptions' are generally difficult to identify and quantify. The uncertainties introduced in these categories depends on the models that are available, the choice of the analysis method, to which extent the process is described etc. The uncertainty in mathematical models is linked to the first two categories and is expressed in the results of the mathematical model. If this can be quantified depends on the model type. It is obvious that the output of the model depends for a significant part on the input parameters. Uncertainties can even be propagated by the mathematical model. Therefore the input parameters are often subject to uncertainty. Uncertainty for the input can be caused by natural variation or a lack of knowledge [25].

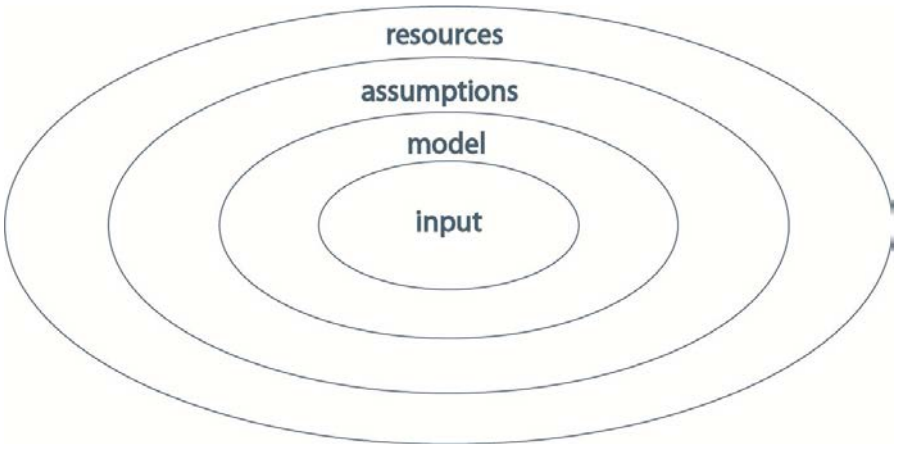

Figure 4.1 Categories in which uncertainties can be introduced [25]

The uncertainties of all of the different categories are often merged in the results of the uncertainty analysis and cannot be quantified in the underlying layers separately. In these results two types of uncertainty can be distinguished. Type A uncertainties are characterised as natural stochastic variations. Type B uncertainties are caused by a lack of knowledge.

The choice of the model determine the accuracy of the predictions. From scientific point of view there is a difference between a research in which statements are made about real world conditions instead of laboratory conditioned experiments. Therefore it must always be considered to what purpose the model is developed, and what the scope of the predictive results of the model is and so how the two types of uncertainty are incorporated in the results. Real world predictions will never be exact and therefore it is important to have knowledge about the range of applicability.

The used simulation programme Ozone can be classified as a time-dependent deterministic model with multi-variable output [25]. Characteristic for this model is that the input data exists of a limited input parameters as described in paragraph 4.1 of the report (x_1,x_2,…,x_n). Subsequently, the mathematical models present the output (y_1, y_2, ..., y_n) for inter alia the RHR, hot and cold zone temperature, fire area, oxygen mass and air pressure as time-dependent deterministic values. This process is shown schematically in Figure 4.2 [25]. As discussed in paragraph 4.1 of the report, a model to adjust the slit on the pressure peak is added manually and this is no part of the simulation programme. The adjustment of the slit is just a adaption on the input parameters.

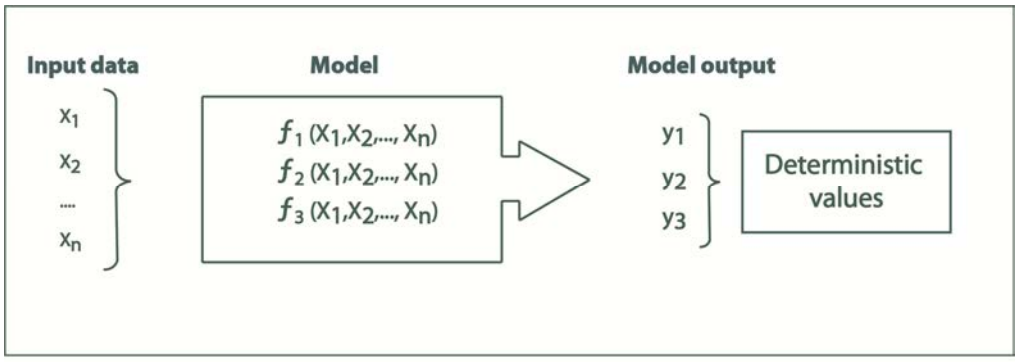

Figure 4.2 Schematic overview Ozone as time-dependent deterministic model [25]

Appendix 5 – Parameter study results

The adjustments which results in higher pressures have been depicted in the Figures 5.1 and 5.3 up to 5.6. For every graph the equivalent surface of the slit is already adapted to the occurring pressure peak.

Rate of Heat Release

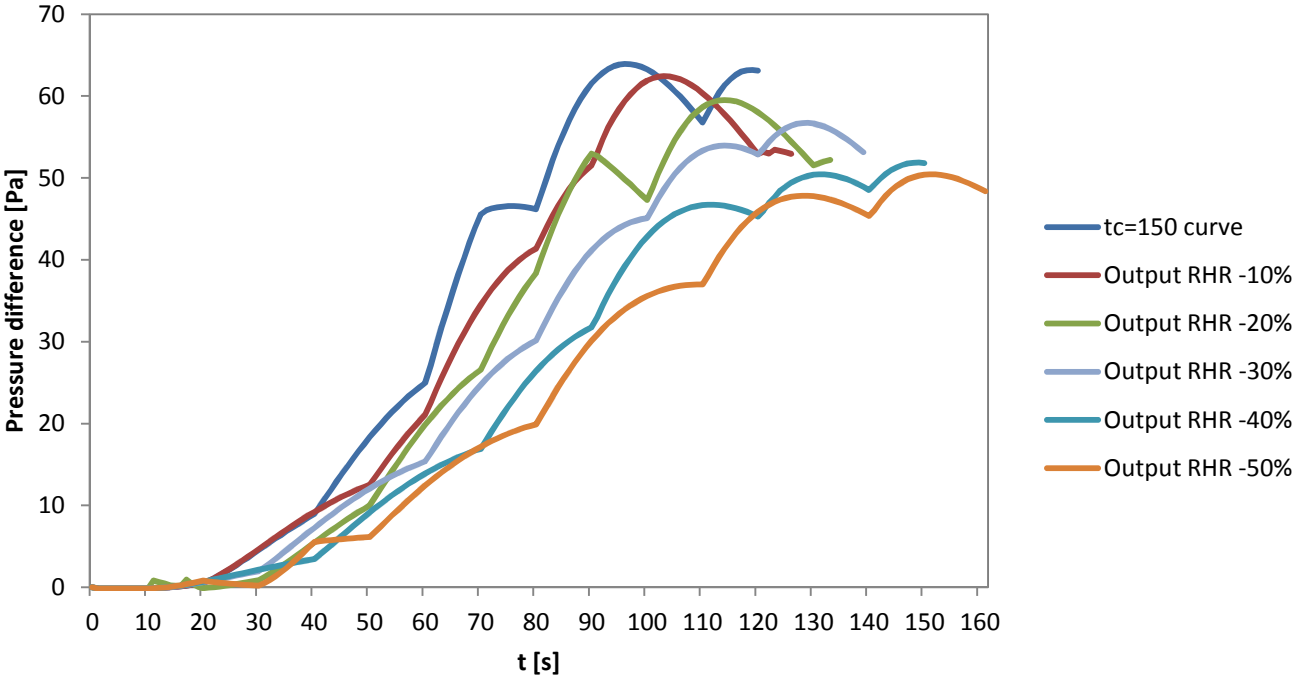

Figure 5.1 Influence on the pressure curve of varying the input Rate of Heat Release

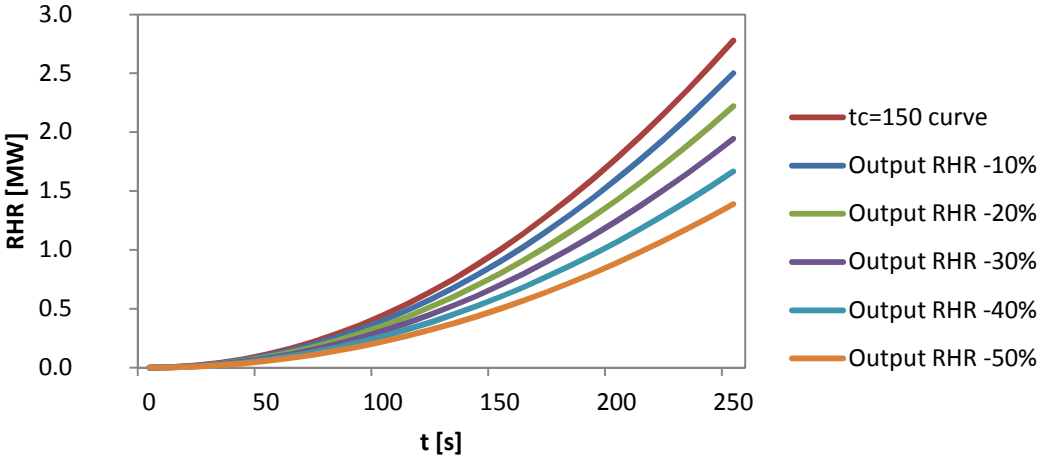

Figure 5.2 Input RHR

The reference line corresponds to the fast growth curve, the t_c = 150 curve. For every step the RHR is reduced with 10%. For the first 50 s. after ignition the curves in Figure 5.1 shows inexplicable behaviour towards the reference line and each other. After 50 s. the lines show that the less steep the input RHR curve is, the lower the pressure peak that occur is. The lower RHR cause a longer fire duration. The difference in fire duration for the reference line and the curve with a 50% decreased RHR is 40 seconds. The pressure peak drops from 64 Pa from the reference line to 48 Pa which is a

difference of 16 Pa. The reduction of the pressure peaks shown a non-linear behaviour. It can be noticed that the absolute pressure peaks occurs at a later stage in the fire when the RHR is lower.

$q_{v;10}$

The reference $q_{v;10}$ value represents the maximum amount of infiltration conform the passive house concept which is 0.15 $dm^3/s.m^2$ floor surface. As the floor surface is 20 m^2 this reference amount of infiltration is 15 dm^3/s. For every simulation this amount of infiltration is decreased with 10%. This results in the pressures as depicted in Figure 5.3. As could be expected the magnitude of the pressure increase when the amount of infiltration decrease. In the graph below the pressure peaks are depicted. The pressure peaks seems to be quadratic with the decrease of the amount of infiltration. The moment of the pressure peak after ignition remains the same and occurs after 97 seconds.

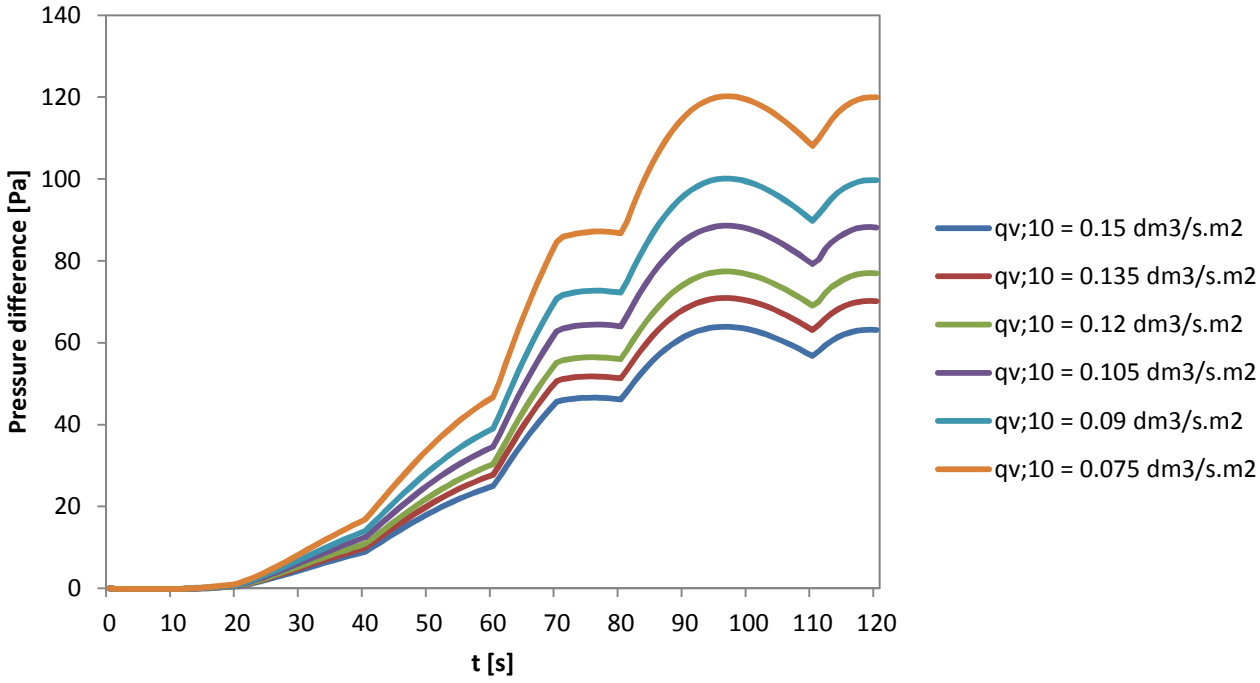

Figure 5.3 Influence on the pressure curve of varying the amount of infiltration

Volume room

As described in paragraph 4.1 the floor space of the enclosure is 20 m^2. In this analysis the floor space increased for every step with 10%. For the height of the enclosure 2.6 m. is maintained. As infiltration the maximum amount of 0.15 $dm^3/s.m^2$ for passive buildings is maintained, as the floor area of the entire dwelling is normative with respect to the amount of infiltration of the fire compartment. The pressure curves shows similar behaviour for the first 90 seconds after ignition. The time that the pressure peaks occur is slightly different and also the pressure peaks are significantly higher for a larger enclosure. The values lie between the 64 Pa for the reference line up to 81.1 Pa for the enclosure which is 50% larger. In the graph below the pressure peaks are depicted.

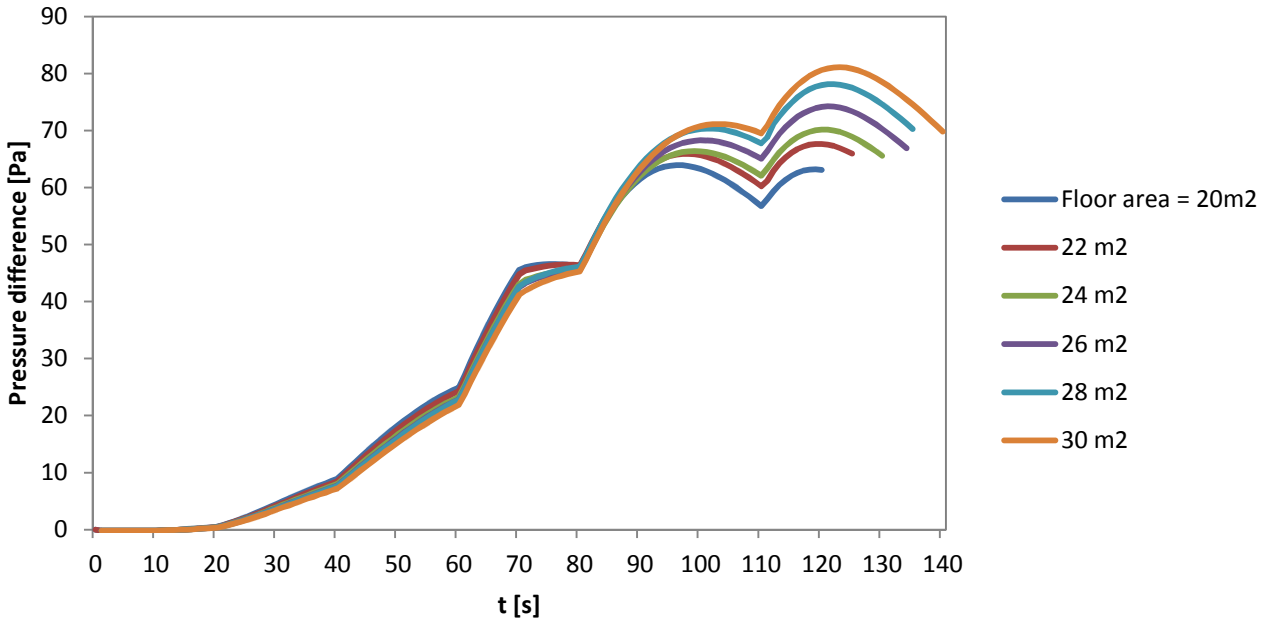

Figure 5.4 Influence on the pressure curve of varying the size of the fire room

Mechanical ventilation

For the reference ventilation rate the in the building code prescribed ventilation rate is applied. As described in paragraph 4.1 minimum amount of ventilation is 0.018 m^3/s. For every step the ventilation rate is increased with 10%. The results shows that the difference between the lines for the first 90 s. is almost negligible. The pressure peaks differs from 64 Pa when the ventilation rate is conform the building code up to 63.6 Pa when the ventilation rate is increased with 50%. However, when the ventilation is shut down the magnitude of the pressure peak is 62 Pa. The output is depicted in Figure 5.5.

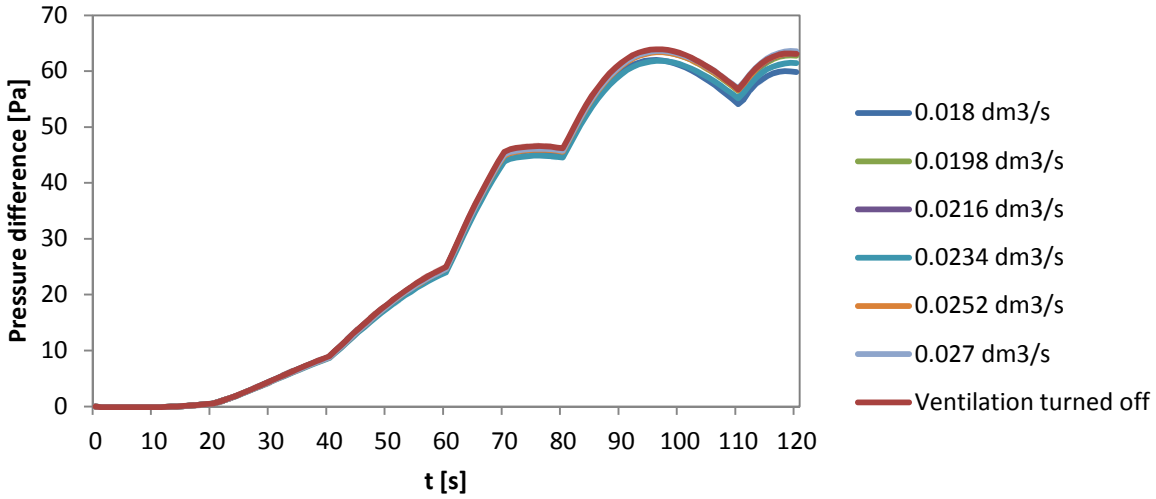

Figure 5.5 Influence on the pressure curve of varying the ventilation rate

Type of enclosure

The enclosure and material of the wall have an influence on the pressure build-up as each construction type has its own thermal inertia and ability for heat accumulation. In the first moments after ignition, thermal thick wall systems will extract heat from the fire enclosure and release heat during the decay period. Therefore the temperature will be overestimated for the first moments

after ignition and underestimated during the decay period. Therefore the characteristics of three common wall materials are used as input and compared with the reference line which refers to an adiabatic situation. The results show that the application of concrete and limestone has limited influence on the pressure. While the pressure peak for the reference line is 64 Pa, these pressure peaks for concrete and limestone are 63.3 Pa and 63.5 Pa respectively. The application of a timber frame construction results in a pressure peak of 68 Pa. This is remarkable as it would be expected that an adiabatic situation results in a higher temperature increase and so higher pressure differences.

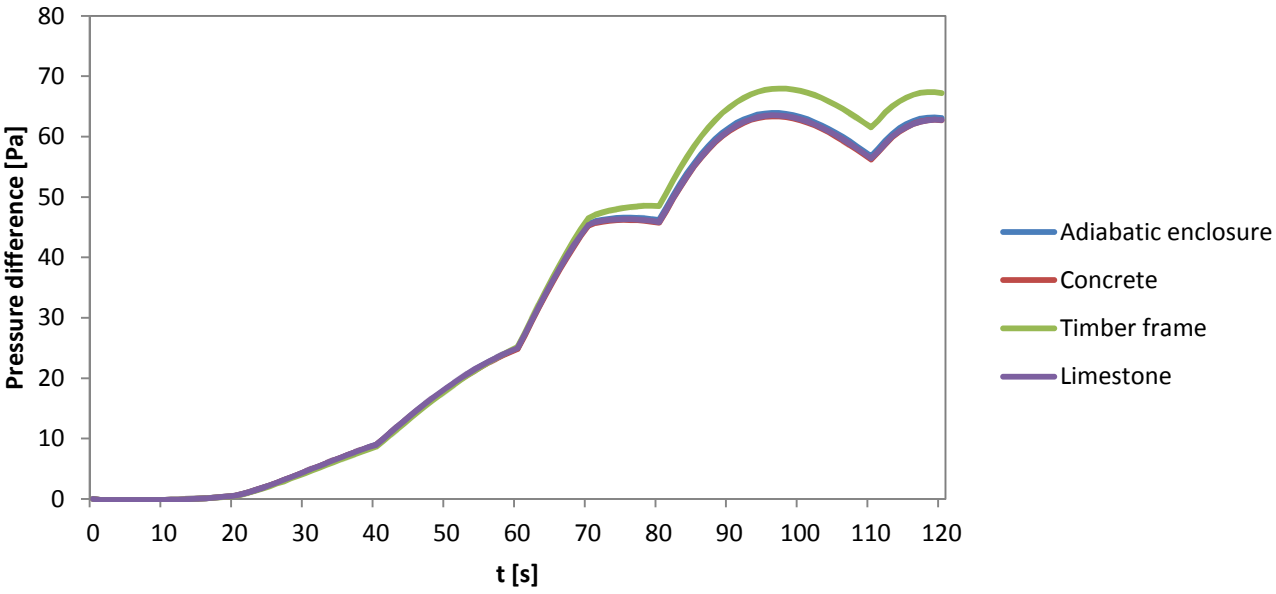

Figure 5.6 Influence on the pressure curve of varying the building system

R_c value enclosure

In this analysis it is assumed that the enclosure is adiabatic. In practice, the insulation will be placed at the outside of the wall. Only when the heat reaches the insulation material the R_c- value of the enclosure becomes a variable of interest. However, the inner wall will have a certain thermal inertia. For all common building systems the walls are too thick for the heat to penetrate the whole thickness of the wall during the short calculation period. Although the R_c- value is expected to play a role in the fire behaviour in well insulated dwellings, this value will not have an direct effect on the pressure behaviour and therefore it is not taken into account in this analysis.

On the next page the results are placed in a Table 5.1. In Table 5.2 all pressure differences as a percentage can be found. These data is the basis of the Pareto analysis.

Table 5.2 Peak pressures

Variable	-50%	-40%	-30%	-20%	-10%	Basis	+10%	+20%	+30%	+40%	+50%
RHR	50.4 Pa	51.8 Pa	56.7 Pa	59.5 Pa	62.4 Pa	64.0 Pa	63.2 Pa	68.0 Pa	70.0 Pa	72.6 Pa	77.4 Pa
$q_{v;10}$ [dm^3/s]	120.2 Pa	100.1 Pa	88.6 Pa	77.4 Pa	71.0 Pa	64.0 Pa	58.2 Pa	53.3 Pa	49.8 Pa	46.7 Pa	42.8 Pa
Volume room [m^3]	42.1	47.3 Pa	52.4 Pa	55.4 Pa	60.4 Pa	64.0 Pa	65.9 Pa	70.2 Pa	74.2 Pa	78.2 Pa	81.1 Pa
Mechanical ventilation [dm^3/s]	63.0 Pa	62.2 Pa	63.4 Pa	63.5 Pa	63.7 Pa	64.0 Pa	63.5 Pa	63.6 Pa	61.8 Pa	63.4 Pa	63.6 Pa
Type of enclosure [-]	-	-	-	-	-	64.0 Pa	63.3 Pa concrete	68.0 Pa Wooden frame	63.5 Pa Lime-stone	-	-
Rc value enclosure [m^2K/W]	64.0 Pa	64.0 Pa	64.0 Pa	64.0 Pa	64.0 Pa	64.0 Pa	64.0 Pa	64.0 Pa	64.0 Pa	64.0 Pa	64.0 Pa

Table 5.3 Pressure change as a percentage*

Variable	-50%	-40%	-30%	-20%	-10%	Basis	+10%	+20%	+30%	+40%	+50%
RHR	-21.25 %	-16%	-11.4%	-7%	-2.5%	0%	-1.25%	6.3%	9.4%	13.4%	20.9%
$q_{v;10}$ [dm^3/s]	87.8%	56.4%	38.4%	20.9%	10.9%	0%	-9.1%	-16.7%	-22.2%	-27.0%	-33.1%
Volume room [m^3]	-34.2%	-26.1%	-18.1%	-13.4%	-5.6%	0%	3%	9.7%	15.9%	22.2%	26.7%
Mechanical ventilation [dm^3/s]	-1.6%	-2.8%	-0.9%	-0.8%	-0.5%	0%	-0.8%	-0.6%	-3.4%	-0.9%	-0.6%
Type of enclosure [-]	-	-	-	-	-	0%	-1.1%	-0.8%	6.3%	-	-
Rc value enclosure [m^2K/W]	0%	0%	0%	0%	0%	0%	0%	0%	0%	0%	0%

* Percentages are with respect to the basic value of 64 Pa in the grey column

Appendix 6 – Results probabilistic scenario analysis

PROBABILISTIC CALCULATION
PRESSURE BUILD-UP IN DWELLINGS

(t^2 CURVE)
CASUS PASSIVE DWELLING 100M^2

	variant study boundary conditions		deterministic avarage x	 pressure peak Pa	sensitivity analysis variation V	 st. deviation s	 variant x + dx	 pressure peak Pa
RHR	rate of heat release	MW	0.64	64	0.5	0.32	0.96	90
t_c	time constant	s	150	64	0.4	60	210	48
mv	mechanical ventilation	dm^3/s	18	64	0.38	6.84	24.84	65
$q_{v;10}$	infiltration	dm^3/s	15	64	0.45	6.75	21.75	59

probability distribution		
dt/dx	s·dt/dx	(s·dt/dx)^2
81.25	26	676
-0.26666667	-16	256
0.14619883	1	1
-0.74074074	-5	25
	variance (P)=	958
	s (P)=	30.9515751

	normative event:	local fire			
	floor area [m^2] :	100			
	lifetime of the building [jr]:	55			
Probability	occurrence of fire [m^{-2}]:	4.00E-05			
	risk on fire (P_{fi}):	1.60E-04			
		p(f)	**p(f|fi)**	**beta (f|fi)**	
	CC2: beta(f) > 3,8	**7.23E-05**	**4.52E-01**	**0.12**	
	CC3: beta(f) > 4,3	8.54E-06	5.34E-02	1.61	

reliability and exceedance probability			
P [Pa]	s(t)	beta ($\Delta P \mid P_{fi}$)	P($\Delta P \mid P_{fi}$)
0	30.951575	-2.067746143	0.98066805
10	30.951575	-1.744660808	0.959478035
20	30.951575	-1.421575473	0.922425235
30	30.951575	-1.098490139	0.864004739
40	30.951575	-0.775404804	0.780949751
50	30.951575	-0.452319469	0.674480574
60	30.951575	-0.129234134	0.551413806
70	30.951575	0.193851201	0.423146197
80	30.951575	0.516936536	0.302600231
90	30.951575	0.840021871	0.200448062
100	30.951575	1.163107206	0.122393004
110	30.951575	1.48619254	0.0686141
120	30.951575	1.809277875	0.035203922
130	30.951575	2.13236321	0.0164885
140	30.951575	2.455448545	0.007035445
150	30.951575	2.77853388	0.002730241
160	30.951575	3.101619215	0.000962327
170	30.951575	3.42470455	0.000307734
180	30.951575	3.747789885	8.91998E-05
190	30.951575	4.070875219	2.34184E-05
200	30.951575	4.393960554	5.5652E-06

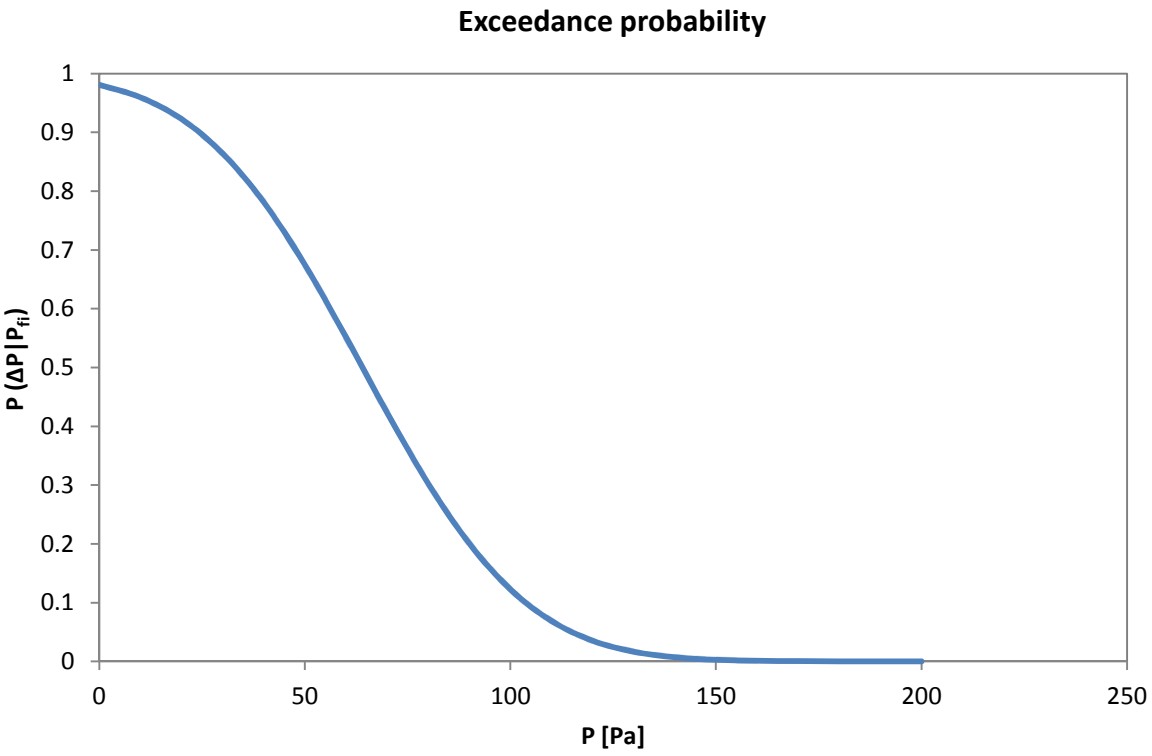

Figure 6.1 Probabilistic scenario analysis; Exceedance probability scenario Chapter 3

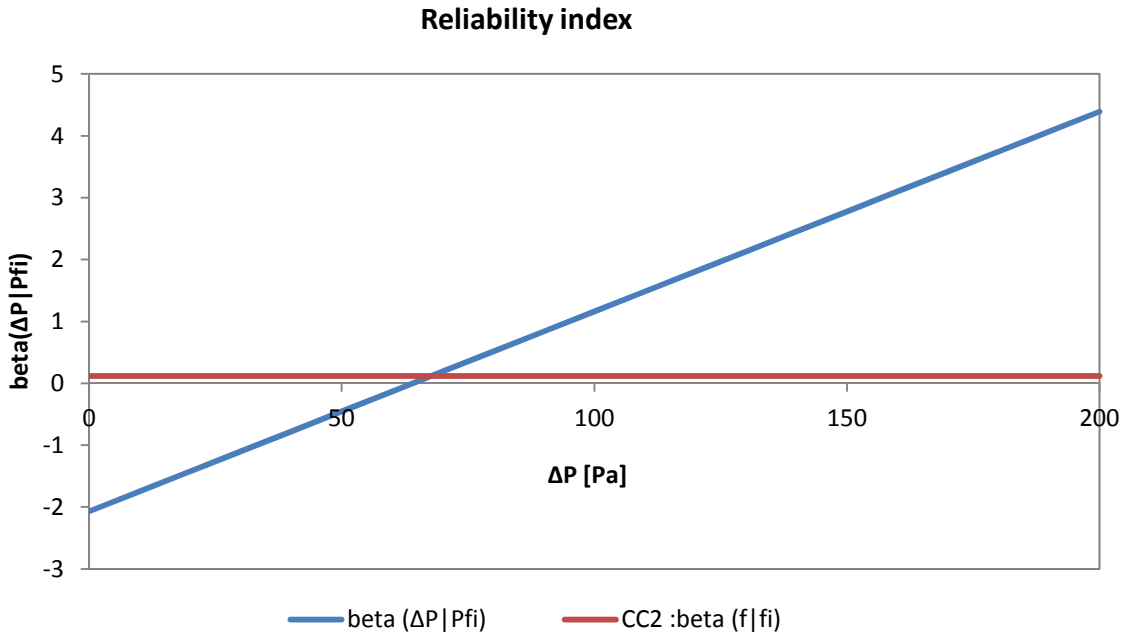

Figure 6.2 Probabilistic scenario analysis; Reliability index scenario Chapter 3

Appendix 7 – Multiple linear regression model

SUMMARY OUTPUT

Regression data	
Multiple correlation coefficient R	0.9478
R Square	0.8984
Adjusted R Square	0.8872
Standard Error	6.3947
Observations	21

ANOVA

	Degree of freedom	*Sum of square(SS)*	*Mean square (MS)*	*F*	*Significance F*
Regression	2	6514.5	3257.2	79.6	1.1 E-09
Residual	18	736.0	40.8		
Total	20	7250.5			

	Coefficients	*St. error*	*T- Stat*	*P- value*	*Lower 95%*	*Upper 95%*
Intercept	102.8	9.5	10.8	2.6 E-09	82.8	122.7
$A_{\text{fire room}}$	1.7	0.3	4.9	9.8 E-05	1.0	2.4
$q_{v;10}$ value	-471.5	40.6	-11.6	8.6 E-10	-556.9	-386.1

Appendix 8 – Calculation insulation covering

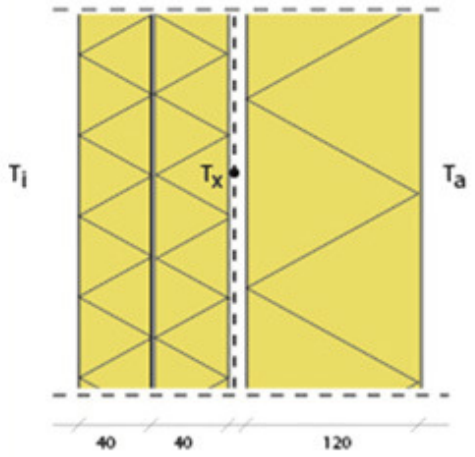

Figure 8.1 Existing enclosure covered with the foil and rockwool

$$T_a = 20\ ^0C = 293\ K$$
$$T_i = 235\ ^0C = 508\ K$$
$$R_d\ rockwool = 1.05\ m^2K/W$$

$$R_{tot} = 0.04 + 2 * 1.05 + 3.5 + 0.13 = 5.77\ m^2K/W$$

$$\frac{T_i - T_x}{T_i - T_a} = \frac{r_i + r_{rockwool}}{R_{tot}}$$

$$\frac{508 - T_x}{508 - 293} = \frac{2.14}{5.77}$$

$$\frac{508 - T_x}{215} = 0.371$$

$$T_x = 428.26K$$
$$T_x = 155.26\ ^0C$$

On the basis of some simple calculations the required thickness of the rockwool can be determined for a steady state situation. For these calculations, an inner temperature of 235 ^{0}C is maintained which is based on the Ozone calculations discussed later in this chapter. However, the maintained temperature will not be present during the entire time the fire is burning. This simplification results in a higher temperature load as it is now assumed that the temperature is at a constant value of 235 ^{0}C, instead of an increasing temperature which will be present during the experiments. This simplification make it possible to estimates quickly the required thickness of the insulation.

The calculation shows that for the front façade it is sufficient to apply two layers of 40mm Rockwool Bouwplaat 210 to protect the foil, as the calculated temperature of 155.26 ^{0}C at point T_x in Figure 40 will be not be reached in a dynamic state situation.

Voltra model

In the model a horizontal section at the location of the insulated façade is modelled into Voltra as this is the most critical part. In the Voltra model, there is no difference in heat exposure between a horizontal part right above the fire or a vertical part in the wall. Also viewing angles are not taken into account in the calculation. So the calculations are also valid for the screws and rosettes directly above the fire.

As the input must fit in an orthogonal grid the surface of the rosette and screw is recalculated into a squared surface. For the material of the screw and rosette, steel is maintained. As fire curve the standard fire curve is maintained. This approximation is valid as it results in higher inner temperatures in the enclosure compared to the calculated temperatures in Ozone for the test setup simulated in paragraph 4.2. Conform the standard fire curve, the inner temperature is about 400 ^{0}C after 120 seconds. The calculation is done in time steps of 10 s. during a time period of 120 s. In the model two output nodes are inserted; one at the position of the rosette and the second at the end of the screw at the position of the foil. The results are depicted in Figure 8.2 and 8.3. On the basis of the output it can be concluded that at the location of the foil the temperature exceeds no critical value.

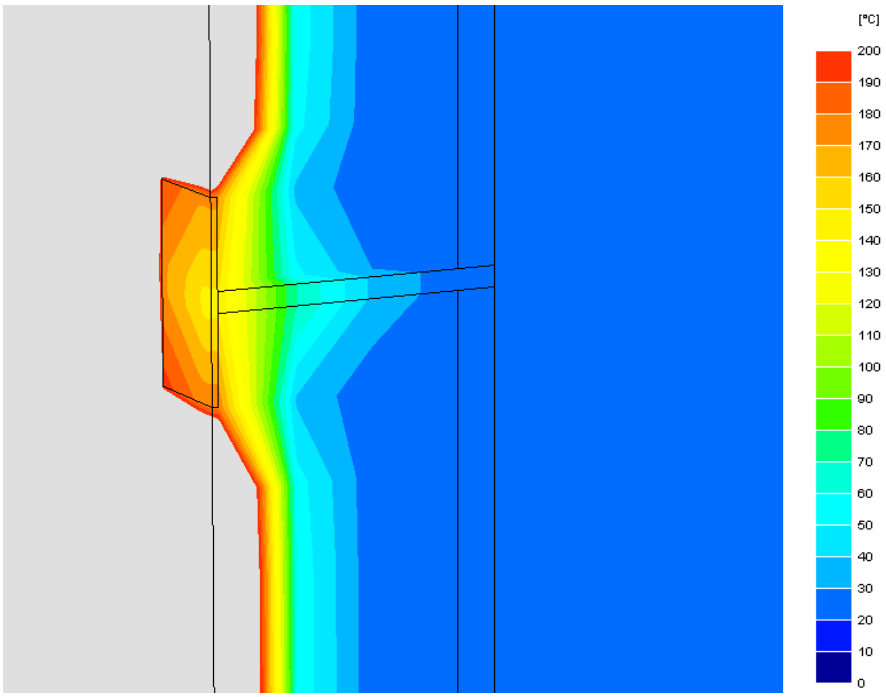

Figure 8.2 Voltra temperature output at 120 s.

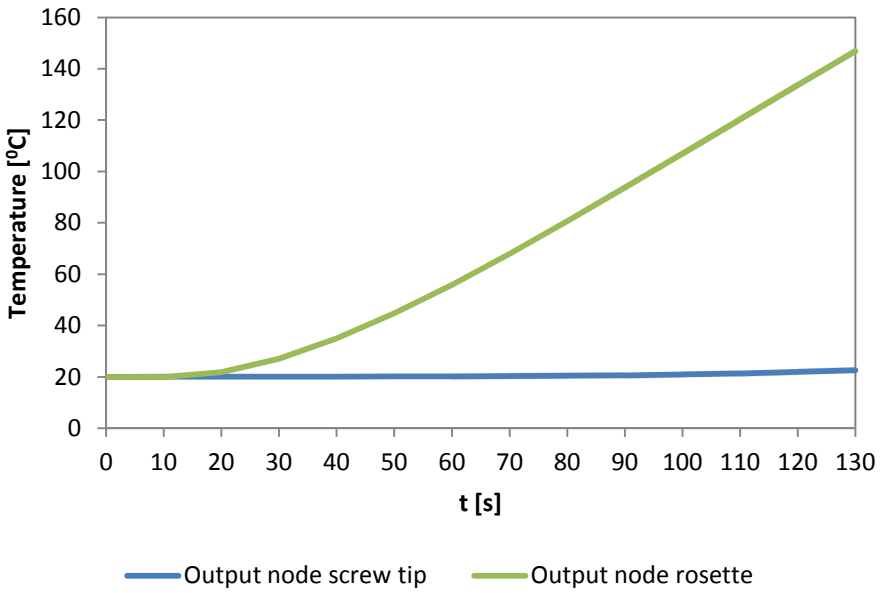

Figure 8.3 Temperature of the output nodes at the location of the rosette and screw tip at the location of the vapour resistant and airtight foil

Appendix 9 – Results blowerdoor test

During the blowerdoor test, a pressure difference between the enclosure and surrounding is created. Then, the amount of air which flows through the leaks is measured at different pressure differences generated by the fan. This will be carried out conform the standard NEN 2686 *Air permeability of Buildings – Measurement methods*.

According to the standards, the amount of air flowing through the leaks must be defined at six different pressure differences, whereby the smallest pressure is at least 15 Pa and the largest 100 Pa. The difference between two consecutive points must be 8- 15 Pa. The six measured air flows are placed in a pressure- volume flow characteristic graph, wherein a regression line is drawn. The error between a certain point at which the air flow is measured and the regression line may not exceed 5%. The output is given as an n- value. This n- value describes the infiltration rate per hour; the volume of air flowing through the façade per hour in relation to the volume of the space. Therefore, the unit for the n- value is h^{-1}. From the pressure/ volume characteristic graph the $q_{v;10}$ value with the unit $dm^3/s.m^2$ can be abstracted. This value describes the volume of the air flow at a pressure difference of 10 Pa.

Infiltration of the test setup

During the test day, the maximum hour average wind speed was 2.0 m/s and the maximum temperature was 24.3 ^{0}C. As a result of this temperature, the starting temperature for the experiments is defined at 30 ^{0}C. The used measuring equipment for the blowerdoor test exists of a Retrotec Q4E Automated Blowerdoor and DM-2A digital pressure gauge. Moreover, as back-up a second pressure gauge without time logger is used. For the blowerdoor test the enclosure is only put on overpressure as the expected main direction of the air flow during the experiments will be from inside to the outside. As a result of the small surface of the experimental setup in relation to the passive standards, the volume of the air flow through the enclosure during the blowerdoor test is small. Therefore it was not possible to carry out the measurements conform the standard NEN 2686, as the used equipment cannot detect such small air flow automatically. Therefore, the measurement points for the pressure differences at which the flow is measured, are determined manually. For determining the amount of infiltration 4 instead of the, conform the standard NEN 2686, required 6 reference points are used. These points, and the corresponding air flows of the enclosure can be seen in Table 9.1.

Table 9.1 Measurements

Pressure difference (ΔP_{facade})	Air flow volume ($q_{v;n}$)
36 Pa	4 dm^3/s
53 Pa	5 dm^3/s
147 Pa	12 dm^3/s
194 Pa	15 dm^3/s

The results can also be presented in a graph which can be seen in Figure 9.1. Through these point a regression line is drawn. The different measurement points are within the error range of 5%. The infiltration of the enclosure is determined at a n_{50} value of 1.01 h^{-1} and corresponds to a $q_{v;10}$ value of 0.173 $dm^3/s.m^2$. However, there may be a large influence of the used blowerdoor. These results must therefore be seen as the minimum performance of the enclosure with regard to the air-tightness. An overview of the results of the blowerdoor test can be found on the next page.

Air tightness of the building ($q_{v;10}$)

Measurement conform the standard NEN2686; Measurement carried out with Retrotec Q4E Automated blowerdoor`

Project data	
Project	Research at Troned
Date	05-09-2014

Measurement situation	
Heated floor area	7.9 m^2
Volume	17.7 m^3
Particularities	None

Measured values	
Pressure difference (ΔPa_{facade})	Air volume flow (q_v)
36 Pa	4 dm^3/s
53 Pa	5 dm^3/s
147 Pa	12 dm^3/s
194 Pa	15 dm^3/s

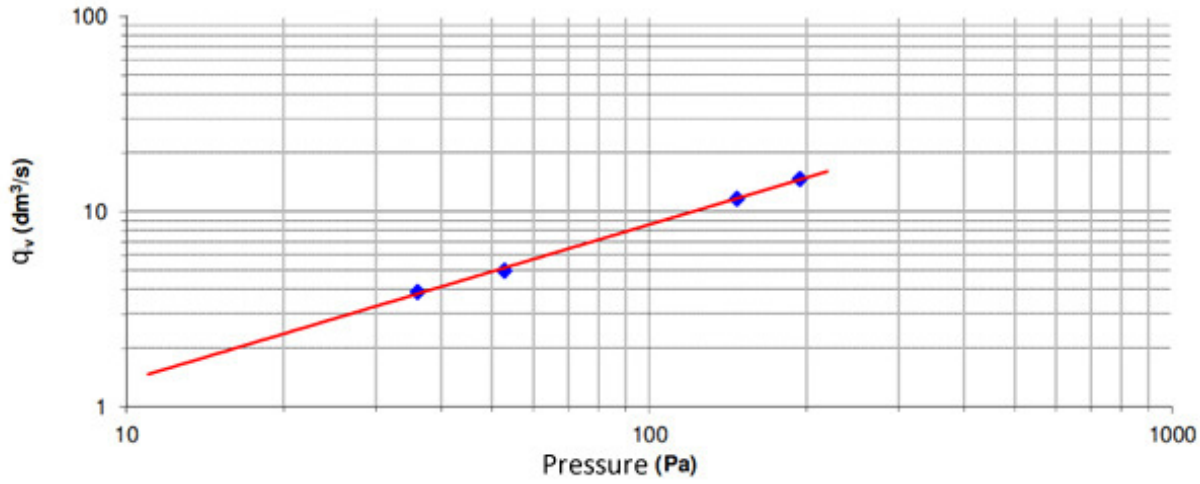

Figure 9.1 Pressure/flow characteristic

Measurement results		
air leakage coefficient (C)		**0.216**
flow exponent (n)		**0.7995**
equivalent surface leakage area (A_e)		**0.0001 m^2**
Air permeability negative pressure (q_v) at	**10 Pa**	**1.4 dm^3/s**
Air permeability per m^2 floor area		**0.173 $dm^3/s.m^2$**
Ventilation rate at	**50 Pa**	**1.01 h-1**

Appendix 10 – Simulation experimental scenarios

In order to predict the fire scenario within the enclosure for the experimental set up, simulations for all scenarios are carried out in accordance with the calculation method described in Chapter four – Computational approach. Compared to this described input, only the geometry of the enclosure with its corresponding values, as described in paragraph 4.1 of the report, is changed.

Scenario 1

Figures 10.1 up to 10.4 give an overview of the expected fire behaviour for the first scenario on the basis of the fast growth curve (t_c = 150 curve). As described earlier, the amount of infiltration is conform the passive house standard. This amount of infiltration is translated into a slit which is adjusted to the maximum occurring pressure using the iterative calculation process.

On the basis of the oxygen mass, it can be determined that the fire extinguishes or smother from 65 s. after ignition as a result of a lack of oxygen. During this period it is expected that the pressure increases gradually up to 485 Pa while the RHR is only 0.25 MW. The temperature will increase up to 204 ^{0}C.

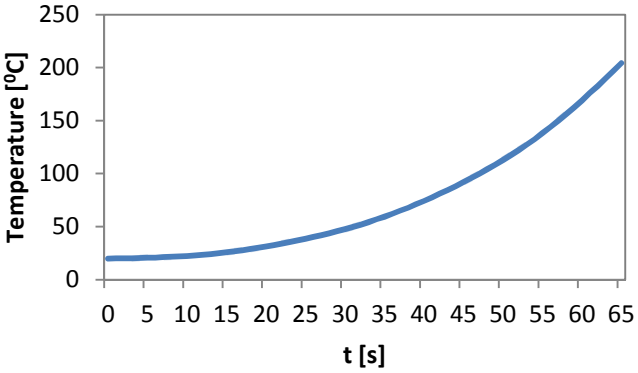

Figure 10.1 Temperature

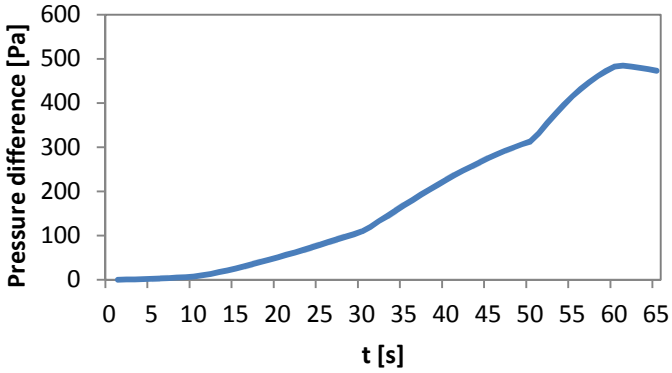

Figure 10.2 Pressure difference

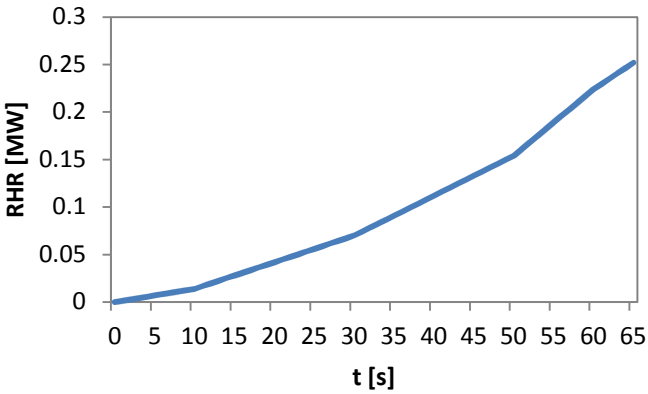

Figure 10.3 Rate of Heat Release

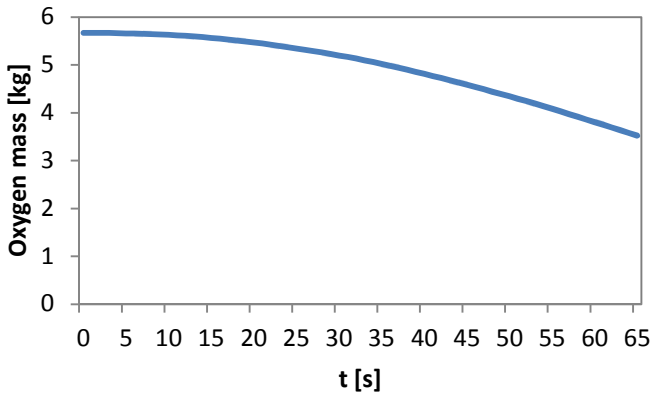

Figure 10.4 Oxygen mass

Scenario 2

These simulations can be conducted in the same way for scenario 2. The Figures 10.5 up to 10.8 give a complete overview of the expected fire behaviour within the enclosure. As described earlier the amount of infiltration is based on the approach that the fire room is a part of a dwellings of 100 m^2. Therefore, the $q_{v;10}$ value is based on 100 m^2 so, based on a $q_{v;10}$ value of 0.15 dm^3/s.m^2, the air flow amounts 15 dm^3/s. This is translated in a larger slit compared to scenario 1, and the slit is also adjusted to the maximum occurring pressure.

On the basis of the oxygen mass it can be determined that the fire extinguishes or remains smouldering after 65 s. after ignition, which is exact the same moment as in scenario 1. The Ozone model suggests the that the $q_{v;10}$ value has no influence on the fire duration, only on the magnitude of the pressure peak. During this period it is expected that the pressure increase up to 59 Pa while the RHR is only 0.25 MW. The temperature will increase up to 204 ^{0}C.

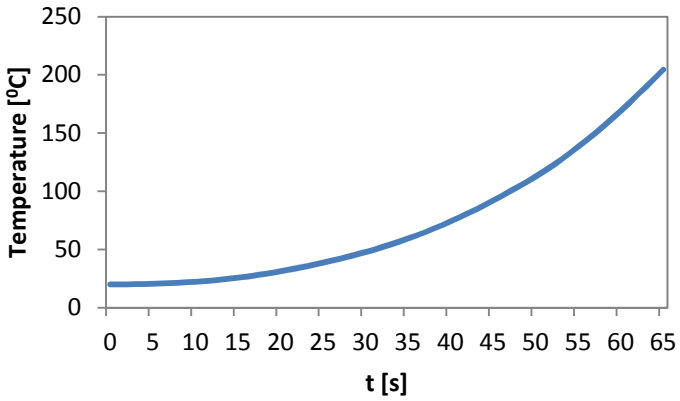

Figure 10.5 Temperature

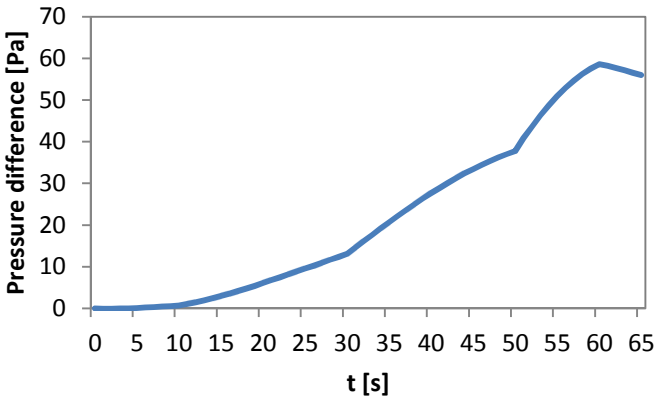

Figure 10.6 Pressure difference

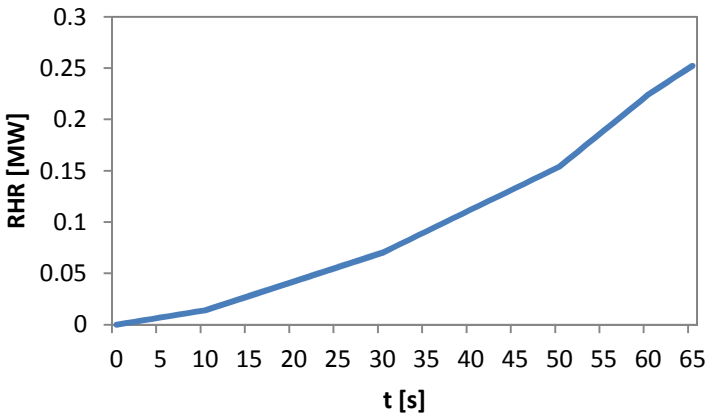

Figure 10.7 Rate of Heat Release

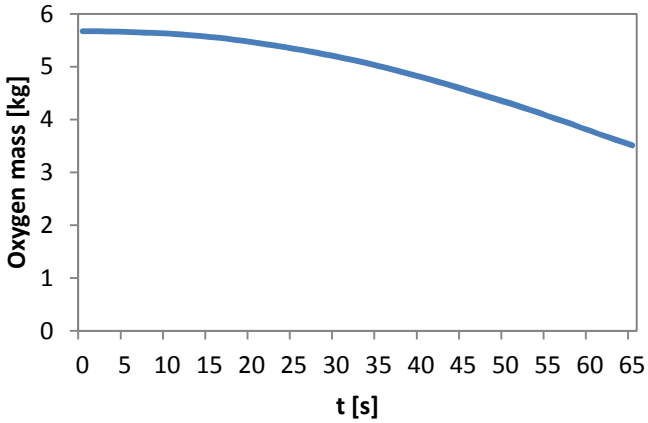

Figure 10.8 Oxygen mass

Scenario 3

In the third scenario all parameters are equal to scenario 2, only the RHR is halved. The $q_{v;10}$ value and so the size of the slit is equal to scenario 2, but the size of the slit is adjusted on the maximum occurring pressure to compensate the flow exponent of n = 0.5 in Ozone instead of n = 0.625 which is characteristic for such openings. Figures 10.9 up to 10.12 gives an overview of the expected results for scenario 3.

Halving the RHR compared to scenario 2 results in a maximum pressure of 39.7 Pa. As the RHR is lower, and so the oxygen consumption is lower, the fire extinguishes or remains smouldering after 85 s. At this moment the RHR will be 0.2 MW and a temperature of 203 ^{0}C will be reached. This is slightly lower compared to scenario 2.

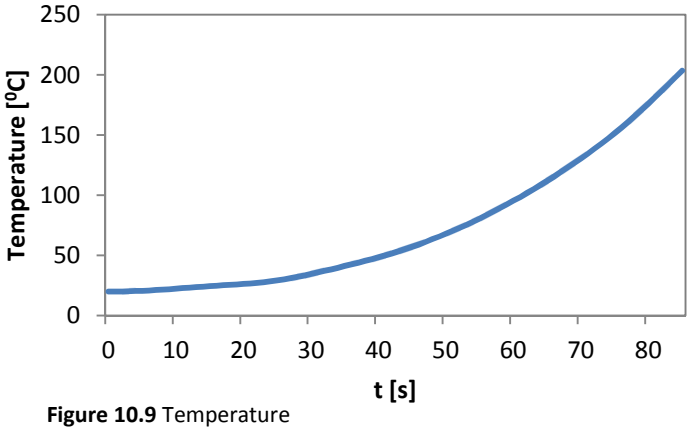

Figure 10.9 Temperature

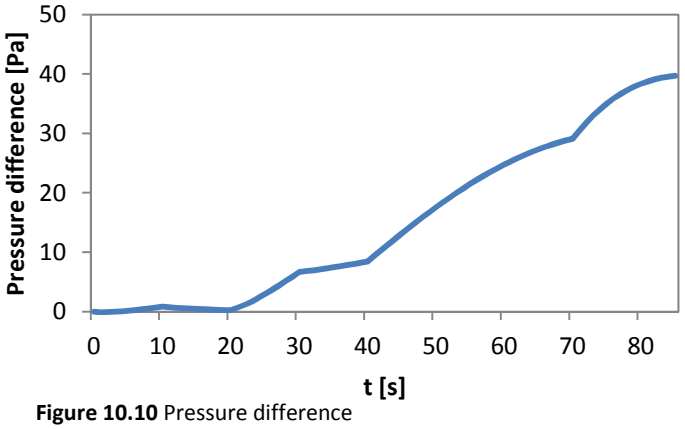

Figure 10.10 Pressure difference

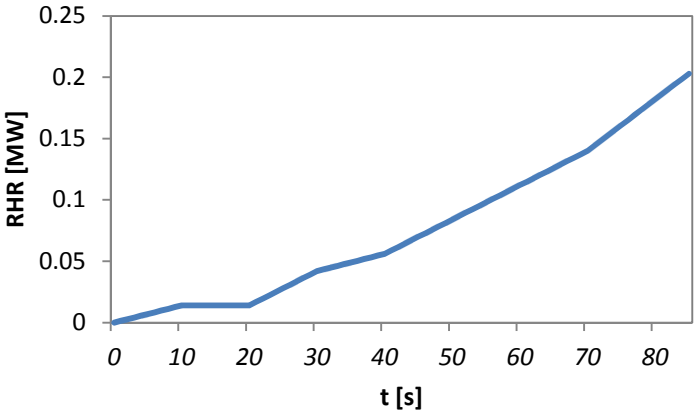

Figure 10.11 Rate of Heat Release

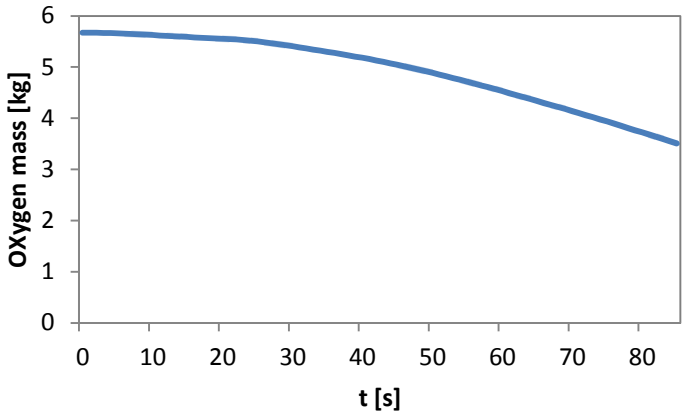

Figure 10.12 Oxygen mass

Scenario 4

Compared to scenario 2, only the $q_{v;10}$ value is doubled and is made 0.3 $dm^3/s.m^2$ for scenario 4. This results in a air flow of 30 dm^3/s. The slit is based on this $q_{v;10}$ value and adapted to the maximum occurring pressure. Figures 10.13 up to 10.16 gives an overview of the expected results for scenario 4.

The results show that a peak pressure of 24.5 Pa can be expected. It can be observed that the other graphs are exact the same as in scenario 2. The RHR is 0.25 MW after 65 s. After this moment the fire is expected to smother or extinguishes as a results of a lack of oxygen.

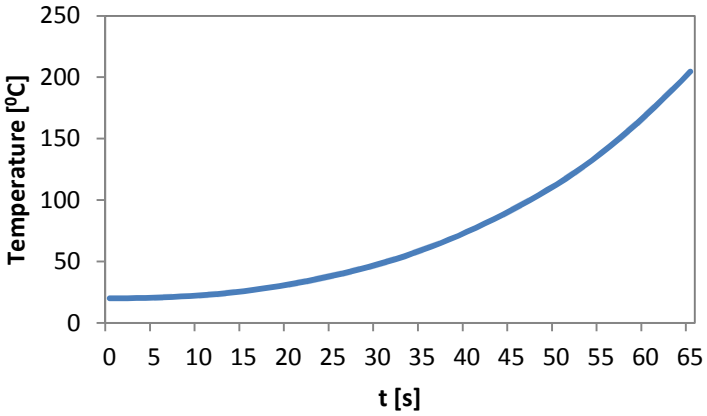

Figure 10.13 Temperature

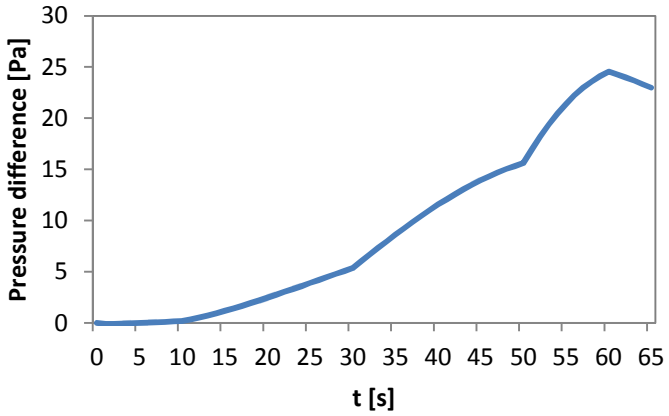

Figure 10.14 Pressure difference

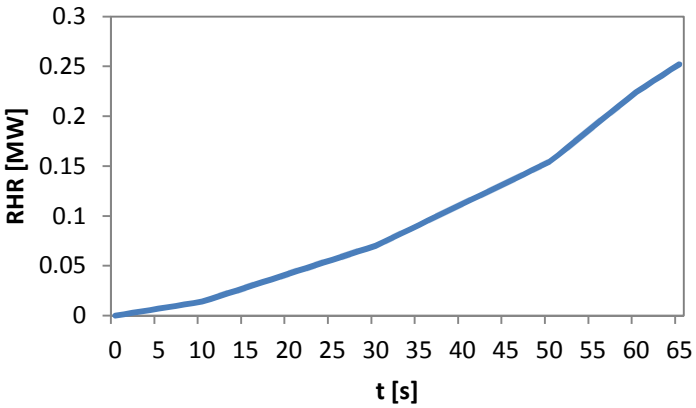

Figure 10.15 Rate of Heat Release

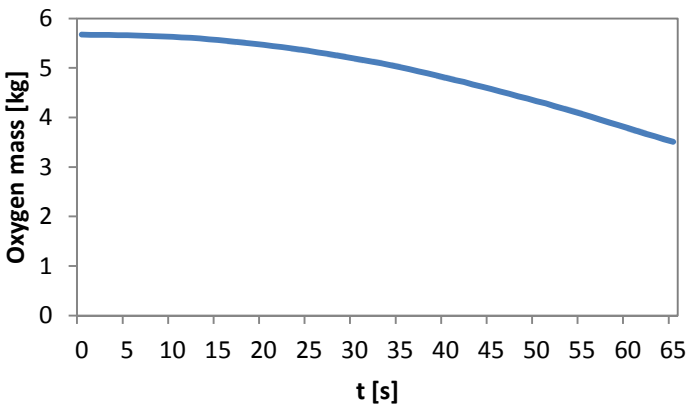

Figure 10.16 Oxygen mass

Appendix 11 – Fuel calculation experiments

A guidance for the required amount of fuel for the experiments can be abstracted from the simulated scenarios above. As described in paragraph 5.2 of the report, as fire source a pool fire will be used. The advantage of a pool fire is that it has a clean combustion, the RHR can be approached more closely and it allows the opportunity to conduct the experiments more time efficiently. In contrast to the used $t_c = 150$ curve used for the simulations, a pool fire will generate a constant RHR. Moreover, the full heat release is present from the moment of ignition. As fuel, 100% bio-ethanol will be used. The size of the pan fire must be chosen such that it compensates the fact that the full heat release is present after ignition. To this end, the constant RHR which results in similar magnitude of the pressure peak for scenario 1 and 2 is determined experimentally with the Ozone model. In Figure 11.1 the pressure curve of scenario 1 is depicted as a result of the $t_c = 150$ curve. Figures 11.2 and 11.3 shows the constant RHR which is required to produce an equal magnitude of the pressure peak. It has turned out that with a constant RHR of 0.1 MW an approximately equal pressure peak of 427 Pa can be expected.

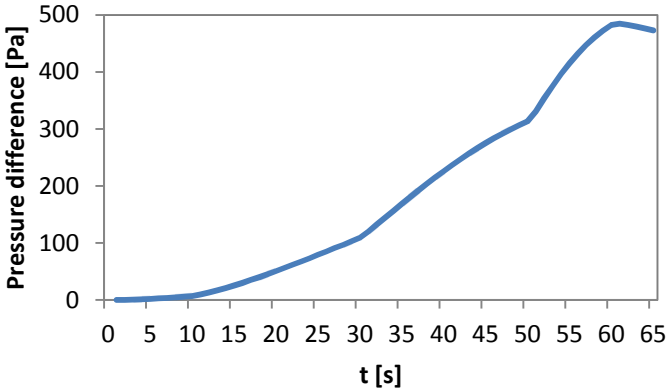

Figure 11.1 Pressure difference simulation on the basis of t^2-curve

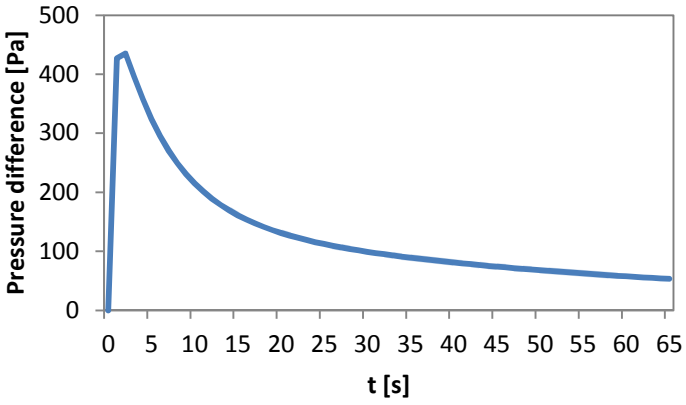

Figure 11.2 Pressure difference as result of a constant RHR

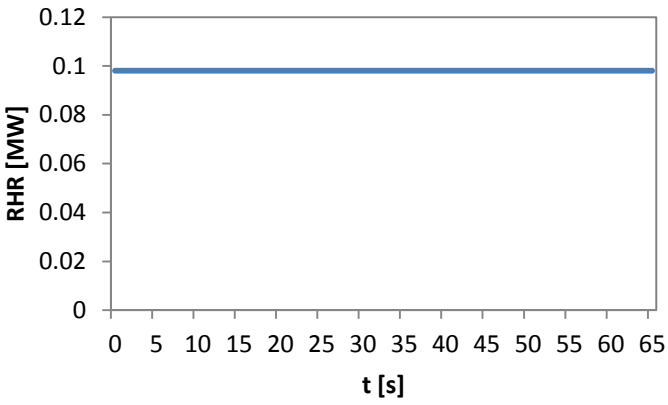

Figure 11.3 Constant Rate of Heat Release

Figures 11.2 and 11.3 can be used to determine the size of the pool fire and the amount of fuel. Because bio ethanol has a fairly clean burning, a purity of nearly 100% and evaporates not quickly, this fuel will be used for the experiments. The required dimensions of the pool fire can be determined with the following equation [30]:

$$Q = A_f * m'' * \chi * \Delta H_c \qquad (11.1)$$

The released energy is determined by Ozone and has a value of 0,098 MW. For the combustion efficiency a value of 0.7 can be maintained for hydrocarbons [30]. The value for gasification can be found in the literature [30]. With regard to the mass flow a distinction between small and large pool fires must be made. When the burning diameter is < 0.2 m a correction factor *k* for the extinction-absorption coefficient and a factor ß for the mean beam length corrector must be applied on the free burning rate. However, as this value is negligible for alcohols it is justified to assume that m_∞" = m". When the values are substituted into Equation (11.2) this gives the following equation:
0.098 = A_f x 0.015 x 0.7 x 26.8. Now it is easy to determine the surface for the pool fire, which must be 0.35 m^2. Then, with the following equation [30] the required amount of fuel can be determined:

$$Fire\ duration\ [s] = \frac{fuel\ mass}{total\ mass\ loss\ rate} \qquad (11.2)$$

The duration of the fire is determined manually on the basis of the oxygen mass from the output of Ozone in the same manner as in chapter three. As can be seen in Figure 65, the fire will have a duration of approximately 70s. The mass loss rate of the surface is 0.35 m^2 x 0.015. Now, the mass of the required fuel can be determined and is 0.3675 kg. This can be converted into litre with the equation fuel mass = (l/ 1000) * ρ. So the required amount of fuel is 0.315 = (l/ 1000) x 794. Therefore, the required amount of fuel is 0.4628 l.

Fuel calculation scenario 2

In the same manner the required amount of fuel for scenario 2 can be determined. The simulated pressure curve of scenario 2 is depicted in Figure 11.4. With the Ozone model it is determined experimentally which RHR leads to an equal pressure peak of 59 Pa. It appears that a constant RHR of 0.1 MW results in a pressure peak of 60.9 Pa, which is similar to the t_c = 150 curve simulation which gives a pressure peak of 59 Pa.

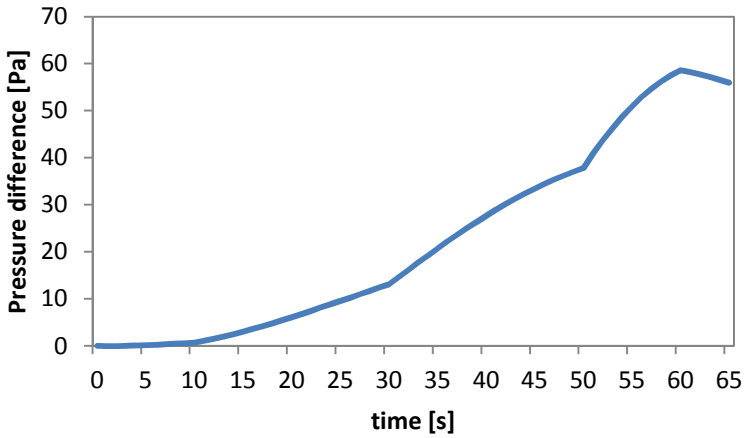

Figure 11.4 Pressure difference simulation on the basis of t^2-curve

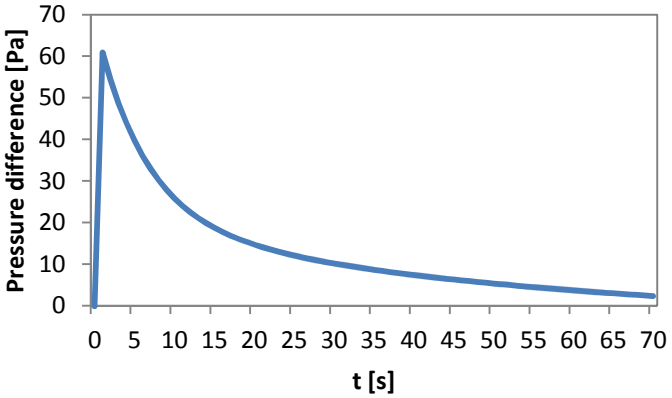

Figure 11.5 Pressure difference as a result of a constant RHR

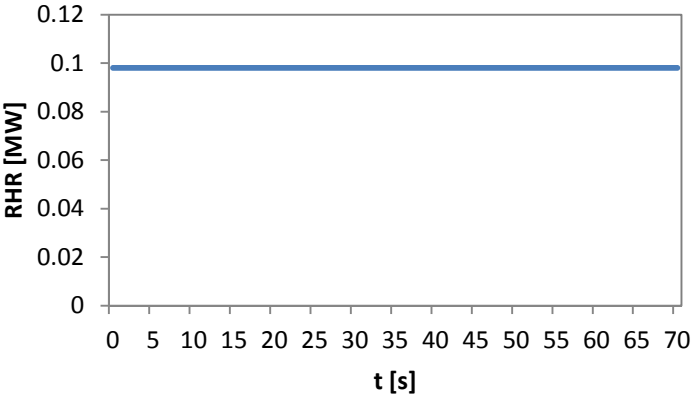

Figure 11.6 Pressure difference constant RHR

On the basis of these data and Equation (11.1) it is possible to calculate the required amount of fuel. The released energy is determined by Ozone and has a value of 0.098 MW. For the combustion efficiency 0.7 can be maintained. As already described it can be assumed for alcohols that m∞” = m” and remains 0.015. This gives the same equation for scenario 1 whereby the pool fire area remains the same, so the area of the pool fire remains 0.35 m^2. The expected duration of the fire remains also the same and will be 70 seconds. This means that the required amount of fuel remains also the same so that 0.4628 l. is needed. As the changed $q_{v;10}$ value has no influence on the temperature, it is not known if the Ozone simulations are accurate. Therefore, a surplus of fuel will be applied.

The purpose of scenario 3 and 4 is to examine the influence of varying the parameters on the pressure build-up. This is only possible when one single parameter is changed. To this end, with respect to scenario 1 and 2, the dimensions of the pool fire will be halved for scenario 3. For scenario 4 the size of the pool fire will be equal to scenario 1 and 2, but only the size of the slit is changed and the amount of fuel will be equal to scenario 1 and 2.

Appendix 12 – Determining moment of deflection by using slopes

In the figure below the moment of deflection is made visible by determining the slopes of the linear part of the upper thermocouple for each scenario.

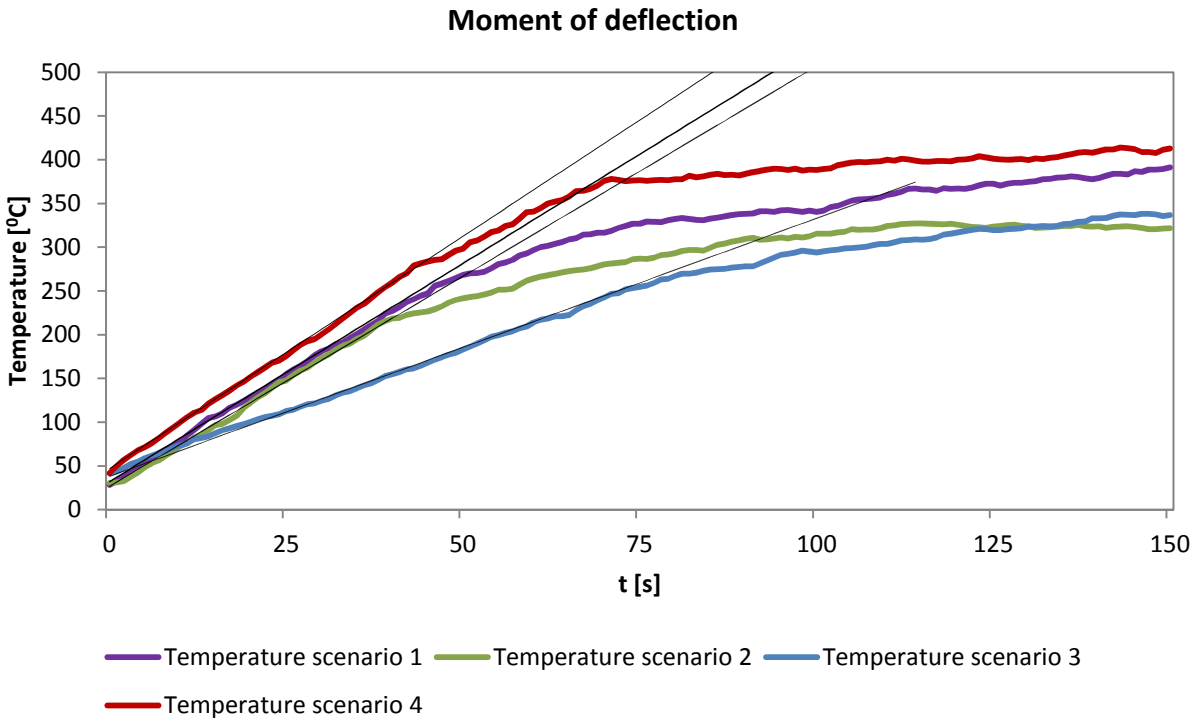

Appendix 13 – Overview fitted simulation models

Table 13.1 Overview models and corresponding results

	Model *(simulation approach)*	**P_{max}**	**Temperature**		
			100 ^{0}C	*200 ^{0}C*	*300 ^{0}C*
	Results conducted experiment scenario 2	**530 Pa**	**17 s.**	**37 s.**	**86 s.**
1.	Infiltration is translated into an equivalent surface of a slit. The slit is not adjusted conform Figure 10. The combustion model is turned off.	887 Pa	32 s.	85 s.	139 s.
2.	Infiltration is translated into an equivalent surface of a gap of 0.04 x 0.15 m. The combustion model is turned off.	807 Pa	32 s.	85 s.	139 s.
3.	Combustion model is turned on, and external fire duration is selected. The infiltration is translated into an equivalent surface of a slit, which is adjusted conform Figure 10 to the maximum occurring pressure	37 Pa	33 s.	88 s.	146 s.
4.1	Combustion model is turned on, and external fire duration is selected. The infiltration is translated into an equivalent surface of a gap of 0.04 x 0.15 m.	758 Pa	33 s.	88 s.	145 s.
4.2	Combustion model is turned on, and external fire duration is selected. The infiltration is translated into an equivalent surface of a slit, which is not adjusted conform Figure 10 to the maximum occurring pressure	826 Pa	33 s.	88 s.	145 s.
5.	Combustion model is turned off and all fire aspects are defined by hand. The infiltration is translated into an equivalent surface of a gap of 0.04 x 0.15 m.	4914 Pa	8 s.	24 s.	41 s.

* The models in which a slit is applied, this slit is already adjusted to the maximum occurring pressure.

Appendix 14 – Mass loss rate free burning experiment

Before the experiments in the enclosure are conducted, the free burning rate of the fuel is determined. For a proper measurement, the pan is levelled on a scale. The pan with the dimensions 0.3 x 0.39 m is filled with 0.4 kg 100% bio-ethanol. After ignition the fuel mass loss rate in relation to the time is depicted (Figure 14.1). As a result of inaccuracy during levelling the pan, the surface of the fire starts to decrease after 130 s. In the graph this can be seen as after t = 130 s when the mass loss rate becomes non-linear. For the linear decrease a mass loss rate of 0.002 kg/s can be maintained. The mass loss rate from the literature [30] is 0.015 kg/(m^2s). For a surface of 0.47 x 0.47 m and a combustion efficiency of 0.7 the mass loss rate according the literature must be 0.0023 kg/s. So the measured value and the literature are in line with each other.

The shape of the RHR is irregular. It is expected that this is caused by a incorrect readout of the scale and as a result of the inaccuracy of the scale.

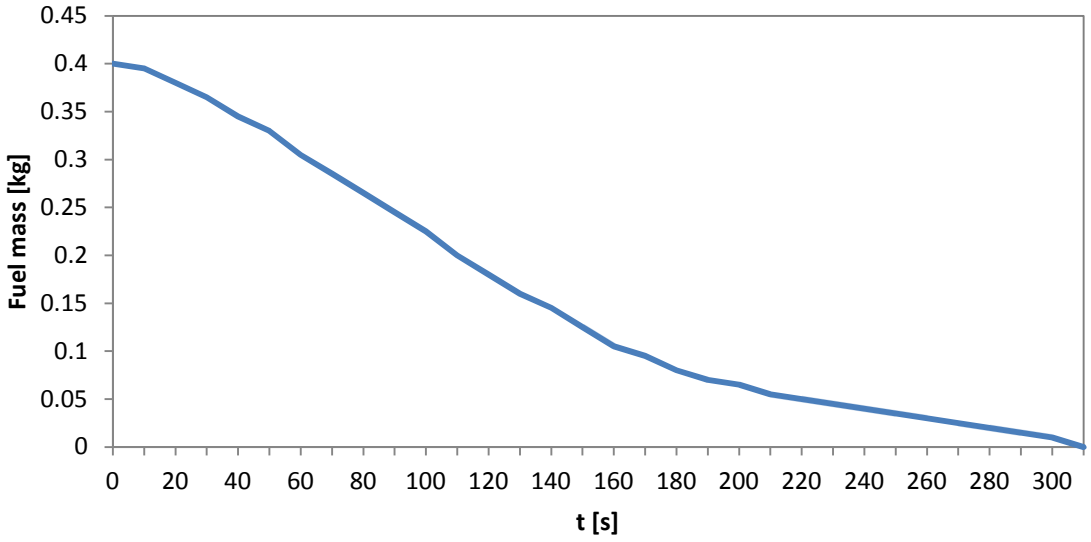

Figure 14.1 Fuel mass decrease for the free burning experiment

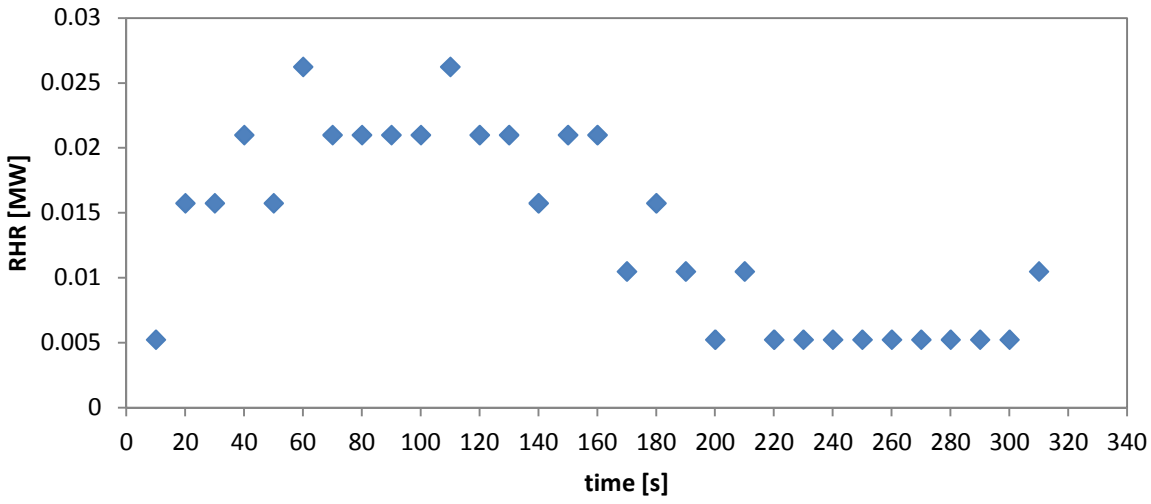

Figure 14.2 RHR of the free burning experiment

Appendix 15 – Stepwise increase RHR in 20 s.

The figures below show the pressure curve of scenario 2,3 and 4 respectively with a stepwise increase of the RHR in 20 seconds. The remarkable progress of the pressure curve seems to be caused by the small steps of the RHR increase. As a result of the low RHR, the steps are such small that the numbers are rounded in Ozone.

As a result of the RHR increase in 20 seconds the simulated pressure peak for scenario 2 is 474 Pa. This is an underestimation of the experimental pressure peak of 56 Pa. With regard to scenario 3 the simulated pressure peak is 114 Pa. This is an underestimation of the experimental pressure peak with 58 Pa. When the RHR is build up in 20 seconds for scenario 4, the simulated pressure peak is 118 Pa. As the experimental pressure peak for scenario 4 is 118 Pa, the simulation underestimates the pressure peak with 54 Pa.

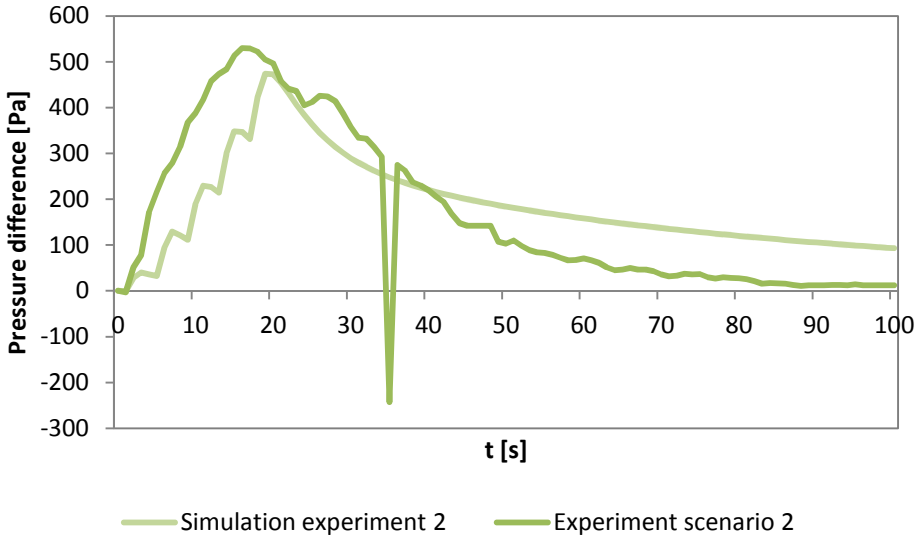

Figure 15.1 Fitted pressure curve scenario 2 with a stepwise increase of the RHR in 20 seconds

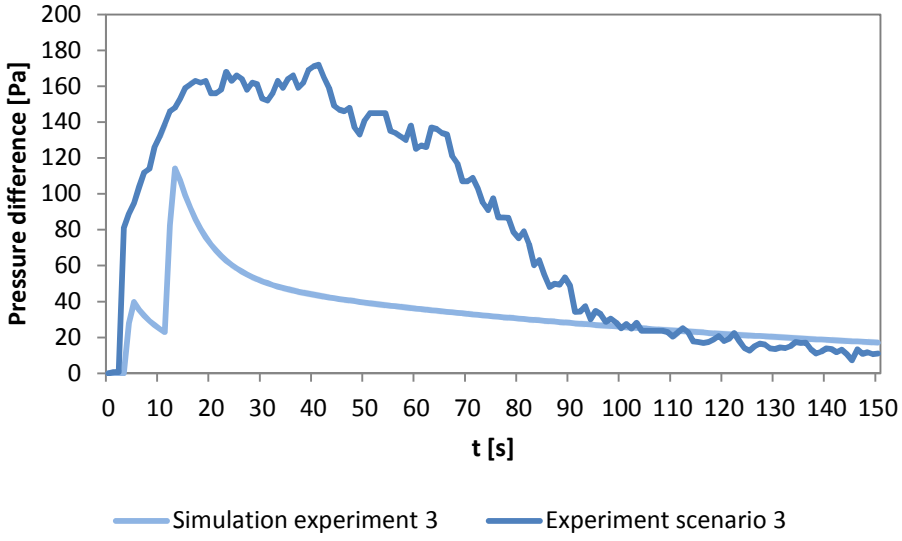

Figure 15.2 Fitted pressure curve scenario 3 with a stepwise increase of the RHR in 20 seconds

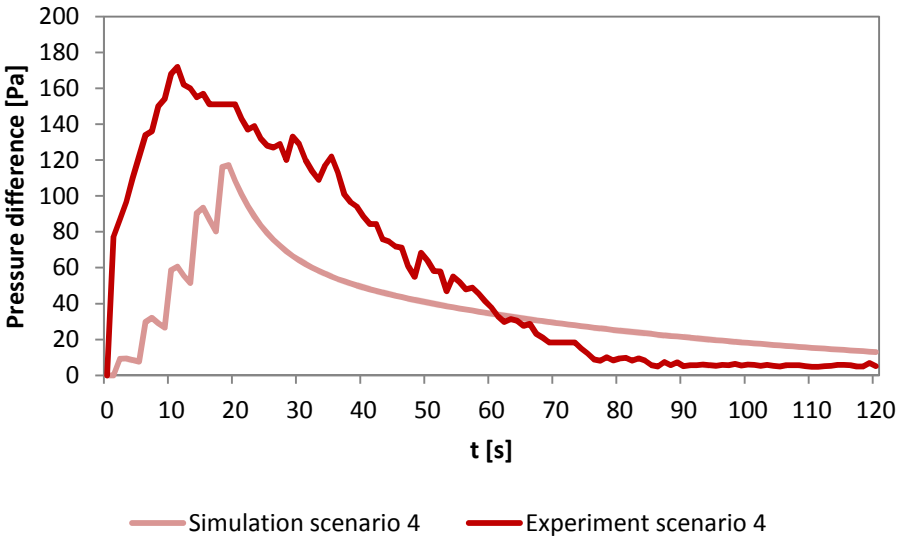

Figure 15.3 Fitted pressure curve scenario 4 with a stepwise increase of the RHR in 20 seconds

Appendix 16 – Temperature behaviour scenario 3 and 4

The temperature lines of scenario 3 shows a large deviation between the experimental result and the simulation for scenario 3. In practice the temperature will reach much higher values (Figure 16.1). As mentioned by scenario 2, this difference may be caused by the fact that during the experiments also the heat radiation instead of only the convective heat is measured.

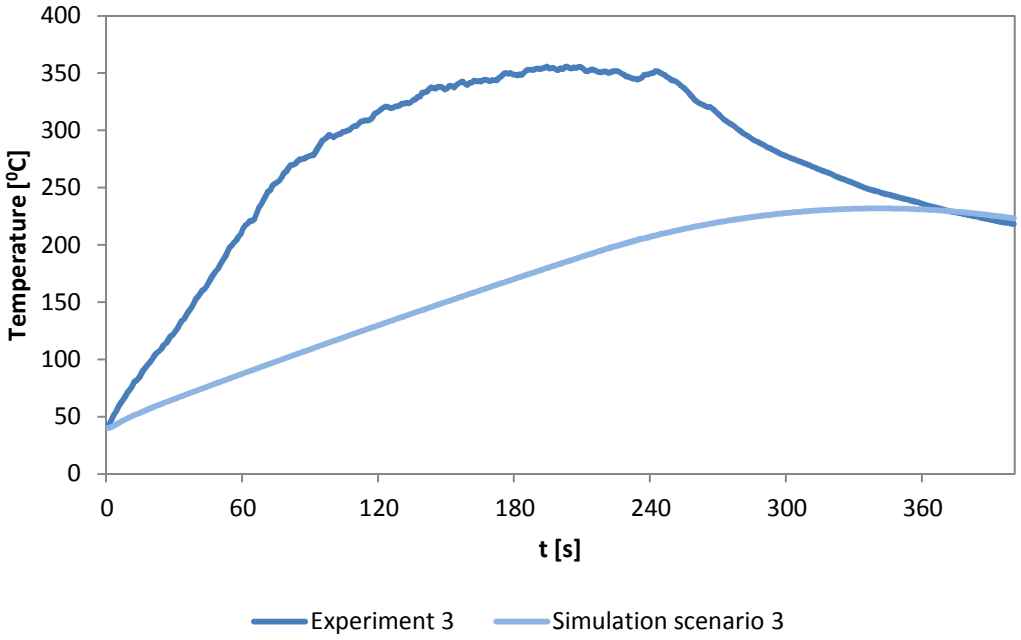

Figure 16.1 Simulated and measured temperature curve scenario 3

Scenario 4

In line with scenario 2 and 3, the simulated temperature curve of the model differs from the experimental result (Figure 16.2). It can be observed that the shape of the simulated temperature curve of scenario 2 is exact the same, but the 10 ^{0}C lower. This is caused by the fact that the starting temperature in scenario 2 in 10 ^{0}C lower. This implies that the size of the opening has no influence on the temperature curve. However, for the conducted experiment a temperature difference of approximately 17 % is measured between the curves of experiment 2 and 4. So in practice the size of the opening does play a role in the temperature behaviour.

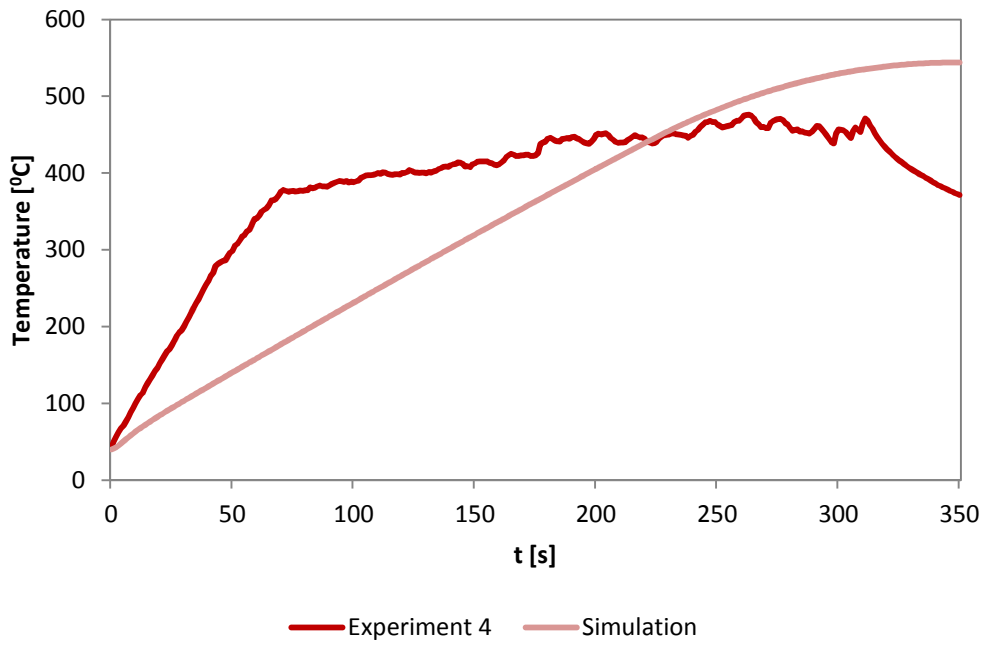

Figure 16.2 Simulated and measured temperature curve scenario 4

On the basis of the oxygen mass fraction it can be calculated that the simulated fire extinguishes or remain smouldering after approximately 63 s. due to a lack of oxygen (Figure 16.3). This corresponds to the moment the experimental temperature curve deflects in Figure 16.2. However, the Ozone RHR graph in Figure 16.4 indicates that the fire will be ventilation controlled after approximately 220 seconds.

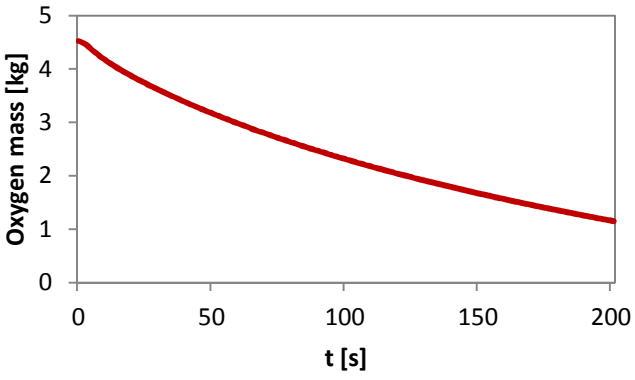

Figure 16.3 Oxygen mass simulation scenario 4

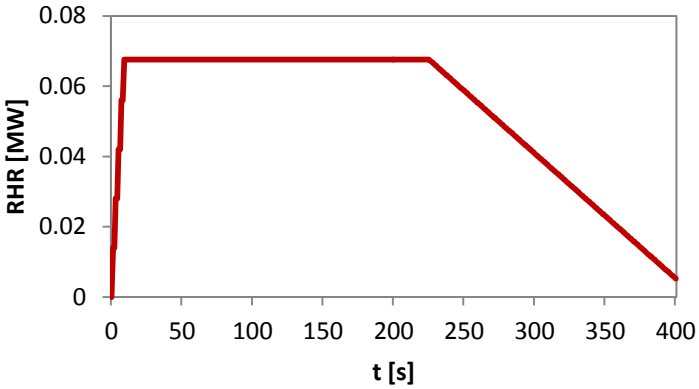

Figure 16.3 Stepwise increase of the RHR for the first 10 s. after ignition

TU/e Technische Universiteit Eindhoven University of Technology
BRANDWEER Nederland
IFV Instituut Fysieke Veiligheid